DISCRETE SCHEMES FOR THERMOVISCOELASTICITY WITH THERMORHEOLOGICALLY-SIMPLE NONLINEAR COUPLING

A thesis submitted for the degree of Doctor of Philosophy

by

Fatmir Qirezi

Department of Mathematical Sciences
School of Information Systems, Computing and Mathematics
Brunel University
February 2014

Abstract

In this thesis, we consider the deformation of a non-ageing solid linear viscoelastic compressible isotropic body, the interior of which occupies the region $\Omega \subset \mathbb{R}^n$, $n \in \{1, 2, 3\}$, with convex polygonal boundary $\partial\Omega$. We employ the finite element method to discretise in space, whereas for time discretisation the trapezoidal rule for approximation is used. We assume that the acceleration is negligible. This, from Newton's law of motion, yields the *quasistatic force balance* equation,

$$-\sigma_{ij,j} = f_i(\boldsymbol{x}, t),$$

with Dirichlet and/or Neumann boundary conditions, where $i, j = 1, \ldots, n$. Here σ_{ij} is the stress tensor written in component form and $,j$ denotes $\frac{\partial}{\partial x_j}$, with repeated indices implying the summation convention. The above body deformation is under the action of body forces $\boldsymbol{f} := (f_i(\boldsymbol{x}, t))_{i=1}^n$ and surface tractions and is considered for every time $t \in I := [0, T]$ at some position $\boldsymbol{x}$ in Ω. Only small strains are considered, thus confining ourselves to the linear theory of deformation.

In addition to the body forces and tractions, we also consider the effects of temperature on the deformation of the above physical body. Thus, assume that for every $t \in I$, a temperature field is applied externally to the body under consideration, where the temperature comes from the solution of the *heat conduction* problem, given by,

$$\kappa\dot{\theta}(\boldsymbol{x}, t) - Q\nabla^2\theta(\boldsymbol{x}, t) = l(\boldsymbol{x}, t).$$

Here $\theta(\boldsymbol{x}, t)$ is temperature, l is a given heat source, $\dot{\theta}(\boldsymbol{x}, t)$ is the partial derivative of θ with respect to time t and ∇^2 is the Laplace operator. κ and Q are assumed to be constants. We assume that, due to heat, the body expands in a volumetric manner, which in turn means that only direct strain is present. In this case, we use the following stress-strain law written in vector-matrix notation,

$$\boldsymbol{\sigma}(\boldsymbol{u}(t)) = \boldsymbol{D}\left[\boldsymbol{\varepsilon}(\boldsymbol{u}(t)) - \alpha(\theta(t) - \theta_r)\boldsymbol{I_0}\right] - \int_0^t \boldsymbol{D}_s(t - s)\left[\boldsymbol{\varepsilon}(\boldsymbol{u}(s)) - \alpha(\theta(s) - \theta_r)\boldsymbol{I_0}\right] ds,$$

where $\boldsymbol{D}$ is the constitutive matrix from the elasticity theory, α is known as the coefficient of thermal expansion, θ_r is a reference temperature and $\boldsymbol{I_0} = [1 \quad 1 \quad 0]$. The above law then leads to a linear coupled problem between the heat equation and the force balance equation.

The notion of a *thermorheologically simple* polymer is also introduced and we explain the nonlinear coupling that results from the introduction of reduced time ρ in the stress-strain law above, which then takes the following form,

$$\boldsymbol{\sigma}(\boldsymbol{u}(t)) = \boldsymbol{D}\left[\boldsymbol{\varepsilon}(\boldsymbol{u}(t)) - \alpha(\theta(t) - \theta_r)\boldsymbol{I_0}\right] - \int_0^t \boldsymbol{D}_s(\rho(t) - \rho(s))\left[\boldsymbol{\varepsilon}(\boldsymbol{u}(s)) - \alpha(\theta(s) - \theta_r)\boldsymbol{I_0}\right] ds.$$

For clarity, in both laws above the $\boldsymbol{x}$ dependence of $\boldsymbol{u}$, θ and ρ is suppressed. Both coupled problems, linear and nonlinear, represent a novel study as part of this thesis. Theoretical results such as stability and a *priori* error estimates are derived. We also conduct experimental work and show some computational results in terms of the convergence rates in the H^1 and L_2 norms.

Acknowledgement

I am very grateful to my supervisor, Dr Simon Shaw, for his excellent supervision throughout my PhD studies. I would like to thank him for his support and encouragement, and, in particular, for introducing me to the world of numerical analysis and finite element methods. Without his guidance this work would have not been possible.

I would also like to thank many people in the maths department for their support and their warm words during the time I have spent here; they know who they are. However, special gratitude goes to Brunel University for awarding me the prestigious Isambard scholarship, which has been very beneficial to me in many aspects and made my research easier.

Finally, I am very grateful to my family, especially my parents, for their patience and moral support throughout my studies, and more.

Contents

List of Tables

List of Figures

List of Symbols

Chapter 1

Introduction

1.1 Outline

In this thesis we initially deal with the mathematical modelling of the behaviour of a solid viscoelastic material body under the action of given forces and tractions. Only small strains are considered. A second constraint is that we only consider the quasistatic case, meaning that the inertia term in the equilibrium equation is neglected, after all the transients have died away. We then extend this problem: a temperature field, coming from the solution of the heat conduction problem, is applied externally to the body under consideration. This results in a coupled problem: first, the heat equation is solved, then this is fed into viscoelasticity. There is a tendency of materials to expand under the influence of heat. The phenomenon of thermal expansion is modelled by modifying the stress-strain law for viscoelasticity. Finally, we introduce a special class of materials known as "thermorheologically-simple materials", and a nonlinearity in the memory integral for thermoviscoelasticity. We use the finite element method and the trapezoidal rule for time integrals to solve the system of equations modelling such behaviour. The theoretical analysis plays a very important part in this thesis. We consider stability and a *priori* error estimates. Stability analysis is needed to ensure that the problem solution is bounded by data and initial conditions in a continuous manner. Error estimates are important to show how error depends on the mesh size and time steps (for time dependent problems) and then one can investigate whether these are consistent with any computational results (e.g convergence rates) achieved. All the computational results are derived using Matlab. The original sources of codes are Alberty et al. (1999) and Alberty et al. (2002). This thesis is organized as follows:

Chapter 1

It contains a brief outline of the thesis and review of preliminary functional analysis. We define Banach space L_p and Sobolev spaces W_p^m and norms related with spaces. We state important theorems such as: Friedrich's inequality and Ritz representation theorem. Some inequalities are presented which are used extensively in this thesis. A brief overview of Volterra equations is given, followed by two versions of the Gronwall's lemmas, continuous and discrete.

Chapter 2

We discuss basic elements of continuum mechanics. Definitions of displacement, stress and strain are given. Also, we show how a strain-displacement relation is derived when small deformations are assumed. Brief introduction into elasticity theory is presented. Properties of viscoelastic materials are discussed, and stress-strain law for linear viscoelasticity is given. This is followed by a brief introduction into heat conduction theory, phenomenon of thermal expansion and the concept of reduced time. Then, we present the proposed model problem for this thesis. New forms of stress-strain laws are given. We define the linear and nonlinear problem, where we give weak formulations to these.

Chapter 3

In this chapter we show how the finite element method is used to find an approximate solution by discretizing in space. We apply this to the elasticity and heat problem. In the case of the heat problem we also discretize in time, where we use Crank-Nicolson method. We then give fully discrete schemes to viscoelasticity and heat problem. For viscoelasticity we also give some numerical results. Finally, in this chapter fully discrete schemes to linear and nonlinear problem are given.

Chapter 4

This is the first chapter where we start to work on the theoretical aspect of thesis. Here we derive a stability bound in energy norm for the linear problem, the continuous and discrete formulation. To achieve this, stability bounds for continuous and discrete temperature are also needed; they are too derived in this chapter. Theorems 4.1.1 and 4.2.1 show the two results for the stability bounds for displacement. We give detailed proofs to the theorems.

Chapter 5

We now move to error analysis for the linear problem. Here we derive *a priori* error estimates in energy norms for the heat problem and the linear problem. Theoretical results derived are shown in Theorems 5.1.1 and 5.2.1. Detailed proofs of theorems are given. We end this chapter by showing some numerical results for the linear problem.

Chapter 6

Stability bounds for the nonlinear problem are derived, both continuous and discrete. These results are presented in Theorems 6.1.1 and 6.2.3.

Chapter 7

In this chapter we derive *a priori* error estimate for the nonlinear problem. Theorem 7.2.1 shows the error estimate derived for this problem. Finally, we give some numerical results for this problem.

Chapter 8

In the last chapter we review what is achieved in this thesis in the form of conclusions, both the theoretical and computational aspect. We also give suggestions for future work, that is, we propose some potential ideas to extend the work presented in this thesis.

1.2 The finite element method

The finite element method (FEM) is a technique for generating discrete algorithms for approximating the solutions of differential equations. It is the preferred method of the engineering community for the numerical solution of partial differential equations. This method is based on earlier works of Galerkin, Rayleigh and Ritz. It was first proposed in a seminal work by Courant in 1943, Zienkiewicz (2004). FEM finds a widespread application in mechanics, fluid dynamics, electromagnetism, medicine, financial modelling etc. FEM is based on the Galerkin method for finding approximate solutions of PDE‘s.

The determination of suitable basis functions for use in the Galerkin method can be extremely difficult, especially when the domain does not have a simple shape. The finite element method overcomes this difficulty by providing a systematic means for generating basis functions on domains of fairly arbitrary shape. The domain is partitioned in a finite number of subdomains called *finite elements*. Based on this partition, then an approximate solution is sought, Reddy (1998). More about this method, later.

1.3 Preliminary functional analysis and notation

The smoothness of the analytical solution to a partial differential equation (PDE) under consideration, together with the smoothness of the data, plays an important role on the accuracy of finite element approximation to the equation.

By considering *function spaces* of functions with specific differentiability and integrability properties one can conveniently formulate precise assumptions about the regularity of the solution and the data. In this section we present a brief overview of the mathematics that will be used throughout this thesis. This includes basic definitions and simple results from the theory of function spaces, however most notation is introduced as it appears. We remark here, for future reference, that all functions that appear in this thesis will be assumed to be real-valued. For more details on these topics we can refer to Brenner and Scott (2002) and Reddy (1998).

Overview of Function Spaces

We first introduce some useful definitions which are of crucial importance in analysis that will be carried out later in this thesis.

Definition 1.3.1. *Given a linear space V, a norm $\|\cdot\|$ is a function from V to $\mathbb{R}$ with the following properties:*

1. $\|v\| \geqslant 0$ *for any* $v \in V$, *with* $\|v\| = 0$ *if and only if* $v = 0$,
2. $\|cv\| = |c|\|v\|$ *for any* $v \in V$ *and* $c \in \mathbb{R}$,
3. $\|u + v\| \leqslant \|u\| + \|v\|$ *for any* $u, v \in V$.

It is possible to define an inner product as well (on *real* vector spaces).

Definition 1.3.2. *The inner product* (u, v) *of* $u, v \in V$ *is an operation that satisfies the following properties, for all* $u, v, w \in V$ *and* $\alpha, \beta \in \mathbb{R}$:

1. $(u, v) \in \mathbb{R}$,
2. $(u, v) = (v, u)$ *(the operation is symmetric),*
3. $(\alpha u + \beta v, w) = \alpha(u, w) + \beta(v, w)$ *(linearity),*
4. $(u, u) \geqslant 0$ *and* $(u, u) = 0$ *if and only if* $u = 0$ *(positive-definiteness).*

Definition 1.3.3. *A linear space* V *together with an inner product defined on it is called an* ***inner-product space*** *and is denoted by* $(V, (\cdot, \cdot))$.

Definition 1.3.4. *A normed linear space* V *is called a* ***Banach space*** *if it is complete with respect to the metric induced by the norm* $\| \cdot \|$.

Definition 1.3.5. *Let* $(V, (\cdot, \cdot))$ *be an inner-product space. If the associated normed linear space* $(V, \| \cdot \|)$ *is complete, then* $(V, (\cdot, \cdot))$ *is called a* ***Hilbert space***.

Given an inner-product space $(V, (\cdot, \cdot))$, there is an associated norm defined on V namely $\|v\| = \sqrt{(v, v)}$, which means that an inner product space can be made into a normed linear space. A normed space is said to be complete if and only if every Cauchy sequence from the space converges to an element in the space. Since every inner product defines a norm, every Hilbert space is a Banach space.

Let Ω be an open bounded connected subset of $\mathbb{R}^n$ with a Lipschitz boundary $\partial\Omega$. A generic point in $\mathbb{R}^n$ is denoted by $\boldsymbol{x} = (x_1, \ldots, x_n)$. For multi-variable functions, it is convenient to use the *multi-index* notation for partial derivatives. A multi-index, τ, is an n-tuple of non-negative integers, τ_i, whose length is given by

$$|\tau| := \sum_{i=1}^{n} \tau_i.$$

For the multi-index τ we denote by

$$D^\tau u := \frac{\partial^{|\tau|} u}{\partial x_1^{\tau_1} \partial x_2^{\tau_2} \dots \partial x_n^{\tau_n}},$$

the partial derivative of order τ of u.

We denote by $C(\Omega)$ the space of all continuous functions defined on Ω, whereas by $C(\bar{\Omega})$ we denote the space of all functions that are continuous on the closed set $\bar{\Omega} = \Omega \cup \partial\Omega$. The space $C^m(\Omega)$ is the space of functions which together with all their derivatives up to and including those of order m, are continuous on Ω. Using the multi-index notation these can be written as,

$$C^m(\Omega) = \{u \in C(\Omega) : D^\tau u \in C(\Omega) \quad \text{for} \quad |\tau| \leq m\}$$

and

$$C^m(\bar{\Omega}) = \{u \in C(\bar{\Omega}) : D^\tau u \in C(\bar{\Omega}) \quad \text{for} \quad |\tau| \leq m\}.$$

We denote by $L_p(\Omega)$ the Banach space of all functions equipped with the norm,

$$\|u\|_{L_p(\Omega)} := \begin{cases} \left(\int_\Omega |u(\boldsymbol{x})|^p d\Omega\right)^{1/p} & 1 \leq p < \infty, \\ \operatorname*{ess\,sup}_{\boldsymbol{x}\in\Omega} |u(\boldsymbol{x})| & p = \infty, \end{cases}$$

where the *essential supremum* is defined to be the infimum of the constants γ that bound $|u|$ almost everywhere:

$$\operatorname*{ess\,sup}_{\boldsymbol{x}\in\Omega} |u(\boldsymbol{x})| = \inf\{\gamma : |u(\boldsymbol{x})| \leqslant \gamma \;\; a.e.\}.$$

A special case corresponds to taking $p = 2$. Then,

$$\|u\|_{L_2(\Omega)} = \left(\int_\Omega |u|^2 d\Omega\right)^{1/2}.$$

The space $L_2(\Omega)$ is defined by

$$L_2(\Omega) := \{u : \; u \text{ is defined on } \Omega, \; \int_\Omega u^2 d\Omega < \infty\}.$$

An important extension to the $L_p(\Omega)$ spaces are the Sobolev spaces $W_p^m(\Omega)$. These are spaces of functions which together with all their partial derivatives of order up to and including m belong to $L_p(\Omega)$. Then, the Sobolev space of order $m \geqslant 0$, $p \geqslant 1$ is defined as

$$W_p^m(\Omega) := \{u : D^m u \in L_p(\Omega) \quad \forall \tau \quad \text{such that} \quad 0 \leqslant |\tau| \leqslant m\},$$

whose norm is given by

$$\|u\|_{W_p^m(\Omega)} := \begin{cases} \left(\displaystyle\sum_{|\tau|\leqslant m} \int_\Omega |D^\tau u|^p dx\right)^{1/p} & 1 \leqslant p < \infty, \\ \displaystyle\max_{|\tau|\leqslant m} \|D^\tau u\|_{L_\infty(\Omega)} & p = \infty. \end{cases}$$

The spaces $L_p(\Omega)$ are called Lebesgue spaces. When $p = 2$ it is common to write $H^m(\Omega) := W_2^m(\Omega)$. Both $L_2(\Omega)$ and $H^m(\Omega)$ are Hilbert spaces equipped with the inner products,

$$(u, v)_\Omega = \int_\Omega uvdx \quad \text{and} \quad (u, v)_{H^m(\Omega)} = \sum_{|\tau| \leqslant m} (D^\tau u, D^\tau v)_\Omega \,, \tag{1.3.1}$$

respectively. It is possible to define the functions from the L_2 space on the manifold $\partial\Omega$ as follows:

$$L_2(\partial\Omega) := \left\{ v : \oint_{\partial\Omega} v^2 d\Gamma < \infty \right\},$$

which is a Hilbert space when equipped with the inner product:

$$(u, v)_{L_2(\partial\Omega)} := \oint_{\partial\Omega} uvd\Gamma,$$

and the norm:

$$\|v\|_{L_2(\partial\Omega)} := \sqrt{(v, v)_{L_2(\partial\Omega)}}.$$

One can also define the space $L_2(\Gamma)$ for $\Gamma \subset \partial\Omega$. Sometimes it is useful to bound the norm of a function in terms of the norm of the gradient of the same function. The following theorem enables us to do just that and it plays an important role in the analysis; this is shown in (Oden and Reddy, 1970, p.82), for example.

Theorem 1.3.1 (Friedrich's inequality)**.** *Let Ω be an open bounded domain with Lipschitz boundary $\partial\Omega$, then there is a positive constant C_F such that*

$$\|v\|^2_{L_2(\Omega)} \leqslant C_F \|\nabla v\|^2_{L_2(\Omega)},$$

for all $v \in H^1(\Omega)$ such that $v = 0$ on $\partial\Omega$. ∇ is the gradient operator.

Very useful in this thesis is also the following norm,

$$\|u\|_{L_2(0,t;V)} := \left(\int_0^t \|u(s)\|^2_V ds \right)^{1/2}. \tag{1.3.2}$$

In continuum mechanics it is useful to define the product space

$$(H^m(\Omega))^n := H^m(\Omega) \times \ldots \times H^m(\Omega) \quad (n \text{ times}),$$

which for a vector $\boldsymbol{u} := (u_i)_{i=1}^n$, we equip with the product norm

$$\|\boldsymbol{u}\|_{H^m(\Omega)} = \left(\sum_{i=1}^{n} \|u_i\|^2_{W_2^m} \right)^{1/2}, \quad \boldsymbol{u} \in (H^m(\Omega))^n .$$

The normed linear space $\left(W_p^m(\Omega)\right)^n$ can be defined in the obvious way. We define the seminorm on $W_p^m(\Omega)$ by

$$|u|_{W_p^m(\Omega)} = \left(\sum_{|\tau|=m} \|D^\tau u\|_{L_p(\Omega)} \right)^{1/p}, \quad u \in W_p^m(\Omega).$$

The concept of a *(symmetric) bilinear form* and that of a *linear functional* are very important in the analysis of boundary value problems, and hence in the analysis that will be presented in this thesis. For their definitions the reader may refer to Brenner and Scott (2002) and Reddy (1998). We say that a linear functional $L : V \to \mathbb{R}$ is continuous if there exists a constant K, such that

$$L(v) \leqslant K\|v\|, \qquad \forall v \in V.$$

If V is a normed space, then the space of all *continuous linear functionals* is called the *dual* space of V, denoted by V', with associated norm

$$\|L\|_{V'} := \sup_{0 \neq v \in V} \frac{|L(v)|}{\|v\|_V}. \tag{1.3.3}$$

The following theorem is also an important result in numerical analysis, Atkinson and Han (2010).

Theorem 1.3.2 (Riesz representation theorem)**.** *Let $(V, (\cdot,\cdot))$ be a Hilbert space and let $L \in V'$. Then there is a unique $u \in V$, for which*

$$L(v) = (v, u), \qquad \forall v \in V.$$

Furthermore, we have

$$\|L\|_{V'} = \|u\|_V.$$

Some inequalities

Here we give some useful inequalities that will be used extensively in this thesis. These can be found, for example, in Atkinson and Han (2010).

Inequality 1.3.1 (Young's Inequality)**.** *For all $a, b \in \mathbb{R}$ and $\forall \epsilon > 0$,*

$$ab \leqslant \frac{\epsilon}{2}a^2 + \frac{1}{2\epsilon}b^2.$$

Inequality 1.3.2 (Hölder's Inequality)**.** *For $1 \leq p, q \leq \infty$, $u \in L_p(\Omega)$ and $v \in L_q(\Omega)$, with $\frac{1}{p} + \frac{1}{q} = 1$ then, $uv \in L_1(\Omega)$ and*

$$\|uv\|_{L_1(\Omega)} \leq \|u\|_{L_p(\Omega)} \|v\|_{L_q(\Omega)}.$$

Inequality 1.3.3 (Minkowski's Inequality)**.** *For $1 \leq p \leq \infty$ and $u, v \in L_p(\Omega)$, we have*

$$\|u + v\|_{L_p(\Omega)} \leq \|u\|_{L_p(\Omega)} + \|v\|_{L_p(\Omega)}.$$

Inequality 1.3.4 (Cauchy-Schwartz Inequality)**.** *If $(V, (\cdot,\cdot))$ is an inner product* *space with norm defined by* $\|\cdot\| = \sqrt{(\cdot,\cdot)}$*, then*

$$|(u,v)| \leqslant \|u\|\|v\|.$$

1.4 Volterra equations

It is worthwhile to present here a brief review of the so-called *Volterra equations*. Let $b(t,s) \in C([0,T]\times[0,T])$ and $f(t) \in C[0,T]$ be two given functions, where T is some positive number, and s and t are such that $0 \leqslant s \leqslant t \leqslant T$. The simplest form of Volterra equation is the equation of the second type and is given by

$$u(t) = f(t) + \int_0^t b(t,s)u(s)ds, \qquad t \in [0,T], \tag{1.4.1}$$

where b is known as the kernel and u is the function to be found. So we note that the function u appears under the integral and outside the integral. In the case of the generic *Volterra equation of the first type* the function u appears only under the integral,

$$f(t) = \int_0^t b(t,s)u(s)ds, \qquad t \in [0,T]. \tag{1.4.2}$$

An important lemma in the study of both theoretical and numerical aspects of time-dependent problems is the Gronwall type inequality which we present here.

Lemma 1.4.1 (Continuous Gronwall lemma, c.f. Shaw (1993))**.** *Let* $u \geqslant 0$ *be an integrable function and* $v \geqslant 0$ *a non-decreasing function, both defined on* $I := [0,T]$*,* $T > 0$*. Then, the inequality*

$$u(t) \leqslant v(t) + C\int_0^t u(s)ds, \qquad \forall t \in I, \tag{1.4.3}$$

where $C \geqslant 0$ is a constant, implies that $u(t) \leqslant v(t)\exp(Ct)$ for all $t \in I$.

Proof. For the case when $t = 0$, this is obviously true, since the integral vanishes. For $t > 0$, let $u(t) = z(t)\exp(Ct)$, and for some arbitrary $\tau \in (0, T]$ let $\hat{t} \in [0, \tau]$ so that $z(\hat{t}) = \max_{t\in[0,\tau]} z(t)$. Then, from (1.4.3), we have the following:

$$
\begin{aligned}
u(\hat{t}) = z(\hat{t})\exp(C\hat{t}) &\leqslant v(\hat{t}) + C\int_0^{\hat{t}} z(s)\exp(Cs)ds \\
&\leqslant v(\hat{t}) + Cz(\hat{t})\int_0^{\hat{t}} \exp(Cs)ds, \quad \text{(since } z(\hat{t}) \text{ is a max in } [0,\hat{t}]) \\
&= v(\hat{t}) + z(\hat{t})(\exp(C\hat{t}) - 1), \quad \text{(integrating the above)} \\
&\leqslant v(\tau) + z(\hat{t})(\exp(C\hat{t}) - 1),
\end{aligned}
$$

because v is a non-decreasing function and $\hat{t} \leqslant \tau$. From $z(\hat{t})\exp(C\hat{t}) \leqslant v(\tau) + z(\hat{t})(\exp(C\hat{t}) - 1)$ we have that $0 \leqslant v(\tau) - z(\hat{t})$, which gives $z(\hat{t}) \leqslant v(\tau)$. Since by definition, $z(\tau) \leqslant z(\hat{t})$, then it is obvious that also $z(\tau) \leqslant v(\tau)$. Thus, the fact that $u(\tau) = z(\tau)\exp(C\tau)$, gives $u(\tau) \leqslant v(\tau)\exp(C\tau)$. Since τ is arbitrary, this completes the proof. □

There is also the discrete version of the Gronwall inequality which we introduce here.

Lemma 1.4.2 (Discrete Gronwall lemma, c.f. Lees (1960))**.** *Given a positive integer N, let $u \geqslant 0$ be a function defined on $I^k := \{t_i \in I : t_i = ik,\ \ i = 0, \dots,\ N = T/k\}$ with $u_i := u(t_i)$ and $v \geqslant 0$ a non-decreasing function also defined on I^k. Then the inequality*

$$
u_i \leqslant v_i + Ck\sum_{j=0}^{i-1} u_j, \qquad \forall t_i \in I^k, \tag{1.4.4}
$$

where $C \geqslant 0$ is a constant, implies that $u_i \leqslant v_i \exp(Ct_i)$ for all $t_i \in I^k$.

Proof. For the case when $i = 0$, we define the sum to be an empty set. For $i > 0$, define z_i by $u_i = z_i \exp(Ct_i)$. For some $m \in \{1, \dots, N\}$, choose $n \in \{0, \dots, m\}$ so that $z_n = \max_{i \in \{0,\dots,m\}} z_i$. Then this implies the following:

$$z_n \exp(Ct_n) \leqslant v_n + z_n Ck \sum_{j=0}^{n-1} \exp(Ct_j).$$

From here, we can write,

$$k \sum_{j=0}^{n-1} \exp(Ct_j) \leqslant \int_0^{t_n} \exp(Cs) ds = \frac{1}{C}\big(\exp(Ct_n) - 1\big).$$

Since v_i is a non-decreasing sequence, then the last two results give,

$$z_n \exp(Ct_n) \leqslant v_n + z_n(\exp(Ct_n) - 1),$$

which implies that $z_n \leqslant v_m$, since $v_n \leqslant v_m$. Therefore,

$$u_m = z_m \exp(Ct_m) \leqslant v_m \exp(Ct_m).$$

Since m is arbitrary, this completes the proof. □

1.5 Summary

In this chapter an outline of the thesis was given. Some preliminary functional analysis was presented: spaces of functions, norms, as well as some useful notation and inequalities. In the next chapter we give a brief overview of continuum mechanics.

Chapter 2

Basic Continuum Mechanics

The fundamental postulate of continuum mechanics is the continuum concept of matter. This concept implies that any material body, whether it be solid, liquid or gas, can be modelled by disregarding molecular considerations and by assuming the material to be continuously distributed throughout its volume and to completely fill the space it occupies. The material may be satisfactorily considered as a continuum when the distance between physical particles is very small compared to the characteristic dimensions of the problem. Other classical theories such as aerodynamics, fluid mechanics, elasticity, plasticity, and viscoelasticity are special branches of continuum theory. The continuum theory is a mathematical theory. A material is said to be *homogeneous* if it has identical properties at all points. A material is said to be *isotropic* if it does not have a characteristic orientation.

2.1 Displacement, stress and strain

The continuum concept allows us to identify a material body with an open bounded subset of $\mathbb{R}^n$. Thus, let $\mathcal{B}$ be a compressible solid body, initially in its undeformed state, defined in the region $\Omega \subset \mathbb{R}^n$, $n \in \{1, 2, 3\}$ with boundary $\partial\Omega$. We say that Ω is the *reference configuration* or the *placement* of $\mathcal{B}$ in $\mathbb{R}^n$. Assume that at some time t this body is acted upon by body and surface forces. *Body forces* are forces which are not due to physical contact between bodies, for example, the gravitational force, or are due to self-weight. *Surface forces*, which are also called surface tractions, represent forces that are due to physical contact between bodies. These forces are referred to as external forces. The boundary $\partial\Omega$ is partitioned into disjoint subsets, Γ_D, called the Dirichlet boundary, and Γ_N, called the Neumann boundary. The partition is such that $\partial\Omega \equiv \Gamma_D \cup \Gamma_N$, $\Gamma_D \cap \Gamma_N = \emptyset$, the empty set.

Displacement, stress and strain. Under the action of body forces and tractions, as a consequence, the body $\mathcal{B}$ will deform to a new shape, unless it is perfectly rigid. Let the displacement of a particle at a point $\boldsymbol{x} \in \Omega$ be denoted by $\boldsymbol{u}(\boldsymbol{x}, t) = (u_i)_{i=1}^n$, and the new position of particle will be $\boldsymbol{x} + \boldsymbol{u}$. In order to measure the deformation of the body $\mathcal{B}$ in terms of relative displacement of particles in the body, it is necessary to define what strain is. *Strain* is the measure of deformation of a body under the influence of forces; it measures the relative movement between particles in the body. *Stress* at a point in the body $\mathcal{B}$ is a measure of the local force intensity and describes the action of neighbouring parts of $\mathcal{B}$ on that point. Stress can be *direct* or *shear*, depending on direction.

We consider two neighbouring particles occupying points $\boldsymbol{x}$ and $\boldsymbol{x} + \triangle\boldsymbol{x}$ before deformation and points $\boldsymbol{X}$ and $\boldsymbol{X} + \triangle\boldsymbol{X}$ in the deformed configuration, Masse (1970). Due to external force, particle at position $\boldsymbol{x}$ will move to a new position $\boldsymbol{X} = \boldsymbol{x} + \boldsymbol{u}$. Let the differential element of length between $\boldsymbol{X}$ and $\boldsymbol{X} + \triangle\boldsymbol{X}$ be dL

and the differential element between $\boldsymbol{x}$ and $\boldsymbol{x} + \triangle\boldsymbol{x}$ be dl. We use the difference $(dL)^2 - (dl)^2$ as a measure of deformation that occurs between the initial (or the undeformed) state and the final (or the deformed) state. Then we have,

$$(dL)^2 = d\boldsymbol{X}^T \cdot d\boldsymbol{X}. \tag{2.1.1}$$

We also have that

$$(dl)^2 = d\boldsymbol{x}^T \cdot d\boldsymbol{x}, \tag{2.1.2}$$

where $d\boldsymbol{X}$ is given by

$$d\boldsymbol{X} = \begin{bmatrix} dX_1 \\ dX_2 \\ dX_3 \end{bmatrix} = \begin{bmatrix} \frac{\partial X_1}{\partial x_1}dx_1 + \frac{\partial X_1}{\partial x_2}dx_2 + \frac{\partial X_1}{\partial x_3}dx_3 \\ \frac{\partial X_2}{\partial x_1}dx_1 + \frac{\partial X_2}{\partial x_2}dx_2 + \frac{\partial X_2}{\partial x_3}dx_3 \\ \frac{\partial X_3}{\partial x_1}dx_1 + \frac{\partial X_3}{\partial x_2}dx_2 + \frac{\partial X_3}{\partial x_3}dx_3 \end{bmatrix}$$

$$= \begin{bmatrix} \frac{\partial X_1}{\partial x_1} & \frac{\partial X_1}{\partial x_2} & \frac{\partial X_1}{\partial x_3} \\ \frac{\partial X_2}{\partial x_1} & \frac{\partial X_2}{\partial x_2} & \frac{\partial X_2}{\partial x_3} \\ \frac{\partial X_3}{\partial x_1} & \frac{\partial X_3}{\partial x_2} & \frac{\partial X_3}{\partial x_3} \end{bmatrix} \begin{bmatrix} dx_1 \\ dx_2 \\ dx_3 \end{bmatrix} := \boldsymbol{F}d\boldsymbol{x}, \quad \text{where} \quad \boldsymbol{F} = \begin{bmatrix} \frac{\partial X_1}{\partial x_1} & \frac{\partial X_1}{\partial x_2} & \frac{\partial X_1}{\partial x_3} \\ \frac{\partial X_2}{\partial x_1} & \frac{\partial X_2}{\partial x_2} & \frac{\partial X_2}{\partial x_3} \\ \frac{\partial X_3}{\partial x_1} & \frac{\partial X_3}{\partial x_2} & \frac{\partial X_3}{\partial x_3} \end{bmatrix}.$$

The matrix $\boldsymbol{F}$ is the deformation gradient. In terms of the displacement $\boldsymbol{u}$, it can be written as

$$\boldsymbol{F} = \begin{bmatrix} 1 + \frac{\partial u_1}{\partial x_1} & 0 + \frac{\partial u_1}{\partial x_2} & 0 + \frac{\partial u_1}{\partial x_3} \\ 0 + \frac{\partial u_2}{\partial x_1} & 1 + \frac{\partial u_2}{\partial x_2} & 0 + \frac{\partial u_2}{\partial x_3} \\ 0 + \frac{\partial u_3}{\partial x_1} & 0 + \frac{\partial u_3}{\partial x_2} & 1 + \frac{\partial u_3}{\partial x_3} \end{bmatrix} = \boldsymbol{I} + \nabla\boldsymbol{u},$$

where $\boldsymbol{I}$ is a 3×3 identity matrix and the gradient of displacement $\nabla \boldsymbol{u}$ is defined by

$$\nabla \boldsymbol{u} := \begin{bmatrix} \frac{\partial u_1}{\partial x_1} & \frac{\partial u_1}{\partial x_2} & \frac{\partial u_1}{\partial x_3} \\ \frac{\partial u_2}{\partial x_1} & \frac{\partial u_2}{\partial x_2} & \frac{\partial u_2}{\partial x_3} \\ \frac{\partial u_3}{\partial x_1} & \frac{\partial u_3}{\partial x_2} & \frac{\partial u_3}{\partial x_3} \end{bmatrix}.$$

Using (2.1.1), $(dL)^2$ can now be written as

$$(dL)^2 = d\boldsymbol{X}^T \cdot d\boldsymbol{X} = d\boldsymbol{x}^T \boldsymbol{F}^T \boldsymbol{F} d\boldsymbol{x}. \tag{2.1.3}$$

We can now express the difference $(dL)^2 - (dl)^2$ as

$$(dL)^2 - (dl)^2 = d\boldsymbol{x}^T [\boldsymbol{F}^T \boldsymbol{F} - \boldsymbol{I}] d\boldsymbol{x} = 2 d\boldsymbol{x}^T \boldsymbol{E} d\boldsymbol{x}, \tag{2.1.4}$$

where,

$$\boldsymbol{E} := \frac{1}{2}(\boldsymbol{F}^T \boldsymbol{F} - \boldsymbol{I}). \tag{2.1.5}$$

Substituting for $\boldsymbol{F}$ in the above gives,

$$\boldsymbol{E} = \frac{1}{2}\left[\nabla \boldsymbol{u} + (\nabla \boldsymbol{u})^T\right] + \frac{1}{2}\left[(\nabla \boldsymbol{u})^T \nabla \boldsymbol{u}\right]. \tag{2.1.6}$$

If we confine our study to the small deformation theory, then a sufficient requirement is that the components of the displacement gradients ought to be small compared to unity, Masse (1970). Thus, neglecting the second term in (2.1.6), since it is much smaller than the sum of the first two terms, we may express $\boldsymbol{E}$ as,

$$\boldsymbol{E} = \begin{bmatrix} \frac{\partial u_1}{\partial x_1} & \frac{1}{2}\left(\frac{\partial u_1}{\partial x_2} + \frac{\partial u_2}{\partial x_1}\right) & \frac{1}{2}\left(\frac{\partial u_1}{\partial x_3} + \frac{\partial u_3}{\partial x_1}\right) \\ \frac{1}{2}\left(\frac{\partial u_2}{\partial x_1} + \frac{\partial u_1}{\partial x_2}\right) & \frac{\partial u_2}{\partial x_2} & \frac{1}{2}\left(\frac{\partial u_2}{\partial x_3} + \frac{\partial u_3}{\partial x_2}\right) \\ \frac{1}{2}\left(\frac{\partial u_3}{\partial x_1} + \frac{\partial u_1}{\partial x_3}\right) & \frac{1}{2}\left(\frac{\partial u_3}{\partial x_2} + \frac{\partial u_2}{\partial x_3}\right) & \frac{\partial u_3}{\partial x_3} \end{bmatrix}.$$

The elements of this matrix are the strain components, which we denote by tensor notation ε_{ij}, and it is known as *infinitesimal strain tensor*. Thus, the strain tensor can be expressed as,

$$\varepsilon_{ij}(\boldsymbol{u}) := \frac{1}{2}\left(\frac{\partial u_i}{\partial x_j} + \frac{\partial u_j}{\partial x_i}\right), \qquad (2.1.7)$$

where $i, j \in \{1, 2, 3\}$ for three-dimensional cases. In this thesis, for computational modelling we confine ourself to the two-dimensional case. The expression (2.1.7) implies a linear relation between the strain ε and the gradient of displacement $\nabla \boldsymbol{u}$ and is used throughout the thesis. Recall that the nonlinear product term $(\nabla \boldsymbol{u})^T \nabla \boldsymbol{u}$ has been neglected due to assumptions on small strain deformation since it is much smaller than the linear term.

Linear elasticity. In elastic materials, for a fixed stress, the strain stays constant and upon removal of load it disappears immediately. In linear elasticity theory, the *constitutive relation* which relates $\boldsymbol{\sigma}$ and $\boldsymbol{\varepsilon}$ for an isotropic and compressible material is linear and is given by *Hooke's law*,

$$\sigma_{ij} = \lambda \nabla \cdot \boldsymbol{u} \delta_{ij} + 2\mu \varepsilon_{ij}(\boldsymbol{u}), \qquad (2.1.8)$$

where δ_{ij} above is the Kronecker delta. This can also be written in the form,

$$\sigma_{ij} = D_{ijkl} \varepsilon_{kl}, \qquad (2.1.9)$$

where $1 \leqslant i, j, k, l \leqslant n$. Stress is a symmetric tensor, that is $\sigma_{ij} = \sigma_{ji}$.

In matrix form, we can express strain as,

$$\boldsymbol{\varepsilon} = \begin{bmatrix} \varepsilon_{11} & \varepsilon_{12} & \varepsilon_{13} \\ \varepsilon_{21} & \varepsilon_{22} & \varepsilon_{23} \\ \varepsilon_{31} & \varepsilon_{32} & \varepsilon_{33} \end{bmatrix}.$$

For computational purposes, it is useful to arrange the strain components into an array. So for a three-dimensional case, this would be,

$$\boldsymbol{\varepsilon}(\boldsymbol{u}) := [\varepsilon_{11}, \varepsilon_{22}, \varepsilon_{33}, 2\varepsilon_{12}, 2\varepsilon_{13}, 2\varepsilon_{23}]^T = \begin{bmatrix} \frac{\partial u_1}{\partial x_1} \\ \frac{\partial u_2}{\partial x_2} \\ \frac{\partial u_3}{\partial x_3} \\ \frac{\partial u_1}{\partial x_2} + \frac{\partial u_2}{\partial x_1} \\ \frac{\partial u_1}{\partial x_3} + \frac{\partial u_3}{\partial x_1} \\ \frac{\partial u_2}{\partial x_3} + \frac{\partial u_3}{\partial x_2} \end{bmatrix}. \tag{2.1.10}$$

For a two-dimensional case, this will reduce to

$$\boldsymbol{\varepsilon}(\boldsymbol{u}) := [\varepsilon_{11}, \varepsilon_{22}, 2\varepsilon_{12}]^T = \begin{bmatrix} \frac{\partial u_1}{\partial x_1} \\ \frac{\partial u_2}{\partial x_2} \\ \frac{\partial u_1}{\partial x_2} + \frac{\partial u_2}{\partial x_1} \end{bmatrix}. \tag{2.1.11}$$

In vector-matrix notation, (2.1.9) can be written as,

$$\boldsymbol{\sigma} = \boldsymbol{D}\boldsymbol{\varepsilon}, \tag{2.1.12}$$

where $\boldsymbol{D}$ is a positive definite, fourth order tensor representing the elastic response of the material called the *constitutive matrix*, which in two dimensions is given by

$$\boldsymbol{D} = \begin{pmatrix} \lambda + 2\mu & \lambda & 0 \\ \lambda & \lambda + 2\mu & 0 \\ 0 & 0 & \mu \end{pmatrix}.$$

We shall adopt the vector-matrix notation (2.1.12) for our analysis in later chapters. The material constants λ and μ are the Lamé coefficients. They describe the volumetric and shear behaviour of the material and are given by

$$\lambda = \frac{E\nu}{(1+\nu)(1-2\nu)}, \quad \mu = \frac{E}{2(1+\nu)}, \tag{2.1.13}$$

where ν and E are Poisson ratio and Young's modulus, respectively. The Poisson ratio may be defined as the fraction of expansion divided by the fraction of compression, for small values of these changes. This is the Possion effect: when a material is compressed in one direction, it tends to expand in the other two perpendicular directions. Young's modulus is a measure of the stiffness of an elastic isotropic material.

2.2 Properties of viscoelastic materials

The theory of viscoelasticity is concerned with materials which exhibit strain rate effects in response to applied stresses, and *vice-versa*. This means that under constant stress a phenomenon of creep will occur, which is a slow continuous deformation of the material. On the other hand, under constant strain a phenomenon of stress relaxation will occur where stress gradually decreases. Viscoelastic materials exhibit both viscous and elastic characteristics when undergoing deformation. Other phenomena which are common to many viscoelastic materials are: instantaneous elasticity, instantaneous recovery and delayed recovery, (Findley et al., 1989, chap. 5). Common examples of viscoelastic materials in engineering science are the thermoplastic polymers. An important feature of a viscoelastic medium is that the stress at any given time at a point depends on the entire strain history from the moment that stress is applied for the first time. Because of this property viscoelastic materials are described as having *memory*, which mathematically suggests that stress can be expressed as a functional of strain, or *vice-versa*, in the form of *Volterra* equations. In general there are two alternative forms used to represent the stress-strain-time relations of viscoelastic materials. These are the differential operator method and the integral representation. Both methods are dealt with in Findley et al. (1989). The second method can be easily extended to describe the effect of temperature in the deformation of material. The hereditary form of stress-strain law (i.e the constitutive relation) for linear viscoelasticity is given by

$$\boldsymbol{\sigma}(t) = \boldsymbol{D}(0)\boldsymbol{\varepsilon}(t) - \int_0^t \boldsymbol{D}_s(t-s)\boldsymbol{\varepsilon}(s)ds. \tag{2.2.1}$$

This can be derived using the Boltzmann type of superposition, as shown in Shaw (1993). Taking the $\boldsymbol{x}$-dependence into account, we can write (2.2.1) in the following form,

$$\boldsymbol{\sigma}(\boldsymbol{u};\boldsymbol{x},t) = \boldsymbol{D}(\boldsymbol{x},0)\boldsymbol{\varepsilon}(\boldsymbol{u}(\boldsymbol{x},t)) - \int_0^t \boldsymbol{D}_s(\boldsymbol{x},t-s)\boldsymbol{\varepsilon}(\boldsymbol{u}(\boldsymbol{x},s))ds, \tag{2.2.2}$$

where the subscript s in the above equations denotes differentiation with respect to the history variable s itself. One can assume that the viscoelastic body under consideration is synchronous. We say that a viscoelastic material is synchronous if $\lambda(\boldsymbol{x},t) = \varphi(t)\lambda(\boldsymbol{x})$ and $\mu(\boldsymbol{x},t) = \varphi(t)\mu(\boldsymbol{x})$, meaning that $\lambda(\boldsymbol{x},t)$ and $\mu(\boldsymbol{x},t)$ are such that their time-dependence is the same. $\varphi(t)$ is called the relaxation function. Then, there exists a temporally constant matrix $\boldsymbol{D}(\boldsymbol{x},0)$ and the scalar function $\varphi(t-s)$ such that

$$\boldsymbol{D}(\boldsymbol{x},t-s) = \boldsymbol{D}(\boldsymbol{x},0)\varphi(t-s), \tag{2.2.3}$$

where $\boldsymbol{D}(\boldsymbol{x},0)$ is the same constant matrix that appears in linear elasticity.

Assumptions 2.2.1. *We make the following assumptions on the relaxation function:*

(i) Fading memory hypothesis:

$$\varphi(t) > 0 \quad \textit{and} \quad \varphi'(t) < 0, \qquad \forall t \in I,$$

(ii) Normalisation: $\varphi(0) = 1$.

Next we have the following corollary.

Corollary 2.2.1. *Using Assumptions 2.2.1, we deduce the following:*

(a) $0 < \varphi(t) \leqslant 1$, $\forall t \in (0,T]$, *which follows from (i) and (ii) above,*

(b) $\varphi_s(t-s) > 0$ *in* $\{0 \leqslant s \leqslant t \leqslant \infty\}$, *which follows from (i) above.*

In practice, there are some possible choices for $\varphi(t)$, but from the computational standpoint, a popular and convenient form is the Dirichlet series which is a sum of decaying exponentials. This choice comes from a generalisation of the spring and dashpots models, Golden and Graham (1988). The relaxation function is given by,

$$\varphi(t) = \varphi_0 + \sum_{p=1}^{N_\varphi} \varphi_p e^{-\alpha_p t}, \tag{2.2.4}$$

where $\varphi_0 > 0$ for solid and $\varphi_0 = 0$ for fluid, $\varphi_p \geqslant 0$, $\alpha_p > 0$, and $\sum_{p=0}^{N_\varphi} \varphi_p = 1$ for normalization, N_φ takes a positive integer value. The constitutive law (2.2.2) then becomes,

$$\boldsymbol{\sigma}(\boldsymbol{u}; \boldsymbol{x}, t) = \boldsymbol{D}(\boldsymbol{x}, 0)\boldsymbol{\varepsilon}(\boldsymbol{u}(\boldsymbol{x}, t)) - \int_0^t \boldsymbol{D}(\boldsymbol{x}, 0)\varphi_s(t-s)\boldsymbol{\varepsilon}(\boldsymbol{u}(\boldsymbol{x}, s))ds. \tag{2.2.5}$$

For clarity, in what follows we shall suppress the $\boldsymbol{x}$ dependence, and for the constitutive matrix above we shall just write $\boldsymbol{D}$.

Remark 1. *We note here that the $\boldsymbol{x}$ and t dependence of $\boldsymbol{D}$ is assumed generally. For this study, since we assume a homogeneous material, $\boldsymbol{D}$ is independent of $\boldsymbol{x}$ and t. This is due to that fact that λ and μ, which $\boldsymbol{D}$ depends on, are parameters which depend on material properties.*

2.3 Inclusion of temperature

The pioneer of the modern mathematical theory of heat conduction was Joseph Fourier. He was the first to consider the transfer of heat between a finite number of bodies arranged in a straight line, Hill and Dewynne (1987). For three dimensional heat flow he obtained the equation

$$\kappa \frac{\partial \theta}{\partial t} = Q \nabla^2 \theta,$$

where κ is the thermal diffusivity and Q is the thermal conductivity. $\theta = \theta(\boldsymbol{x}, t)$ is the temperature at position $\boldsymbol{x}$ and time t, ∇^2 is the Laplace operator. In deriving the heat equation, the knowledge that the rate of flow across an isothermal surface per unit area is proportional to the temperature gradient at the surface is crucial.

This may be expressed, using the *Fourier's law* of heat conduction, as

$$\boldsymbol{j} = -Q\nabla\theta,$$

where $\boldsymbol{j}$ denotes the heat flux vector. In general, heat flow is accompanied by temperature change. One can talk about "the heat in a body" as long as there is temperature difference between the body and its surroundings. Temperature and heat flow are two important quantities in problems of heat conduction. Temperature at any point in a body is completely defined by its numerical value since it is a scalar quantity, whereas heat flow is defined by its numerical value and direction since it is a vector quantity. For details on how to derive heat equation one can refer, for example, to Hill and Dewynne (1987) and Ozisik (1968).

Thermal expansion. One may wish to consider the effect of temperature on the behaviour of materials, in particular on viscoelastic solid materials. There is a tendency of matter to change in volume under the influence of an applied temperature field. The ratio of the degree of expansion to the change in temperature is known as the *coefficient of thermal expansion*, which we may denote with α. It describes how the size of a body changes with a change in temperature. For a one-dimensional case, this is given by

$$\frac{\triangle\mathcal{L}}{\mathcal{L}} = \alpha(\theta - \theta_r), \tag{2.3.1}$$

where θ_r is a reference temperature, at which nothing happens in terms of the volume of the body if no other external forces are applied. $\mathcal{L}$ is the (initial) length at θ_r and $\triangle\mathcal{L}$ is the change in length after the change of temperature. When the body is heated to some temperature θ, it expands. Hence the stress, in the case of linear elasticity, may be written as

$$\sigma = E\left(\varepsilon - \alpha(\theta - \theta_r)\right), \tag{2.3.2}$$

where E is the Young's modulus and ε is the strain in the x-direction. The term inside the brackets is subtracted because when the body expands due to heat there is no stress induced, and the amount subtracted is the strain which would have been induced anyway. We assume the expansion is volumetric. This argument is used in Morland and Lee (1960) and Fagan (1992).

Reduced time. In general, it is possible to consider the effect of temperature on the constitutive equations by assuming that the relaxation modulus $\boldsymbol{D}$ in the hereditary representation can be written as a function of temperature and time. This means that the right side of

$$\boldsymbol{D}(t-s) = \boldsymbol{D}\varphi(t-s), \tag{2.3.3}$$

coming from (2.2.3), becomes $\boldsymbol{D}\varphi(\theta, t-s)$, where θ is temperature, Findley et al. (1989). In (2.3.3) the matrix $\boldsymbol{D}$ is identical to the matrix $\boldsymbol{D}(\boldsymbol{x}, 0)$ in 2.2.3).

Theoretical and experimental results indicate that for this class of material the effect due to time and temperature can be embedded into a single variable using the following relation

$$\varphi(\theta, t) = \varphi(\theta_b, \rho), \tag{2.3.4}$$

where

$$\rho(\theta, t) = t/\psi(\theta), \tag{2.3.5}$$

where t is the real time of observation measured from first application of load, θ is the temperature, ψ is the temperature shift factor and ρ is the "reduced time", Findley et al. (1989). Relations (2.3.4) and (2.3.5) represent a translational shift of the relaxation modulus plotted against the logarithm of time at different uniform temperatures. The relaxation modulus at an arbitrary uniform temperature, θ, is thus expressed in terms of a base temperature, θ_b, and a new time scale which depends on the temperature θ. Materials exhibiting this property are classified as "thermorheologically simple" by Schwarzl and Staverman (1952). The equivalence relation (2.3.4) can be rewritten as

$$\varphi(\theta, \ln t) = \varphi(\theta_b, \ln t + f(\theta)), \tag{2.3.6}$$

where the relaxation function $\varphi(\theta, \ln t)$ is written as a function of $\ln t$ at a uniform temperature θ and $f(\theta)$ is measured relative to some arbitrary θ_b and is a positive increasing function for $\theta > \theta_b$. The above equivalence relations imply that the relaxation modulus curve will shift towards shorter times with increase of temperature. In Williams et al. (1955), Williams, Landel and Ferry propose the following analytical expression, which relates the shift factor ψ and temperature θ,

$$\log_{10} \psi(t) \equiv \frac{k_1(\theta - \theta_g)}{k_2 + \theta - \theta_g}, \tag{2.3.7}$$

where k_1 and k_2 are assumed to be universal constants with values -17.44 and 51.6, respectively. θ_g is the glass transition temperature and can take different values for different systems. This is the temperature at which a polymer solid changes to liquid. In Findley et al. (1989), a loglog plot of relaxation modulus is shown at different temperature levels. The curve at 70°F is fixed. If all other curves are shifted parallel to the time axis, eventually they will lie along a single line known as the *master curve*. We shall later refer to (2.3.7) also as the "WLF formula".

For the case where a general temperature field $\theta(\boldsymbol{x}, t)$ is considered where each particle has a temperature varying with time, Morland and Lee (1960) propose the following reduced time

$$\rho(\theta, t) = \int_0^t \frac{d\xi}{\psi(\theta(\xi))}. \tag{2.3.8}$$

In what follows, for clarity, we shall write $\rho(t)$ rather then $\rho(\theta, t)$. In the next section, we shall define the model for study in this thesis.

2.4 Model problem

The proposed model problem is as follows. Consider the deformation of a non-ageing solid linear viscoelastic compressible isotropic body, the interior of which occupies the region $\Omega \subset \mathbb{R}^n$, where $n \in \{1, 2, 3\}$, with convex polygonal boundary $\partial\Omega$. We assume that the acceleration is negligible, that is, the inertia term $\ddot{u}_i = \frac{\partial^2 u_i}{\partial t^2}$ is not included. This, from Newtons law of motion, yields the quasistatic force balance given by

$$-\sigma_{ij,j} = f_i(\boldsymbol{x}, t), \qquad \boldsymbol{x} \in \Omega,$$

$$u_i(\boldsymbol{x}, t) = 0, \quad \boldsymbol{x} \in \Gamma_{D_1}, \qquad \sigma_{ij}\widehat{\boldsymbol{n}}_j = g_i(\boldsymbol{x}, t), \quad \boldsymbol{x} \in \Gamma_{N_1}, \tag{2.4.1}$$

where $i, j = 1, \dots, n$ and $,j$ denotes partial derivative of σ_{ij} with respect to the variable x_j with repeated indices implying summation convention. We assume that the above deformation is under the action of a body force $\boldsymbol{f} := (f_i(\boldsymbol{x}, t))_{i=1}^n$ and a surface traction $\boldsymbol{g} := (g_i(\boldsymbol{x}, t))_{i=1}^n$ and is considered for every time $t \in I := [0, T]$, for some real positive number $T > 0$. The *Neumann* boundary Γ_{N_1} and the *Dirichlet* boundary Γ_{D_1} form a disjoint and time independent partition of the boundary $\partial\Omega$, see Fig. 2.1. We denote by $\boldsymbol{u} := (u_i)_{i=1}^n$ the resulting displacement at a point $\boldsymbol{x} := (x_i)_{i=1}^n \subset \overline{\Omega} := \Omega \cup \partial\Omega$. Here σ_{ij} and ε_{ij} denote the components of the symmetric stress and strain tensors, respectively, where $1 \leqslant i, j \leqslant n$; $\widehat{\boldsymbol{n}} := (\widehat{n}_i)_{i=1}^n$ is the unit outward normal vector to Γ_{N_1}. Only small strains are considered, thus confining ourselves to the linear theory of deformation. For the purposes of computation the components of stress are arranged into an array. Thus, for example, for $n = 3$,

$$\boldsymbol{\sigma} = (\sigma_{11}, \sigma_{22}, \sigma_{33}, \sigma_{12}, \sigma_{13}, \sigma_{23})^T, \tag{2.4.2}$$

whereas for $n = 2$,

$$\boldsymbol{\sigma} = (\sigma_{11}, \sigma_{22}, \sigma_{12})^T, \tag{2.4.3}$$

The strain tensor is given by (2.1.7), whereas for computational purposes (2.1.11) and (2.1.10) are used. For the sake of clarity, the $\boldsymbol{x}$ dependence for the terms in (2.4.1) will be suppressed. The meaning of $-\sigma_{ij,j} = f_i$ in 2.4.1 can be explained as follows. In our notation, for a 2-dim problem, where $i, j = 1, 2$, we have $x_1 = x$ and $x_2 = y$. Thus, for example, $f_1 = -\dfrac{\partial \sigma_{11}}{\partial x} - \dfrac{\partial \sigma_{12}}{\partial y}$ and $f_2 = -\dfrac{\partial \sigma_{21}}{\partial x} - \dfrac{\partial \sigma_{22}}{\partial y}$. The values of σ_{ij} will be derived using the stress-strain laws.

If we were to include the inertia term in our model problem, then this would appear on the left side of (2.4.1) and the additional initial conditions would be: $u_i(\boldsymbol{x}, 0) = u_i^0(\boldsymbol{x})$ and $\dot{u}_i(\boldsymbol{x}, 0) = u_i^1(\boldsymbol{x})$, $\boldsymbol{x} \in \Omega$.

Remark 2. *We note here that in this study we do not consider a specific viscoelastic material, however we assume that the material is a solid.*

In addition to the body forces and tractions, we are also interested to consider the effects of temperature on the deformation of the above physical body. Thus, assume that for every $t \in I$, a temperature field is applied externally to the body under consideration, where the temperature comes from the solution of the heat conduction problem, given by

$$\begin{aligned} \kappa\dot{\theta}(\boldsymbol{x}, t) - Q\nabla^2\theta(\boldsymbol{x}, t) &= l(\boldsymbol{x}, t), & \boldsymbol{x} \in \Omega, \\ \nabla\theta(\boldsymbol{x}, t) \cdot \hat{n} &= q(\boldsymbol{x}, t), & \boldsymbol{x} \in \Gamma_{N_2}, \\ \theta(\boldsymbol{x}, t) &= 0, & \boldsymbol{x} \in \Gamma_{D_2}. \end{aligned} \tag{2.4.4}$$

Here $\theta(\boldsymbol{x}, t)$ is the temperature at $\boldsymbol{x} \in \Omega$ at time $t \in I = (0, T]$, $l(\boldsymbol{x}, t)$ is a given (external) heat source, $q(\boldsymbol{x}, t)$ is the temperature gradient. Also, $\dot{\theta}(\boldsymbol{x}, t) = \dfrac{\partial \theta(\boldsymbol{x}, t)}{\partial t}$,

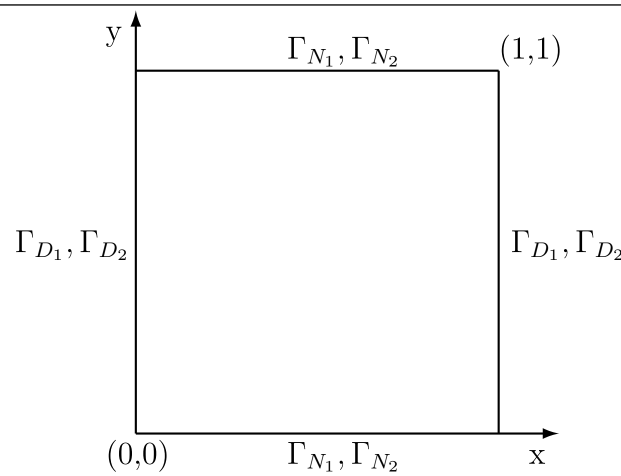

Figure 2.1: 2D domain for the displacement and heat problem.

$\hat{n}$ is the unit outward normal vector to Γ_{N_2}, the Neumann boundary. Γ_{D_2} denotes the Dirichlet boundary, see Fig. 2.1. κ and Q are constants. We denote by $\theta^0=\theta(\boldsymbol{x},0)$ a given initial temperature. For the sake of clarity, the $\boldsymbol{x}$ dependence of the terms in (2.4.4) will be suppressed. We assume that the viscoelastic body under consideration expands in a volumetric manner. Then, we suggest we use the same reasoning in our model problem that was used in the elasticity case (2.3.2) in the previous section. We modify the strain inside and outside the time integral in the stress-strain law for viscoelasticity, given by (2.2.1). With the inclusion of temperature effects, this law now takes the following form,

$$\boldsymbol{\sigma}(t) = \boldsymbol{D}\big[\boldsymbol{\varepsilon}(\boldsymbol{u}(t)) - \alpha(\theta(t)-\theta_r)\boldsymbol{I_0}\big] - \int_0^t \boldsymbol{D}_s(t-s)\big[\boldsymbol{\varepsilon}(\boldsymbol{u}(s)) - \alpha(\theta(s)-\theta_r)\boldsymbol{I_0}\big]\,ds. \tag{2.4.5}$$

Here $\boldsymbol{I_0} = [1 \quad 1 \quad 0]$. The effect of $\boldsymbol{I_0}$ is such that the amount of strain subtracted, $\alpha(\theta(s)-\theta_r)\boldsymbol{I_0}$, has zero shear strain. Thus, we can write

$$\boldsymbol{\varepsilon}(\boldsymbol{u}(t)) - \alpha(\theta(t)-\theta_r)\boldsymbol{I_0} = \begin{bmatrix} \varepsilon_{11} \\ \varepsilon_{22} \\ 2\varepsilon_{12} \end{bmatrix} - \begin{bmatrix} \alpha(\theta(t)-\theta_r) \\ \alpha(\theta(t)-\theta_r) \\ 0 \end{bmatrix}.$$

The presence of temperature, $\theta(t)$, in the stress-strain law (2.4.5), implies that we now have a coupled problem, via (2.4.5), between the quasistatic force balance equation (2.4.1) and the heat conduction problem (2.4.4).

Introducing the nonlinearity. With the inclusion of the reduced time, now the viscoelasticity consitutive equation (2.2.1) takes the form,

$$\boldsymbol{\sigma}(t) = \boldsymbol{D}\boldsymbol{\varepsilon}(\boldsymbol{u}(t)) - \int_0^t \boldsymbol{D}_s(\rho(t) - \rho(s))\boldsymbol{\varepsilon}(\boldsymbol{u}(s))ds, \qquad (2.4.6)$$

where now the integral kernel has a nonlinear time argument due to the presence of the reduced time which in turn depends on temperature via a logarithmic function, as shown in the WLF formula (2.3.7). If we now consider the thermal expansion of such materials, the stress-strain law becomes,

$$\begin{aligned}\boldsymbol{\sigma}(t) = \boldsymbol{D}\big[\boldsymbol{\varepsilon}(\boldsymbol{u}(t)) - \alpha(\theta(t) - \theta_r)\boldsymbol{I_0}\big] \\ - \int_0^t \boldsymbol{D}_s(\rho(t) - \rho(s))\big[\boldsymbol{\varepsilon}(\boldsymbol{u}(s)) - \alpha(\theta(s) - \theta_r)\boldsymbol{I_0}\big]ds. \qquad (2.4.7)\end{aligned}$$

The fact that we now have two different constitutive laws, (2.4.5) and (2.4.7), it is obvious that consequently we shall have two different problems to consider. We shall refer to the problem arising from the thermal expansion via (2.4.5) as the *linear problem*. Whereas, the problem arising from the reduced time via (2.4.7) will be referred to as the *nonlinear problem*.

It is of crucial importance to state here that both problems represent a novel study, and that we are not aware up to now that these have been studied elsewhere in literature, particularly deriving stability and error estimates and numerical results. The study on viscoelasticity at constant temperature has been advanced in terms of deriving stability and error estimates as well as numerical results, for example, Shaw et al. (1994), Shaw et al. (1997), Shaw and Whiteman (1998). The analysis on the heat problem is not new in this study, however we present a more detailed analysis that can hardly be found in literature, especially the work on error estimate. Work on heat problems can be found, for example, in Johnson (2009) and Thomée (2006).

Weak formulations for displacement

The first step in deriving fully-discrete formulations is to obtain the so-called weak formulations of the problems. We start by deriving the weak formulation for the equilibrium equation (2.4.1). We define a test space V as:

$$V := \left\{ \boldsymbol{v} \in \left(H^1(\Omega)\right)^n : \boldsymbol{v} = 0 \text{ on } \Gamma_{D_1} \right\}. \tag{2.4.8}$$

Let $(V, (\cdot,\cdot)_V)$ be a Hilbert space with its dual $(V', (\cdot,\cdot)_{V'})$. We assume that $\boldsymbol{f} \in (C(\Omega))^n$ and $\boldsymbol{g} \in (C(\Gamma_{N_1}))^n$ for each t. Also, let $w \in H^1(\Omega)$. In order to derive the weak formulation, we need the following Green's theorem from (Johnson, 2009, chap. 1),

$$\int_\Omega v_i \frac{\partial w}{\partial x_i}\, d\Omega + \int_\Omega w \frac{\partial v_i}{\partial x_i}\, d\Omega = \int_{\partial\Omega} w v_i \hat{n}_i \, d\Gamma, \qquad \text{for} \quad i = 1, \ldots, n \tag{2.4.9}$$

where $\hat{\boldsymbol{n}} = (\hat{n}_1, \ldots, \hat{n}_n)$ is the unit outward normal to $\partial\Omega$. Using the force balance equation (2.4.1), the next step in deriving the weak formulation is to take the scalar product of this equation with a test function $\boldsymbol{v} \in V$ and then to integrate over the domain Ω. This gives,

$$-\int_\Omega \sigma_{ij,j} v_i \, d\Omega = \int_\Omega f_i v_i \, d\Omega \qquad \forall \boldsymbol{v} \in V. \tag{2.4.10}$$

Integrating by parts the left-hand side of (2.4.10) using the Green's formula gives,

$$-\int_\Omega \sigma_{ij,j} v_i \, d\Omega = \int_\Omega \sigma_{ij} v_{i,j} \, d\Omega - \int_{\Gamma_{N_1}} \sigma_{ij} \hat{n}_j v_i \, d\Gamma, \tag{2.4.11}$$

where the summation convention is applied to all terms: summing over the repeated indices. Using the fact that $\sigma_{ij} = \sigma_{ji}$ and the definition of ε_{ij} given by (2.1.7), we have,

$$\sigma_{ij}\varepsilon_{ij}(v) = \frac{1}{2}\left(\sigma_{ij}v_{i,j} + \sigma_{ji}v_{j,i}\right) = \frac{1}{2}\left(\sigma_{ij}v_{i,j} + \sigma_{ij}v_{i,j}\right) = \sigma_{ij}v_{i,j}. \tag{2.4.12}$$

Note the interchange of indices above. Using the above and the traction boundary condition in (2.4.1), we arrive at the weak formulation for the equilibrium equation:

$$\int_{\Omega} \sigma_{ij}\varepsilon_{ij}(\boldsymbol{v})\, d\Omega = \int_{\Omega} f_i v_i \, d\Omega + \int_{\Gamma_{N_1}} g_i v_i \, d\Gamma. \tag{2.4.13}$$

This is rather general, as we have not used a constitutive relationship to derive it. However, this will be very useful when we begin to derive the weak formulation for viscoelasticity later in this chapter. Next, using Hooke's law (2.1.8), we can eliminate σ_{ij} to get,

$$\int_{\Omega} \lambda \nabla \cdot \boldsymbol{u} \nabla \cdot \boldsymbol{v} + \mu \varepsilon_{ij}(\boldsymbol{u})\varepsilon_{ij}(\boldsymbol{v})\, d\Omega = \int_{\Omega} f_i v_i \, d\Omega + \int_{\Gamma_{N_1}} g_i v_i \, d\Gamma. \tag{2.4.14}$$

We have thus arrived at the following weak formulation of the elasticity problem: find $\boldsymbol{u} \in V$, such that

$$a(\boldsymbol{u}, \boldsymbol{v}) = L(\boldsymbol{v}) \qquad \forall \boldsymbol{v} \in V, \tag{2.4.15}$$

where

$$a(\boldsymbol{u}, \boldsymbol{v}) = \int_{\Omega} \lambda \nabla \cdot \boldsymbol{u} \nabla \cdot \boldsymbol{v} + \mu \varepsilon_{ij}(\boldsymbol{u})\varepsilon_{ij}(\boldsymbol{v}) d\Omega \tag{2.4.16}$$

$$L(\boldsymbol{v}) = \int_{\Omega} f_i v_i \, d\Omega + \int_{\Gamma_{N_1}} g_i v_i \, d\Gamma, \tag{2.4.17}$$

where $a(\cdot,\cdot)$ is a symmetric bilinear form and $L(\cdot)$ is a linear functional. Note that (2.4.13) can also be written as

$$(\boldsymbol{\sigma}, \boldsymbol{\varepsilon}(\boldsymbol{v}))_\Omega = (\boldsymbol{f}, \boldsymbol{v})_\Omega + (\boldsymbol{g}, \boldsymbol{v})_{\Gamma_{N_1}}, \qquad \forall \boldsymbol{v} \in V. \tag{2.4.18}$$

Note that here $\boldsymbol{f}$ and $\boldsymbol{g}$ refer to their own values at $t = 0$, since at $t = 0$ viscoelasticity reduces to an elasticity problem. Using (2.4.18) we can derive the weak formulation for linear viscoelasticity. Hence, substituting (2.2.5) in (2.4.18) and using the fact that $\boldsymbol{D}_s(t-s) = \boldsymbol{D}\varphi_s(t-s)$, we arrive at: find $\boldsymbol{u} \in C(0,T;V)$, such that

$$\begin{aligned}(\boldsymbol{D}\boldsymbol{\varepsilon}(\boldsymbol{u}(t)), \boldsymbol{\varepsilon}(\boldsymbol{v}))_\Omega = (\boldsymbol{f}(t), \boldsymbol{v})_\Omega + (\boldsymbol{g}(t), \boldsymbol{v})_{\Gamma_{N_1}} \\ + \int_0^t \varphi_s(t-s)\,(\boldsymbol{D}\boldsymbol{\varepsilon}(\boldsymbol{u}(s)), \boldsymbol{\varepsilon}(\boldsymbol{v}))_\Omega\, ds, \quad \forall \boldsymbol{v} \in V.\end{aligned} \tag{2.4.19}$$

Note that now the linear form $L(t;\boldsymbol{v}) = (\boldsymbol{f}(t), \boldsymbol{v})_\Omega + (\boldsymbol{g}(t), \boldsymbol{v})_{\Gamma_{N_1}}$ is time dependent since we are now dealing with the viscoelasticity problem. A more useful way of stating the weak formulation would be to use the (time independent) bilinear form $a(\cdot,\cdot)$ instead, and write: find $\boldsymbol{u} \in C(0,T;V)$ such that

$$a(\boldsymbol{u}(t), \boldsymbol{v}) = L(t;\boldsymbol{v}) + \int_0^t \varphi_s(t-s) a(\boldsymbol{u}(s), \boldsymbol{v}) ds, \qquad \forall \boldsymbol{v} \in V. \tag{2.4.20}$$

Next, we derive the weak formulation for the linear problem. Substituting the stress-strain law (2.4.5) above in (2.4.18) and using the fact that $\boldsymbol{D}_s(t-s) = \boldsymbol{D}\varphi_s(t-s)$ together with the linearity, we arrive at the weak formulation for the linear problem:

find $\boldsymbol{u} \in C(0,T;V)$ such that

$$\begin{aligned}
a\big(\boldsymbol{u}(t),\boldsymbol{v}\big) - \int_0^t \Big(\boldsymbol{D}\varphi_s(t-s)\boldsymbol{\varepsilon}(\boldsymbol{u}(s)),\boldsymbol{\varepsilon}(\boldsymbol{v})\Big)_\Omega ds \\
= L(t;\boldsymbol{v}) + \Big(\alpha\boldsymbol{D}(\theta(t)-\theta_r)\boldsymbol{I_0},\boldsymbol{\varepsilon}(\boldsymbol{v})\Big)_\Omega \\
- \int_0^t \Big(\alpha\boldsymbol{D}\varphi_s(t-s)(\theta(s)-\theta_r)\boldsymbol{I_0}),\boldsymbol{\varepsilon}(\boldsymbol{v})\Big)_\Omega ds, \quad \forall \boldsymbol{v} \in V.
\end{aligned} \tag{2.4.21}$$

Finally, substituting the stress-strain law (2.4.7) in (2.4.18), using the linearity property and the fact that $\boldsymbol{D}_s(\rho(t)-\rho(s)) = \boldsymbol{D}\varphi_s(\rho(t)-\rho(s))$, we arrive at the weak formulation for the nonlinear problem: find $\boldsymbol{u} \in C(0,T;V)$, such that

$$\begin{aligned}
a(\boldsymbol{u}(t),\boldsymbol{v}) - \int_0^t \Big(\boldsymbol{D}\varphi_s(\rho(t)-\rho(s))\boldsymbol{\varepsilon}(\boldsymbol{u}(s)),\boldsymbol{\varepsilon}(\boldsymbol{v})\Big)_\Omega ds \\
= L(t;\boldsymbol{v}) + \Big(\alpha\boldsymbol{D}(\theta(t)-\theta_r)\boldsymbol{I_0},\boldsymbol{\varepsilon}(\boldsymbol{v})\Big)_\Omega \\
- \int_0^t \Big(\alpha\boldsymbol{D}\varphi_s(\rho(t)-\rho(s))(\theta(s)-\theta_r)\boldsymbol{I_0},\boldsymbol{\varepsilon}(\boldsymbol{v})\Big)_\Omega ds, \quad \forall \boldsymbol{v} \in V.
\end{aligned} \tag{2.4.22}$$

We note here that for the existence of a solution to (2.4.21) and (2.4.22) we assume $\boldsymbol{u} \in C(0,T;V)$, whereas for the forthcoming a *priori* error analysis we require higher regularity, $\boldsymbol{u} \in C^2(0,T;V)$.

Weak formulation for the heat equation

Note that this is needed due to the presence of temperature θ in the coupled problems above, linear and nonlinear. We let $\mathcal{V} \subset H^1(\Omega)$ be a test space given by

$$\mathcal{V} := \left\{ v \in H^1(\Omega) : v = 0 \text{ on } \Gamma_{D_2} \right\}, \tag{2.4.23}$$

where $v \in \mathcal{V}$ is a test function. Let $(\mathcal{V},(\cdot,\cdot)_{\mathcal{V}})$ be a Hilbert space with its dual $(\mathcal{V}',(\cdot,\cdot)_{\mathcal{V}'})$. We multiply (2.4.4) by the test function v and integrate by parts using the First Green Formula. This gives the *weak formulation* of (2.4.4) as: find $\theta \in \mathcal{V}$, such that

$$\int_\Omega \kappa\dot{\theta} v \, d\Omega + \int_\Omega Q\nabla\theta \cdot \nabla v \, d\Omega - \int_{\Gamma_{N_2}} \nabla\theta \cdot \hat{n} v \, d\Gamma$$
$$= \int_\Omega lv d\Omega, \quad \forall v \in \mathcal{V}, \ t \in I(0,T]. \tag{2.4.24}$$

Alternatively, this can be written as:

$$\begin{aligned}(\kappa\dot{\theta}, v)_\Omega + a_H\left(\theta(t), v\right) &= \left(l(t), v\right)_\Omega + \left(q(t), v\right)_{\Gamma_{N_2}}, \qquad \forall v \in \mathcal{V}, \ \ t \in I = (0,T], \\ (\theta(0), v)_\Omega &= (\theta^0, v)_\Omega, \end{aligned} \tag{2.4.25}$$

where $a_H\left(\theta, v\right) = \int_\Omega Q\nabla\theta \cdot \nabla v d\Omega$ is a symmetric bilinear form. We also define the linear functional $\langle G(t), v\rangle := \left(l(t), v\right)_\Omega + \left(q(t), v\right)_{\Gamma_{N_2}}$.

Before we embark on analysis, we show the uniqueness of the solution to (2.4.21). We assume that there are two solutions $\boldsymbol{u}_1$ and $\boldsymbol{u}_2$, satisfying (2.4.21). Then, subtracting one from the other gives,

$$a(\boldsymbol{u}_1(t) - \boldsymbol{u}_2(t), \boldsymbol{v}) = \int_0^t \Big(\boldsymbol{D}\varphi_s(t-s)\boldsymbol{\varepsilon}(\boldsymbol{u}_1(s) - \boldsymbol{u}_2(s)), \boldsymbol{\varepsilon}(\boldsymbol{v})\Big)_\Omega. \tag{2.4.26}$$

Now, using the definition of the energy norm $\|\cdot\|_E$ given in Assumptions 2.4.1 (iii), and putting $\boldsymbol{v} = \boldsymbol{u}_1(t) - \boldsymbol{u}_2(t)$, gives

$$\|\boldsymbol{u}_1(t) - \boldsymbol{u}_2(t)\|_E^2 \leqslant \int_0^t \varphi_s(t-s)\|\boldsymbol{u}_1(s) - \boldsymbol{u}_2(s)\|_E ds \|\boldsymbol{u}_1(t) - \boldsymbol{u}_2(t)\|_E.$$

$$\text{Then,} \quad \|\boldsymbol{u}_1(t) - \boldsymbol{u}_2(t)\|_E \leqslant \int_0^t \varphi_s(t-s)\|\boldsymbol{u}_1(s) - \boldsymbol{u}_2(s)\|_E ds \tag{2.4.27}$$

Using Gronwall's lemma 1.4.3, gives $\|\boldsymbol{u}_1(t) - \boldsymbol{u}_2(t)\|_E \leqslant 0$, which implies that $\|\boldsymbol{u}_1(t) - \boldsymbol{u}_2(t)\|_E = 0$, hence $\boldsymbol{u}_1(t) = \boldsymbol{u}_2(t)$.

Next we prove the continuity of $L(t,\cdot)$. Thus we have,

$$
\begin{aligned}
|L(\boldsymbol{v})| &\leqslant \|\boldsymbol{f}\|_{L_2(\Omega)}\|\boldsymbol{v}\|_{L_2(\Omega)} + \|\boldsymbol{g}\|_{L_2(\Gamma)}\|\boldsymbol{v}\|_{L_2(\Gamma)} \\
&= c_1\|\boldsymbol{v}\|_{L_2(\Omega)} + c_2\|\boldsymbol{v}\|_{L_2(\Gamma)} \\
&\leqslant c_1\|\boldsymbol{v}\|_{H^1(\Omega)} + c_2\|\boldsymbol{v}\|_{H^1(\Omega)} \quad \text{using Trace theorem,} \\
&\leqslant c\|\boldsymbol{v}\|_{H^1(\Omega)}, \quad \text{c=max}\{c_1, c_2\}.
\end{aligned} \tag{2.4.28}
$$

For the Trace theorem see Reddy (1998). Exactly in the same way the continuity of $\langle G(t), v\rangle$ can be shown. With respect to the shift factor ψ, for analysis purposes, we are interested in the behaviour of $1/\psi$ for large values of θ, more precisely, in the limit of $1/\psi$ as θ tends to infinity. This is because, $\rho' = 1/\psi$, coming from (2.3.8), appears in the forthcoming analysis. This limit is,

$$
\lim_{\theta\to\infty} \frac{-17.44(\theta-\theta_g)}{51.6+(\theta-\theta_g)} = -17.44, \quad \Longrightarrow \quad \frac{1}{\psi} = 10^{17.44}. \tag{2.4.29}
$$

In order to facilitate the forthcoming analysis, we make the following assumptions.

Assumptions 2.4.1. *(i) The data* $\boldsymbol{g}$ *and* $\boldsymbol{f}$ *are such that there exists solution* $\boldsymbol{u} \in C(I;V)$ *solving (2.4.21). We also assume that the same solution* $\boldsymbol{u} \in C(I;V)$ *exists and is unique, solving (2.4.22).*

(ii) The data l *and* q *are such that there exists solution* $\theta \in C(I;\mathcal{V})$*, which is unique, solving the heat conduction problem (2.4.4).*

(iii) The symmetric bilinear form $a(\cdot,\cdot)$ *is continuous and coercive and we define an energy norm by* $\|\boldsymbol{v}\|_E = \sqrt{a(\boldsymbol{v},\boldsymbol{v})}$*. Also assume that* $a_H(\cdot,\cdot)$ *for the heat problem is continuous and coercive and define an energy norm by* $\|v\|_{\mathcal{A}} = \sqrt{a_H(v,v)}$*.*

(iv) With regards to the nonlinear problem (2.4.22), we assume the temperature θ

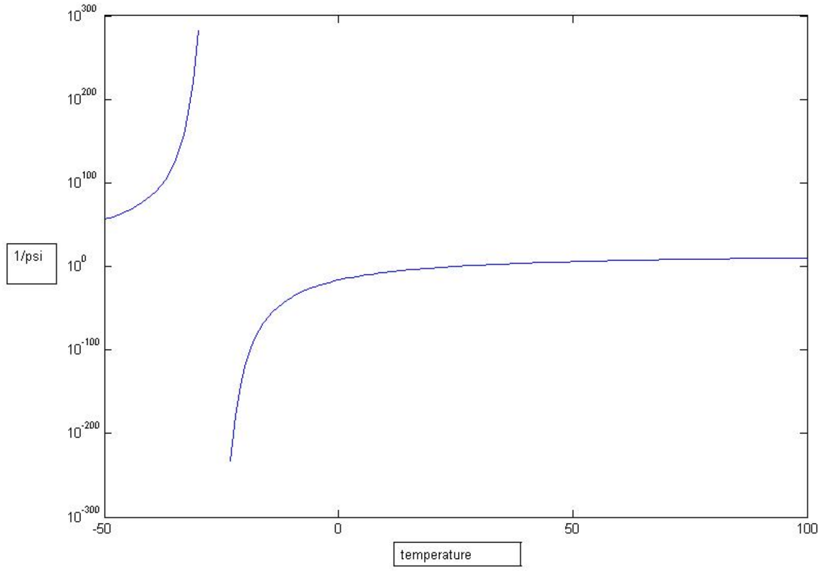

Figure 2.2: $1/\psi$ versus temperature θ. $\theta_g = 25$

to be in the range $\theta > \theta_g - 51.6$. This is due to the fact that at $\theta = \theta_g - 51.6$ there is an asymptote, as shown in Fig. 2.2. In this range, $\rho'(s) = \dfrac{1}{\psi(\theta)}$ has a bound, that is, $\|\rho'\|_{L_\infty([0,T]\times\Omega)} \leqslant C_\rho$, see (2.4.29) and (2.3.7). We also assume here that ψ, ψ' ψ'' exist and are finite.

It is worth mentioning here that for both, displacement and temperature, throughout the thesis, the boundary conditions are as depicted in Fig. 2.1.
The next step towards derivation of fully-discrete schemes corresponding to the weak formulations given in this section is the finite element approximation, also known as discretization in space. This topic is part of the next chapter, where we also derive fully-discrete schemes.

2.5 Summary

In this chapter the concept of continuum mechanics was discussed. Definitions of stress, strain and displacement were introduced, together with some physical derivations. Also a brief discussion on elasticity and linear viscoelasticity was presented. We then introduced the physical concepts of thermal expansion and reduced time. Finally, the model problem for this thesis was introduced together with new forms of stress-strain laws and weak formulations for viscoelasticity and the problems under study.

Chapter 3

Discrete Schemes for Displacement and Heat

In this chapter we show how the finite element method is used to discretize in space, and for time-dependent problems we also discretize in time in order to derive fully-discrete schemes. The first step in the construction of a finite element method (FEM) for a boundary value problem is to convert the problem into a *weak formulation*. This was mainly dealt with in Section 2.4. In order to illustrate the use of FEM in finding an approximate solution to a given problem, we shall apply it to the elasticity and heat conduction problem.

3.1 FEM for elasticity

For the *finite element approximation* we consider a finite dimensional subspace $V^h \subset V$ consisting of piecewise linear functions, where each $\boldsymbol{v} \in V$ can be written as a linear combination of the basis functions ϕ_{k_Ω}, $k_\Omega = 1, \ldots, nM$, and where M is just the number of nodes in the discretized domain of the problem under consideration and n is the dimension of the displacement vector. For computational purposes in this thesis we take $n = 2$. We consider a *triangulation* $\mathcal{T} = \{E_{\hat{\alpha}} : \hat{\alpha} = 1, \ldots, m_{\Omega}\}$ of Ω into non-overlapping closed triangular elements $E_{\hat{\alpha}}$, such that no vertex of one triangle lies on the edge of another triangle, where m_{Ω} is the number of elements in the mesh. Also each edge $e \subset \Gamma$ of an element $E \in \mathcal{T}$ belongs either to $\bar{\Gamma}_{N_1}$ or to $\bar{\Gamma}_{D_1}$, and Γ_{D_1} has a positive measure. We also assume that each triangular element $E_{\hat{\alpha}}$ has diameter $h_{\hat{\alpha}}$, and then set

$$h := \max_{1 \leqslant \hat{\alpha} \leqslant \Omega_m} h_{\hat{\alpha}}. \tag{3.1.1}$$

The finite element approximation to (2.4.15) is defined as: find $\boldsymbol{u}^h \in V^h \subset V$, such that

$$a(\boldsymbol{u}^h, \boldsymbol{v}) = L(\boldsymbol{v}) \quad \forall \boldsymbol{v} \in V^h. \tag{3.1.2}$$

In matrix form this can be written as

$$\boldsymbol{A}\boldsymbol{U} = \boldsymbol{L},$$

where $\boldsymbol{A} \in \mathbb{R}^{nM \times nM}$ is the global stiffness matrix and is given by

$$\boldsymbol{A}_{k_\Omega m} = \sum_{E \in \mathcal{T}} \int_E \boldsymbol{\varepsilon}^T(\phi_{k_\Omega}) \cdot \boldsymbol{D}\boldsymbol{\varepsilon}(\phi_m) dE, \qquad k_\Omega, m = 1, ..., nM,$$

where $\varepsilon(\phi_{k_\Omega})$ is a 3×6 matrix containing the derivatives of the basis functions. The load vector $\boldsymbol{L}$ is given by,

$$\boldsymbol{L}_{k_\Omega} = \sum_{E \in \mathcal{T}} \int_E \boldsymbol{f} \phi_{k_\Omega} dE + \sum_{e \subset \Gamma_{N_1}} \int_e \boldsymbol{g} \phi_{k_\Omega} de, \qquad k_\Omega = 1, ..., nM.$$

Note that, above, $e = \mathcal{T} \cap \Gamma_{N_1}$ for each $\mathcal{T}$, such that $\mathcal{T} \cap \Gamma_{N_1} \neq \emptyset$.

3.2 Discrete schemes for viscoelasticity

Having derived the weak formulation in Section 2.4, we are now able to give a fully-discrete scheme for the linear viscoelasticity problem. We initially derive the discretization in space followed by the discretization in time. This then leads to the full discretization of the problem.

3.2.1 Discretization in space and time

For the finite element approximation, we again consider the subspace $V^h \subset V$. Thus, we have: find $\boldsymbol{u}^h \in C(0, T; V^h)$ such that,

$$a(\boldsymbol{u}^h(t), \boldsymbol{v}) = L(t; \boldsymbol{v}) + \int_0^t \varphi_s(t-s) a(\boldsymbol{u}^h(s), \boldsymbol{v}) ds, \qquad \forall \boldsymbol{v} \in V^h. \tag{3.2.1}$$

This is also known as the *semi-discrete* formulation.

To provide fully discrete approximations to the weak formulation (2.4.20), we use the trapezoidal rule for numerical integration to discretize in time. We assume a constant time step $k := t_i - t_{i-1}$, $t_i = ki$, $i = 1, \ldots, N$, where $k = T/N$. The time domain I is discretized into

$$I^k := \{0 = t_0 < t_1 < \ldots < t_N = T\}. \tag{3.2.2}$$

The trapezoidal rule is given by

$$\int_0^{t_i} m(s)ds \approx \sum_{j=1}^{i} \frac{k}{2}\left(m(t_j) + m(t_{j-1})\right), \tag{3.2.3}$$

see, for example, Scott (2011). Replacing the integral in (3.2.1) by the trapezoidal approximation, we arrive at the following fully discrete approximation of (2.4.20): find $\boldsymbol{u}_i^h \approx \boldsymbol{u}^h(t_i) \in V^h$ for each $i = 1, \dots, N$, such that

$$\begin{aligned} a(\boldsymbol{u}_i^h, \boldsymbol{v}) &= L(t_i; \boldsymbol{v}) \\ &\quad + \frac{k}{2}\sum_{j=1}^{i}\left(\varphi_s(t_i - t_j)a(\boldsymbol{u}_j^h, \boldsymbol{v}) + \varphi_s(t_i - t_{j-1})a(\boldsymbol{u}_{j-1}^h, \boldsymbol{v})\right), \quad \forall \boldsymbol{v} \in V^h. \end{aligned} \tag{3.2.4}$$

In matrix form, this can be written as

$$\boldsymbol{A}\boldsymbol{U}_i = \boldsymbol{L}_i + \frac{k}{2}\boldsymbol{A}\sum_{j=1}^{i}\left(\varphi_s(t_i - t_j)\boldsymbol{U}_j + \varphi_s(t_i - t_{j-1})\boldsymbol{U}_{j-1}\right). \tag{3.2.5}$$

We can re-write (3.2.5) as,

$$\begin{aligned} \boldsymbol{A}\boldsymbol{U}_i &= \boldsymbol{L}_i + \frac{k}{2}\boldsymbol{A}\varphi_s(t_i - t_i)\boldsymbol{U}_i \\ &+ \frac{k}{2}\boldsymbol{A}\sum_{j=1}^{i-1}\varphi_s(t_i - t_j)\boldsymbol{U}_j \\ &+ \frac{k}{2}\boldsymbol{A}\sum_{j=2}^{i}\varphi_s(t_i - t_{j-1})\boldsymbol{U}_{j-1} \\ &+ \frac{k}{2}\boldsymbol{A}\varphi_s(t_i)\boldsymbol{U}_0. \end{aligned} \tag{3.2.6}$$

Hence,

$$\boldsymbol{A}\left(1 - \frac{k}{2}\varphi_s(0)\right)\boldsymbol{U}_i = \boldsymbol{L}_i + \boldsymbol{A}\boldsymbol{H}_i, \tag{3.2.7}$$

where

$$\boldsymbol{H}_i = \frac{k}{2}\varphi_s(t_i)\boldsymbol{U}_0 + k\sum_{j=1}^{i-1}\varphi_s(t_i - t_j)\boldsymbol{U}_j. \tag{3.2.8}$$

Now substituting for φ_s, coming from (2.2.4), in the above result, we arrive at,

$$\begin{aligned}\boldsymbol{H}_i &= \sum_{q=1}^{N_\varphi}\left[\frac{k}{2}\alpha_q\varphi_q e^{-\alpha_q t_i}\boldsymbol{U}_0 + \sum_{j=1}^{i-1} k\alpha_q\varphi_q e^{-\alpha_q(t_i-t_j)}\boldsymbol{U}_j\right] \\ &= \sum_{q=1}^{N_\varphi}\boldsymbol{H}_{iq},\end{aligned} \tag{3.2.9}$$

where we have denoted by $\boldsymbol{H}_{iq}$ the expression inside the square brackets. Now, using the fact that,

$$e^{-\alpha_q t_i} = e^{-\alpha_q(t_i-t_{i-1})}e^{-\alpha_q t_{i-1}} = e^{-\alpha_q k}e^{-\alpha_q t_{i-1}}, \tag{3.2.10}$$

we can write for $\boldsymbol{H}_{iq}$,

$$\boldsymbol{H}_{iq} = e^{-\alpha_q k}\boldsymbol{H}_{(i-1)q} + k\alpha_q\varphi_q e^{-\alpha_q(t_i-t_{i-1})}\boldsymbol{U}_{i-1}. \tag{3.2.11}$$

This is because,

$$\boldsymbol{H}_{(i-1)q} = \frac{k}{2}\alpha_q\varphi_q e^{-\alpha_q t_{i-1}}\boldsymbol{U}_0 + \sum_{j=1}^{i-2} k\alpha_q\varphi_q e^{-\alpha_q(t_{i-1}-t_j)}\boldsymbol{U}_j. \tag{3.2.12}$$

Here $\boldsymbol{A} \in \mathbb{R}^{nM\times nM}$ is exactly as before in the FEM elasticity problem. $\boldsymbol{L}_i$ is the load vector computed at time t_i and is given by

$$(L_i)_{k_\Omega} = \sum_{E\in\mathcal{T}}\int_E f\phi_{k_\Omega}dE + \sum_{e\subset\Gamma_N}\int_e g\phi_{k_\Omega}de, \qquad k_\Omega = 1,\ldots,nM.$$

Also note that, above, $e = \mathcal{T}\cap\Gamma_N$ for each $\mathcal{T}$, such that $\mathcal{T}\cap\Gamma_N \neq \emptyset$.

3.2.2 Numerical results

We now give an algorithm for the viscoelasticity problem. Note that at $t = 0$, from (2.4.20), we have that $a(\boldsymbol{u}(0), \boldsymbol{v}) = L(0; \boldsymbol{v})$, which implies that $\boldsymbol{A}\boldsymbol{U}_0 = \boldsymbol{L}_0$.

`Algorithm 1: Quasistatic viscoelasticity problem`

---

1. Solve $\mathtt{A}\mathtt{U}_0 = \mathtt{L}_0$
2. Initialize $\mathtt{H}_q = \frac{1}{2}\mathtt{k}\alpha_\mathtt{q}\varphi_\mathtt{q}\mathtt{e}^{-\alpha_\mathtt{q}\mathtt{t}_1}\mathtt{U}_0, \qquad \mathtt{q} = 1, \dots, \mathtt{N}_\mathtt{q}$
3. for i=1,...,N
4. Solve $\mathtt{A}(1 - \frac{\mathtt{k}}{2}\varphi_\mathtt{s}(0))\mathtt{U}_\mathtt{i} = \mathtt{L}_\mathtt{i} + \mathtt{A}\sum_{\mathtt{q}=1}^{\mathtt{N}_\mathtt{q}} \mathtt{H}_\mathtt{q}$
5. update $\mathtt{H}_\mathtt{q}$
6. $\mathtt{H}_\mathtt{q} \leftarrow \mathtt{e}^{-\alpha_\mathtt{q}\mathtt{k}}\mathtt{H}_\mathtt{q} + \mathtt{k}\alpha_\mathtt{q}\varphi_\mathtt{q}\mathtt{e}^{-\alpha_\mathtt{q}\mathtt{k}}\mathtt{U}_\mathtt{i}$
7. next i

The values for viscoelastic parameters, for all computational work in this thesis, are as follows: $E = 100000$ and $\nu = 0.3$; then using these, λ and μ are computed using (2.1.13). The values of α_q and φ_q, for $q = 1, \dots, N_\varphi = 3$, are $\alpha_q = [0.1 \;\; 0.05 \;\; 0.01]$ and $\varphi_q = [0.3 \;\; 0.2 \;\; 0.1]$. First, we compute displacement at $t = 0$, as shown in line 1 on the algorithm; this is just the elasticity problem. Next we initialise H_q. Then at each discrete time we solve the matrix equation in line 4 which corresponds to equation (3.2.7) and update H_q using the recursive relation (3.2.12).

To check for convergence of the algorithm, we give three examples. The errors are computed in such a way that the maximum values of components of the error $|\boldsymbol{u} - \boldsymbol{u}_i^h|$ are retrieved over *all* discrete times t_i and over *all* nodes of the mesh, where $\boldsymbol{u}$ is the exact solution (or the "manufactured solution") and $\boldsymbol{u}_i^h$ is the fully discrete (computed) approximate solution for displacement. We may call this the "max error". This is how it is done: for a fixed number of time steps and a fixed mesh size (i.e. the number of elements in the mesh), for each discrete time t_i we compute the max error for the whole mesh (over all nodes), then we retrieve the maximum value out of all these max errors, that is, maxerror = max $\{\text{error}_{t_1}, \text{error}_{t_2}, \ldots, \text{error}_{t_{END}}\}$. To show convergence of the algorithm, we consider the following three examples.

Example 1: Exact solution $\boldsymbol{u}(\boldsymbol{x}, t) = \begin{pmatrix} 3x - 2y \\ 4x + y \end{pmatrix} t$

Table 3.1 shows no displacement errors as the mesh size increases by a factor of two (i.e. horizontally) since the dependence of exact solution on spatial coordinates is linear. However we see that there are errors as the time steps are doubled (i.e. vertically) even though dependence on t is linear and this is due to the fact that the approximation by trapezoidal rule has a second order convergence. It can be seen from the table that the error changes slightly as the mesh size increases; ideally there should be no changes at all. This may be due to quadrature error in the code since the integrals are computed using one point of quadrature which is exact for integrands of order one (center of gravity); the integrands involved here are not linear.

Table 3.1: Displacement *max* errors for viscoelasticity: $\times 10^{-3}$, Example 1

time steps	mesh size 2	4	8	16	32	64
2	0.150280	0.160557	0.165915	0.168193	0.168757	0.168981
4	0.037568	0.040137	0.041476	0.042046	0.042187	0.042243
8	0.009391	0.010034	0.010369	0.010511	0.010546	0.010560
16	0.002347	0.002508	0.002592	0.002627	0.002636	0.002640
32	0.000586	0.000627	0.000648	0.000656	0.000659	0.000660
64	0.000146	0.000156	0.000162	0.000164	0.000164	0.000165

Example 2: Exact solution $\boldsymbol{u}(\boldsymbol{x},t) = \begin{pmatrix} 3x - 2y \\ 4x + y \end{pmatrix} t^2$

As Table 3.2 shows, again there are no displacement errors as the mesh size is increased, and this is because the exact solution is again linear in spatial variables. There are only temporal errors and this is because of the trapezoidal rule and the term t^2. As in the previous example, due to quadrature error in the code, there is a slight change in the error as the mesh size increases.

Table 3.2: Displacement *max* errors for viscoelasticity: $\times 10^{-3}$, Example 2

time steps	mesh size 2	4	8	16	32	64
2	1.871755	1.999757	2.066493	2.094862	2.101886	2.104676
4	0.467918	0.499917	0.516600	0.523692	0.525448	0.526146
8	0.116978	0.124977	0.129148	0.130921	0.131360	0.131535
16	0.029244	0.031244	0.032287	0.032730	0.032840	0.032883
32	0.007311	0.007811	0.008071	0.008182	0.008210	0.008220
64	0.001827	0.001952	0.002017	0.002045	0.002052	0.002055

Example 3: Exact solution $\boldsymbol{u}(\boldsymbol{x},t) = \begin{pmatrix} x^2 + y^3 \\ x^3 + y^2 \end{pmatrix} t^2$

In this case, different from the first two, there are both temporal and spatial errors present. This is due to the fact that the exact solution is not linear either in the spatial coordinates or in time. As Table 3.3 shows, there is second order convergence along the diagonal. That is, the error is reduced by a factor of four as the mesh size and the number of time steps are doubled.

Table 3.3: Displacement *max* errors for viscoelasticity: $\times 10^{-3}$, Example 3

time steps	mesh size 2	4	8	16	32	64
2	22.421437	7.308300	3.141031	2.047279	1.773113	1.701675
4	21.178083	6.063612	1.890683	0.792868	0.513760	0.443045
8	20.867262	5.752457	1.578114	0.479343	0.198939	0.128405
16	20.770131	5.655222	1.480437	0.381368	0.100638	0.049746
32	20.770131	5.655222	1.480437	0.381368	0.100638	0.030097
64	20.765275	5.650361	1.475553	0.376470	0.095740	0.025187

3.3 Discrete schemes for the heat conduction problem

We will first consider a so-called *semi-discrete* analogue of the heat equation (2.4.4), which implies discretization in space. To obtain a fully discrete scheme we will also need to discretize in time. For the time-discretization we shall employ the *Crank-Nicolson method* (CN) and follow the style of Johnson (2009), where the backward Euler method is derived in. This is mainly bookwork, but here we show in more detail the use of CN, something which is omitted in Johnson (2009).

3.3.1 Discretization in space

For the discretization in space we choose a finite-dimensional subspace $\mathcal{V}^h \subset \mathcal{V}$ with basis functions $\{\Psi_1, \ldots, \Psi_M\}$. We assume that $\mathcal{V}^h$ consists of piecewise linear functions on the triangulation of Ω. Next, replacing $\mathcal{V}$ with $\mathcal{V}^h$, we consider the following semi-discrete version of (2.4.25): find $\theta^h(t) \in \mathcal{V}^h$, such that

$$\begin{aligned} \kappa(\dot{\theta}^h, v)_\Omega + a_H\left(\theta^h, v\right) &= (q,v)_{\Gamma_{N_2}} + (l,v)_\Omega\,, && \forall v \in \mathcal{V}^h,\ t \in I. \\ (\theta^h(0), v)_\Omega &= (\theta^0, v)_\Omega. && \end{aligned} \tag{3.3.1}$$

Next we write

$$\theta^h(\boldsymbol{x}, t) = \sum_{p=1}^{M} \xi_p(t)\Psi_p(\boldsymbol{x}), \qquad \boldsymbol{x} \in \Omega,\ t \in I, \tag{3.3.2}$$

with time-dependent coefficients $\xi_p(t) \in \mathbb{R}$, M is the number of nodes in the mesh. Using (3.3.2) and $v = \Psi_r$ in (3.3.1), we get

$$\begin{aligned} \kappa\left(\sum_{p=1}^{M} \dot{\xi}_p(t)\Psi_p, \Psi_r\right)_\Omega + a_H\left(\sum_{p=1}^{M} \xi_p(t)\Psi_p, \Psi_r\right) &= (l, \Psi_r)_\Omega + (q, \Psi_r)_{\Gamma_{N_2}} \\ \sum_{p=1}^{M} \xi_p(0)(\Psi_p, \Psi_r)_\Omega &= (\theta^0, \Psi_r)_\Omega, \end{aligned} \tag{3.3.3}$$

$r = 1, \ldots, M$ and $t \in I$. In matrix form this system reads,

$$\begin{aligned} \kappa B\dot{\xi}(t) + A\xi(t) &= G(t), && t \in I. \\ B\xi(0) &= \Theta^0. && \end{aligned} \tag{3.3.4}$$

3.3.2 Discretization in time

For the time discretization of (3.3.1), and equivalently of (3.3.4), we shall use the Crank-Nicolson method. Taking the average of (3.3.1) over two consecutive time steps gives:

$$\kappa\frac{1}{2}(\dot{\theta}^h(t_i)+\dot{\theta}^h(t_{i-1}),v)_\Omega+\frac{1}{2}a_H\left(\dot{\theta}^h(t_i)+\dot{\theta}^h(t_{i-1}),v\right)$$
$$=\frac{1}{2}\left(l_i+l_{i-1},v\right)_\Omega+\frac{1}{2}\left(q_i+q_{i-1},v\right)_{\Gamma_{N_2}}, \tag{3.3.5}$$

where the subscript i denotes the discrete time t_i. Next we approximate

$$\frac{\dot{\theta}^h(t_i)+\dot{\theta}^h(t_{i-1})}{2}$$

by

$$\frac{\theta^h(t_i)-\theta^h(t_{i-1})}{k},$$

with discretization error $O(k^2)$. Then (3.3.5) becomes: find $\theta_i^h \approx \theta^h(t_i) \in \mathcal{V}^h$, $i=1,\ldots,N$, such that

$$\kappa\left(\frac{\theta_i^h-\theta_{i-1}^h}{k},v\right)_\Omega+a_H\left(\frac{\theta_i^h+\theta_{i-1}^h}{2},v\right)=\left(\frac{l_i+l_{i-1}}{2},v\right)_\Omega+\left(\frac{q_i+q_{i-1}}{2},v\right)_{\Gamma_{N_2}}$$
$$\left(\theta_0^h,v\right)_\Omega=(\theta_0,v)_\Omega\,. \tag{3.3.6}$$

Using (3.3.2) this can be written

$$\kappa\left(\frac{\sum_{p=1}^{M}\xi_p^i\Psi_p-\sum_{p=1}^{M}\xi_i^{i-1}\Psi_p}{k},v\right)_\Omega+a_H\left(\frac{\sum_{p=1}^{M}\xi_p^i\Psi_p+\sum_{p=1}^{M}\xi_p^{i-1}\Psi_p}{2},v\right)$$
$$=\left(\frac{l_i+l_{i-1}}{2},\Psi_p\right)_\Omega+\left(\frac{q_i+q_{i-1}}{2},\Psi_p\right)_{\Gamma_{N_2}}. \tag{3.3.7}$$

Finally, after some algebra the Crank-Nicolson method in matrix form reads:

$$\Big(\kappa B + \frac{1}{2}Ak\Big)\xi^i = \Big(\kappa B - \frac{1}{2}Ak\Big)\xi^{i-1} + \frac{k}{2}\Big(G_i + G_{i-1}\Big), \quad i = 1, \ldots, N, \tag{3.3.8}$$

where

$$\theta_i^h = \sum_{p=1}^{M} \xi_p^i \Psi_p(x), \qquad (\xi_p^i \in \mathbb{R}).$$

In (3.3.8), $A \in \mathbb{R}^{M\times M}$ is the global stiffness matrix and is given by

$$A_{pr} = \sum_{E\in\mathcal{T}} \int_E \nabla\Psi_p \cdot \nabla\Psi_r dE.$$

$B \in \mathbb{R}^{M\times M}$ is the mass matrix and is given by

$$B_{pr} = \sum_{E\in\mathcal{T}} \int_E \Psi_p \Psi_r dE.$$

$G_i \in \mathbb{R}^M$ is the time-dependent load vector computed at time t_i and includes the contributions from both l and q, and it is given by

$$G_i = \sum_{E\in\mathcal{T}} \int_E l\Psi_r dE + \sum_{e\subset\Gamma_{N_2}} \int_e q\Psi_r de.$$

Note that, above $e = \mathcal{T} \cap \Gamma_{N_2}$ for each $\mathcal{T}$, such that $\mathcal{T} \cap \Gamma_{N_2} \neq \emptyset$.

3.4 Discrete schemes for the linear and nonlinear problem

For the fully-discrete approximation to the linear problem (2.4.21), we consider the subspace $V^h \subset V$ and then use the trapezoidal rule, given by (3.2.3), for approximating the time integrals. This gives: for arbitrary $i = 1, \ldots, N$, find $\boldsymbol{u}_i^h \approx \boldsymbol{u}^h(t_i) \in V^h$, such that

$$\begin{aligned} a(\boldsymbol{u}_i^h, \boldsymbol{v}) = & \frac{k}{2} \sum_{j=1}^{i} \Big(\varphi_s(t_i - t_j) a(\boldsymbol{u}_j^h, \boldsymbol{v}) + \varphi_s(t_i - t_{j-1}) a(\boldsymbol{u}_{j-1}^h, \boldsymbol{v}) \Big) \\ & + L(t_i; \boldsymbol{v}) + \Big(\alpha \boldsymbol{D}(\theta_i^h - \theta_r) \boldsymbol{I_0}, \boldsymbol{\varepsilon}(\boldsymbol{v}) \Big)_\Omega \\ & - \frac{k}{2} \sum_{j=1}^{i} \Big(\alpha \boldsymbol{D} \varphi_s(t_i - t_j)(\theta_j^h - \theta_r) \boldsymbol{I_0}, \boldsymbol{\varepsilon}(\boldsymbol{v}) \Big)_\Omega \\ & - \frac{k}{2} \sum_{j=1}^{i} \Big(\alpha \boldsymbol{D} \varphi_s(t_i - t_{j-1})(\theta_{j-1}^h - \theta_r) \boldsymbol{I_0}, \boldsymbol{\varepsilon}(\boldsymbol{v}) \Big)_\Omega. \end{aligned} \tag{3.4.1}$$

Analogously for the fully discrete approximation to the nonlinear problem (2.4.22), we consider the subspace $V^h \subset V$ and employ the trapezoidal rule for approximating the time integrals. This yields: for arbitrary $i = 1, \ldots, N$ find $\boldsymbol{u}_i^h \approx \boldsymbol{u}^h(t_i) \in V^h$, such that,

$$\begin{aligned} a(\boldsymbol{u}_i^h, \boldsymbol{v}) = L(t_i; \boldsymbol{v}) + & \frac{k}{2} \sum_{j=1}^{i} \Big[\big(\boldsymbol{D} \varphi_s(\rho_i^h - \rho_j^h) \boldsymbol{\varepsilon}(\boldsymbol{u}_j^h), \boldsymbol{\varepsilon}(\boldsymbol{v}) \big)_\Omega \\ & + \big(\boldsymbol{D} \varphi_s(\rho_i^h - \rho_{j-1}^h) \boldsymbol{\varepsilon}(\boldsymbol{u}_{j-1}^h), \boldsymbol{\varepsilon}(\boldsymbol{v}) \big)_\Omega \Big] \\ + \Big(\alpha \boldsymbol{D}(\theta_i^h - \theta_r) \boldsymbol{I_0}, \boldsymbol{\varepsilon}(\boldsymbol{v}) \Big)_\Omega - & \frac{k}{2} \sum_{j=1}^{i} \Big[\big(\alpha \boldsymbol{D} \varphi_s(\rho_i^h - \rho_j^h)(\theta_j^h - \theta_r) \boldsymbol{I_0}, \boldsymbol{\varepsilon}(\boldsymbol{v}) \big)_\Omega \\ & + \big(\alpha \boldsymbol{D} \varphi_s(\rho_i^h - \rho_{j-1}^h)(\theta_{j-1}^h - \theta_r) \boldsymbol{I_0}, \boldsymbol{\varepsilon}(\boldsymbol{v}) \big)_\Omega \Big], \qquad \forall \boldsymbol{v} \in V^h, \end{aligned} \tag{3.4.2}$$

where the approximate value ρ_i^h of reduced time is given by,

$$\rho_i^h = \frac{k}{2}\sum_{j=1}^{i}\Big(\frac{1}{\psi(\theta_j^h)} + \frac{1}{\psi(\theta_{j-1}^h)}\Big), \tag{3.4.3}$$

coming from (2.3.8).

3.5 Summary

In this chapter we gave a more detailed account of the finite element method. Finite element approximations were given for the elasticity, viscoelasticity and heat problems. Fully discrete schemes were derived for viscoelasticity and heat problem. Convergence rates were shown for displacement in the case of viscoelasticity. Fully discrete approximations were given for the linear and nonlinear problem. Having done this, in the next chapter we move to the theoretical aspect of thesis, and derive stability bounds for the linear problem.

Chapter 4

Stability Analysis for the Linear Problem

4.1 The continuous formulation

In this section we aim to derive a bound in the energy norm for the continuous formulation for displacement $\boldsymbol{u}$ in the case of the linear coupled problem given by (2.4.21), motivated by the need to show that there is stability in the sense that the solution $\boldsymbol{u}$ in the energy norm is bounded by data, exact solution, derivatives of exact solutions and constants. We state the following theorem.

Theorem 4.1.1. *Let Assumptions 2.4.1 (i) - (iii) and Corollary 2.2.1 hold and let* $\alpha > 0$*, then for* $\boldsymbol{u}$*, the exact solution of (2.4.21), we have the following bound,*

$$\begin{aligned}\|\boldsymbol{u}\|_{L_\infty(0,t;E)} \leqslant & \frac{1}{\varphi(t)}\|L\|_{L_\infty(0,t;E')} \\ & + \frac{2C(\alpha, \boldsymbol{D})}{\varphi(t)}\left(\|\theta_0\|_{L_2(\Omega)} + \frac{1}{\kappa}\|G\|_{L_\infty(0,t;E')} + |\theta_r|\sqrt{Vol(\Omega)}\right), \qquad (4.1.1)\end{aligned}$$

where $C(\alpha, \boldsymbol{D}) = \alpha\|\boldsymbol{D}^{1/2} I_0\|_{L_\infty(\Omega)}$ *is a positive constant.*

Proof. Choosing $\boldsymbol{v} = \boldsymbol{u}(t)$ in (2.4.21) for some $t \in I$, using the energy norm and the Cauchy-Schwartz inequality on the right side gives,

$$\begin{aligned}\|\boldsymbol{u}\|_E^2 \leqslant \|L\|_{E'}\|\boldsymbol{u}\|_E + \int_0^t \varphi_s(t-s)\|\boldsymbol{u}(s)\|_E ds \|\boldsymbol{u}(t)\|_E \\ + C(\alpha, \boldsymbol{D})\|\boldsymbol{u}(t)\|_E\|\theta(t) - \theta_r\|_{L_2(\Omega)} \\ + \int_0^t \varphi_s(t-s) C(\alpha, \boldsymbol{D})\|\theta(s) - \theta_r\|_{L_2(\Omega)} ds \|\boldsymbol{u}(t)\|_E. \end{aligned} \tag{4.1.2}$$

Writing,

$$\begin{aligned}\int_0^t \varphi_s(t-s)\|\boldsymbol{u}(s)\|_E ds &\leqslant \|\boldsymbol{u}\|_{L_\infty(0,t;E)} \int_0^t \varphi_s(t-s) ds \\ &= (1 - \varphi(t))\, \|\boldsymbol{u}\|_{L_\infty(0,t;E)}, \end{aligned} \tag{4.1.3}$$

and substituting this in (4.1.2), yields

$$\|\boldsymbol{u}\|_{L_\infty(0,t;E)} \leqslant \frac{1}{\varphi(t)}\|L\|_{L_\infty(0,t;E')} + \frac{2}{\varphi(t)} C(\alpha, \boldsymbol{D})\|\theta(t) - \theta_r\|_{L_\infty(0,t;L_2(\Omega))}. \tag{4.1.4}$$

We recall here that $0 < \varphi(t) \leqslant 1$. Next step of the proof is to derive an estimate for $\|\theta(t) - \theta_r\|_{L_\infty(0,t;L_2(\Omega))}$. Recall from Assumptions 2.4.1 (iii), that the energy norm for the heat problem is given by

$$\|v\|_{\mathcal{A}} := (Q\nabla v, \nabla v)_\Omega = \|Q^{1/2}\nabla v\|_{L_2(\Omega} \tag{4.1.5}$$

Rewrite the weak formulation (2.4.24) for the heat problem as,

$$(\kappa\theta_t, v)_\Omega + (Q\nabla\theta, \nabla v)_\Omega = \langle G, v\rangle, \qquad \forall v \in \mathcal{V}, \tag{4.1.6}$$

with $\theta(\boldsymbol{x},0)$ given. Next, for some $t \in (0,T]$, choose $v = \theta(t)$ in (4.1.6), to get

$$\frac{\kappa}{2}\frac{d}{dt}\|\theta(t)\|^2_{L_2(\Omega)} + \|Q^{1/2}\nabla\theta\|^2_{L_2(\Omega)} = \langle G, \theta\rangle. \tag{4.1.7}$$

Definition of the dual norm (1.3.3) gives,

$$|\langle G, \theta\rangle| \leqslant \|G\|_{\mathcal{A}'}\|\theta(t)\|_{\mathcal{A}}. \tag{4.1.8}$$

Using the definition of the energy norm above and (4.1.8), we can rewrite (4.1.7) as,

$$\frac{\kappa}{2}\frac{d}{dt}\|\theta(t)\|^2_{L_2(\Omega)} + \|\theta(t)\|^2_{\mathcal{A}} \leqslant \|G(t)\|_{\mathcal{A}'}\|\theta(t)\|_{\mathcal{A}}. \tag{4.1.9}$$

Applying Inequality (1.3.1) with $\epsilon = 1$ on the right-hand side, we get

$$\kappa\frac{d}{dt}\|\theta(t)\|^2_{L_2(\Omega)} + \|\theta(t)\|^2_{\mathcal{A}} \leqslant \|G(t)\|^2_{\mathcal{A}'}. \tag{4.1.10}$$

Integrating this between 0 and t, gives

$$\kappa\int_0^t \frac{d}{ds}\|\theta(s)\|^2_{L_2(\Omega)}ds + \int_0^t \|\theta(s)\|^2_{\mathcal{A}}ds \leqslant \int_0^t \|G(s)\|^2_{\mathcal{A}'}ds, \tag{4.1.11}$$

which then yields,

$$\kappa\|\theta(t)\|^2_{L_2(\Omega)} + \int_0^t \|\theta(s)\|^2_{\mathcal{A}}ds \leqslant \kappa\|\theta(0)\|^2_{L_2(\Omega)} + \int_0^t \|G(s)\|^2_{\mathcal{A}'}ds. \tag{4.1.12}$$

Rearranging this, gives

$$\begin{aligned}\|\theta(t)\|^2_{L_2(\Omega)} &\leqslant \|\theta(0)\|^2_{L_2(\Omega)} + \frac{1}{\kappa}\int_0^t \|G(s)\|^2_{\mathcal{A}'}ds \\ &= \|\theta(0)\|^2_{L_2(\Omega)} + \frac{1}{\kappa}\|G(s)\|^2_{L_2(0,t;\mathcal{A}')}. \end{aligned} \tag{4.1.13}$$

Using the fact that for $a, b, c \geqslant 0$, $a^2 \leqslant b^2 + c^2$ implies $a \leqslant b + c$, enables us to give a bound for θ in the L_2 norm,

$$\|\theta(t)\|_{L_2(\Omega)} \leqslant \|\theta(0)\|_{L_2(\Omega)} + \frac{1}{\sqrt{\kappa}}\|G(s)\|_{L_2(0,t;\mathcal{A}')}. \tag{4.1.14}$$

Next, the triangle inequality gives,

$$\begin{aligned}\|\theta(t) - \theta_r\|_{L_2(\Omega)} &\leqslant \|\theta(t)\|_{L_2(\Omega)} + \|\theta_r\|_{L_2(\Omega)} \\ &\leqslant \|\theta_0\|_{L_2(\Omega)} + \frac{1}{\sqrt{\kappa}}\|G(s)\|_{L_2(0,t;\mathcal{A}')} + |\theta_r|\sqrt{\mathrm{Vol}(\Omega)}. \end{aligned} \tag{4.1.15}$$

Taking the L_∞ norm, we can write,

$$\|\theta - \theta_r\|_{L_\infty(0,t;L_2(\Omega))} \leqslant \|\theta_0\|_{L_2(\Omega)} + \frac{1}{\sqrt{\kappa}}\|G\|_{L_2(0,T;\mathcal{A}')} + |\theta_r|\sqrt{\mathrm{Vol}(\Omega)}. \tag{4.1.16}$$

□

Substituting this back into (4.1.4), proves the theorem.

4.2 Discrete formulation

In this section we aim to derive a bound in the energy norm for the discrete formulation for displacement $\boldsymbol{u}_i^h$ in the case of the linear coupled problem given by (3.4.1), motivated by the need to show that there is stability in the sense that the solution $\boldsymbol{u}_i^h$ in the energy norm is bounded by data, derivatives of exact solutions and constants. We start by stating the following theorem,

Theorem 4.2.1. *Let Assumptions 2.4.1 (i) - (iii) and Corollary 2.2.1 hold and let* $\alpha > 0$. *Then for the fully discrete approximate solution* $\boldsymbol{u}_i^h$ *of (3.4.1), for* k *small* *enough, we have the following bound,*

$$\|\boldsymbol{u}_i^h\|_E \leqslant C_2 e^{C_1 T}, \tag{4.2.1}$$

where C_1 and C_2 are non-negative quantities. C_1 depends on $\max\limits_{0\leqslant j\leqslant i-1} \varphi_s(t_i - t_j)$, whereas C_2 depends on data, initial conditions and other constants.

Proof. First, re-arranging (3.4.1) gives, find $\boldsymbol{u}_i^h \in V^h$ such that,

$$\begin{aligned} a(\boldsymbol{u}_i^h,\boldsymbol{v}) = {} & \frac{k}{2}\varphi_s(0)a(\boldsymbol{u}_i^h,\boldsymbol{v}) - \frac{k}{2}\varphi_s(t_i)a(\boldsymbol{u}_0^h,\boldsymbol{v}) + L(t_i;\boldsymbol{v}) + k\sum_{j=0}^{i-1}\varphi_s(t_i-t_j)a(\boldsymbol{u}_j^h,\boldsymbol{v}) \\ & - \frac{k}{2}\Big(\alpha\boldsymbol{D}\varphi_s(t_i)(\theta_0^h-\theta_r)\boldsymbol{I_0},\boldsymbol{\varepsilon}(\boldsymbol{v})\Big)_\Omega - \frac{k}{2}\Big(\alpha\boldsymbol{D}\varphi_s(0)(\theta_i^h-\theta_r)\boldsymbol{I_0},\boldsymbol{\varepsilon}(\boldsymbol{v})\Big)_\Omega \\ & + \Big(\alpha\boldsymbol{D}(\theta_i^h-\theta_r)\boldsymbol{I_0},\boldsymbol{\varepsilon}(\boldsymbol{v})\Big)_\Omega \\ & - k\sum_{j=1}^{i-1}\Big(\alpha\boldsymbol{D}\varphi_s(t_i-t_j)(\theta_j^h-\theta_r)\boldsymbol{I_0},\boldsymbol{\varepsilon}(\boldsymbol{v})\Big)_\Omega \quad \forall \boldsymbol{v}\in V^h. \end{aligned} \tag{4.2.2}$$

For an arbitrary $i \in \{1,\ldots,N\}$ take $\boldsymbol{v} = \boldsymbol{u}_i^h$ in (4.2.2). Assumptions (2.4.1), (iii), gives

$$\begin{aligned} \|\boldsymbol{u}_i^h\|_E^2 = {} & \frac{k}{2}\varphi_s(0)a(\boldsymbol{u}_i^h,\boldsymbol{u}_i^h) - \frac{k}{2}\varphi_s(t_i)a(\boldsymbol{u}_0^h,\boldsymbol{u}_i^h) + L(t_i;\boldsymbol{u}_i^h) + k\sum_{j=0}^{i-1}\varphi_s(t_i-t_j)a(\boldsymbol{u}_j^h,\boldsymbol{u}_i^h) \\ & - \frac{k}{2}\Big(\alpha\boldsymbol{D}\varphi_s(t_i)(\theta_0^h-\theta_r)\boldsymbol{I_0},\boldsymbol{\varepsilon}(\boldsymbol{u}_i^h)\Big)_\Omega - \frac{k}{2}\Big(\alpha\boldsymbol{D}\varphi_s(0)(\theta_i^h-\theta_r)\boldsymbol{I_0},\boldsymbol{\varepsilon}(\boldsymbol{u}_i^h)\Big)_\Omega \\ & + \Big(\alpha\boldsymbol{D}(\theta_i^h-\theta_r)\boldsymbol{I_0},\boldsymbol{\varepsilon}(\boldsymbol{u}_i^h)\Big)_\Omega \\ & - k\sum_{j=1}^{i-1}\Big(\alpha\boldsymbol{D}\varphi_s(t_i-t_j)(\theta_j^h-\theta_r)\boldsymbol{I_0},\boldsymbol{\varepsilon}(\boldsymbol{u}_i^h)\Big)_\Omega. \end{aligned} \tag{4.2.3}$$

Furthermore, Assumptions (2.4.1), (iii) and (2.4.28), and Cauchy-Schwartz, give

$$\begin{aligned}\|\boldsymbol{u}_i^h\|_E^2 \leqslant \frac{k}{2}\varphi_s(0)\|\boldsymbol{u}_i^h\|_E^2 + Ck\|\boldsymbol{u}_0^h\|_E\|\boldsymbol{u}_i^h\|_E + \tilde{C}k\sum_{j=0}^{i-1}\|\boldsymbol{u}_j^h\|_E\|\boldsymbol{u}_i^h\|_E + \|L\|_{E'}\|\boldsymbol{u}_i^h\|_E \\ + C\|\boldsymbol{u}_i^h\|_E\|\theta_i^h - \theta_r\|_{L_2(\Omega)} + Ck\|\boldsymbol{u}_i^h\|_E\|\theta_0^h - \theta_r\|_{L_2(\Omega)} + Ck\|\boldsymbol{u}_i^h\|_E\|\theta_i^h - \theta_r\|_{L_2(\Omega)} \\ + \tilde{C}k\sum_{j=1}^{i-1}\|\boldsymbol{u}_i^h\|_E\|\theta_j^h - \theta_r\|_{L_2(\Omega)}. \qquad (4.2.4)\end{aligned}$$

Here $\tilde{C} = \max_{0\leqslant j\leqslant i-1}\varphi_s(t_i - t_j)$. Dividing through by $\|\boldsymbol{u}_i^h\|_E$, this simplifies to,

$$\begin{aligned}(1 - \frac{k}{2}\varphi_s(0))\|\boldsymbol{u}_i^h\|_E \leqslant Ck\|\boldsymbol{u}_0^h\|_E + \|L\|_{E'} + C\|\theta_i^h - \theta_r\|_{L_2(\Omega)} + Ck\|\theta_0^h - \theta_r\|_{L_2(\Omega)} \\ + Ck\|\theta_i^h - \theta_r\|_{L_2(\Omega)} + Ck\sum_{j=1}^{i-1}\|\theta_j^h - \theta_r\|_{L_2(\Omega)} + Ck\sum_{j=0}^{i-1}\|\boldsymbol{u}_j^h\|_E, \\ (4.2.5)\end{aligned}$$

where we require $k < \frac{2}{\varphi_s(0)}$. In order to derive a bound on $\|\theta_i^h - \theta_r\|_{L_2(\Omega)}$ we first need to derive a bound for $\|\theta_i^h\|_{L_2(\Omega)}$. From (3.3.6), multiplying by $2k$, gives

$$2\kappa\left(\theta_i^h - \theta_{i-1}^h, v\right) + k\left(Q\nabla(\theta_i^h + \theta_{i-1}^h), \nabla v\right) = k\left(\langle G(t_i), v\rangle + \langle G(t_{i-1}), v\rangle\right). \quad (4.2.6)$$

Using the linearity on the first term, the definition of the energy norm (4.1.5) and that of the dual norm (1.3.3), and then choosing $v = \theta_i + \theta_{i-1}$, yields

$$\begin{aligned}2\kappa\left(\|\theta_i^h\|_{L_2(\Omega)}^2 - \|\theta_{i-1}^h\|_{L_2(\Omega)}^2\right) + k\|\theta_i^h + \theta_{i-1}^h\|_{\mathcal{A}}^2 \\ \leqslant k\left(\|G_i\|_{\mathcal{A}'} + \|G_{i-1}\|_{\mathcal{A}'}\right)\|\theta_i^h + \theta_{i+1}^h\|_{\mathcal{A}}. \qquad (4.2.7)\end{aligned}$$

Summing from $i = 1$ to $m \leqslant N$ gives,

$$2\kappa \sum_{i=1}^{m} \left(\|\theta_i^h\|^2_{L_2(\Omega)} - \|\theta_{i-1}^h\|^2_{L_2(\Omega)} \right) + k \sum_{i=1}^{m} \|\theta_i^h + \theta_{i-1}^h\|^2_{\mathcal{A}}$$
$$\leqslant k \sum_{i=1}^{m} \left(\|G_i\|_{\mathcal{A}'} + \|G_{i-1}\|_{\mathcal{A}'} \right) \|\theta_i^h + \theta_{i+1}^h\|_{\mathcal{A}}. \quad (4.2.8)$$

The first summation on the left side of (4.2.8) gives $\|\theta_m^h\|^2_{L_2(\Omega)} - \|\theta_0^h\|^2_{L_2(\Omega)}$. Using Inequality (1.3.1) with $\epsilon = 1$ on the right side of (4.2.8) and then ignoring the term $\frac{k}{2} \sum_{i=1}^{m} \|\theta_i^h + \theta_{i-1}^h\|^2_{\mathcal{A}}$ on the left, we arrive at:

$$\|\theta_m^h\|^2_{L_2(\Omega)} \leqslant \|\theta_0^h\|^2_{L_2(\Omega)} + \frac{k}{4\kappa} \sum_{i=1}^{m} \left(\|G_i\|^2_{\mathcal{A}'} + \|G_{i-1}\|^2_{\mathcal{A}'} \right). \quad (4.2.9)$$

This can be written as,

$$\|\theta_m^h\|_{L_2(\Omega)} \leqslant \|\theta_0^h\|_{L_2(\Omega)} + C\sqrt{\frac{T}{\kappa}} \max_{0 \leqslant i \leqslant m} \left\{ \|G_i\|_{\mathcal{A}'} \right\}. \quad (4.2.10)$$

After using the triangle inequality to write $\|\theta_i^h - \theta_r\|_{L_2(\Omega)} \leqslant \|\theta_i^h\|_{L_2(\Omega)} + \|\theta_r\|_{L_2(\Omega)}$, substituting (4.2.10) in (4.2.5), gives

$$\|\boldsymbol{u}_i^h\|_E \leqslant \bar{C} + Ck \sum_{j=0}^{i-1} \|\boldsymbol{u}_j^h\|_E, \quad (4.2.11)$$

where $\bar{C}$ and C depend on data, initial conditions and other constants. Finally, using Lemma 1.4.2 (the discrete version of Gronwall's lemma), this becomes

$$\|\boldsymbol{u}_i^h\|_E \leqslant \bar{C} e^{CT}, \quad (4.2.12)$$

□

and this proves our theorem.

4.3 Summary

In this chapter we derived stability bounds for the continuous and discrete formulations for displacement for the linear coupled problem. As part of the proof, we also derived a bound in the L_2 norm for the heat problem, both for the continuous and discrete case.

Chapter 5

A Priori Error Analysis for the Linear Problem

The aim in this chapter is to derive an *a priori* error estimate for the linear coupled problem. We first derive an error bound for the heat conduction problem, as a first result towards deriving the error bound for the linear coupled problem (2.4.21).

5.1 A priori error analysis for the heat conduction problem

In this section we aim to derive a fully discrete error estimate in the L_2 norm for the heat problem. We employ the Ritz or elliptic projection for this purpose.

We recall that weak formulation of the heat equation is given by: find $\theta \in \mathcal{V}$, such that,

$$\kappa\left(\theta_t, v\right)_\Omega + \left(Q\nabla\theta, \nabla v\right)_\Omega = \langle G, v\rangle, \quad \forall v \in \mathcal{V},\ \ t \in I = (0, T] \tag{5.1.1}$$

$$\left(\theta(0), v\right)_\Omega = \left(\theta^0, v\right)_\Omega, \tag{5.1.2}$$

where $\mathcal{V}$ is the Hilbert test space given by (2.4.23), $\theta_t = \dot{\theta}$ and recall that $\langle G, v\rangle = (l, v)_\Omega + (q, v)_{\Gamma_{N_2}}$. $(Q\nabla\theta, \nabla v)_\Omega$ corresponds to the bilinear form $a_H(\theta, v)$. For the fully discrete problem we can write,

$$\kappa\left(\partial_t\theta_n^h, v\right) + \left(Q\nabla\bar{\theta}_n^h, \nabla v\right) = \langle\bar{G}_n, v\rangle, \quad \forall v \in \mathcal{V}^h, \tag{5.1.3}$$

$n = 1, \ldots, N$. Here $\bar{\theta}_n^h$ and $\bar{G}_n$ are averages over two time steps, t_{n-1} and t_n, that is, $\bar{\theta}_n^h := \dfrac{\theta_{n-1}^h + \theta_n^h}{2}$ and $\bar{G}_n := \dfrac{G_{n-1} + G_n}{2}$. We note that above we have adopted the following notation,

$$\partial_t\theta_n^h := \frac{\theta_n^h - \theta_{n-1}^h}{k}. \tag{5.1.4}$$

Definition 5.1.1. *Let the Ritz projection $R\theta \in \mathcal{V}^h$ at each t be defined by*

$$\left(\nabla\left(\theta - R\theta\right), \nabla v\right) = 0, \quad \forall v \in \mathcal{V}^h.$$

The map $R : \mathcal{V} \to \mathcal{V}^h$ maps each element of $\mathcal{V}$ to some element in the subspace $\mathcal{V}^h$.

From the above definition we can write,

$$\begin{aligned}\|\nabla\theta - \nabla R\theta\|^2_{L_2(\Omega)} &= (\nabla\theta - \nabla R\theta, \nabla\theta - \nabla R\theta)\\ &= (\nabla\theta - \nabla R\theta, \nabla\theta - \nabla\pi\theta)\\ &\leqslant \|\nabla\theta - \nabla R\theta\|_{L_2(\Omega)}\|\nabla(\theta - \pi\theta)\|_{L_2(\Omega)}.\end{aligned} \tag{5.1.5}$$

This is because $\pi\theta, R\theta \in \mathcal{V}^h$. Here $\pi\theta$ is known as the linear interpolation of θ and for its definition we refer to Theorem 3.1 in Scott and Zhang (1990). The above then simplifies to the following estimate,

$$\begin{aligned}\|Q\nabla(\theta - R\theta)\|_{L_2(\Omega)} &\leqslant \|Q\nabla(\theta - \pi\theta)\|_{L_2(\Omega)} \\ &\leqslant Ch\|\theta\|_{H^2(\Omega)},\end{aligned} \tag{5.1.6}$$

using a standard estimate from (Johnson, 2009, p.90). Before we give a theorem showing a *priori* error estimate for the heat problem, we give a lemma showing the error estimate for the trapezoidal rule.

Lemma 5.1.1. *For a function $w \in C^2([0,T])$ we have the following error estimate for the trapezoidal rule approximation,*

$$\big|E(\omega)\big| = \Big|\frac{k}{2}\left(\omega(t_n) + \omega(t_{n-1})\right) - \int_{t_{n-1}}^{t_n} \omega(y)dy\Big| \leqslant Ck^2 \int_{t_{n-1}}^{t_n} |\omega''(y)|dy, \quad n > 0. \tag{5.1.7}$$

Proof. Using the Peano-Kernel theorem, (Scott, 2011, p.211), we have the following error estimate for the trapezoidal rule,

$$\begin{aligned}\big|E(\omega)\big| &= \frac{1}{2}\Big|\int_{t_{n-1}}^{t_n} \left(t_n - y\right)\left(t_{n-1} - y\right)\omega''(y)dy\Big| \\ &\leqslant \frac{1}{2}\int_{t_{n-1}}^{t_n} |t_n - y||t_{n-1} - y||\omega''(y)|dy \\ &\leqslant \frac{k^2}{2}\int_{t_{n-1}}^{t_n} |\omega''(y)|dy,\end{aligned} \tag{5.1.8}$$

where $t_{n-1} < y < t_n$, and this proves the lemma. □

Theorem 5.1.1. *Let Assumptions 2.4.1 hold. Let θ and θ_n^h be the solutions of*

(5.1.2) and (5.1.3), respectively. Then,

$$\kappa\|\theta(t_m)-\theta_m^h\|^2_{L_2(\Omega)} + k\sum_{n=1}^{m}\|Q\nabla\left(\bar\theta(t_n)-\bar\theta_n^h\right)\|^2_{L_2(\Omega)}$$
$$\leqslant Ch^2\Big(\|\theta(t_m)\|^2_{H^2(\Omega)}+\|\theta(0)\|^2_{H^2(\Omega)}+\|\theta_t\|^2_{L^2(0,T;H^2(\Omega))}\Big)+Ck^4\|\theta_{ttt}\|^2_{L_2(0,T;L_2(\Omega))}.$$

Proof. The first step is to form an error equation: we average (5.1.2) over two consecutive times, t_n and t_{n-1}, and then subtract (5.1.3) from it. Thus,

$$\kappa\left(\bar\theta_t(t_n)-\partial_t\theta_n^h, v\right)+\left(Q\nabla\left(\bar\theta_n-\bar\theta_n^h\right),\nabla v\right)$$
$$=\langle\bar G_n, v\rangle-\langle\bar G_n, v\rangle = 0, \quad \forall v\in\mathcal{V}^h. \tag{5.1.9}$$

To proceed, we define the following,

$$\eta(t_n) := \theta(t_n)-R\theta(t_n) \quad \text{and} \quad \zeta_n := \theta_n^h - R\theta(t_n). \tag{5.1.10}$$

These imply the following,

$$\theta(t_n)-\theta_n^h = \left(\theta(t_n)-R\theta(t_n)\right)-\left(\theta_n^h-R\theta(t_n)\right)=\eta(t_n)-\zeta_n. \tag{5.1.11}$$

We can also write,

$$\bar\theta_t(t_n)-\partial_t\theta_n^h=\bar\theta_t(t_n)-\partial_t\theta(t_n)+\partial_t\left(\theta(t_n)-\theta_n^h\right). \tag{5.1.12}$$

With this to hand, (5.1.9) can be re-written as,

$$\kappa\left(\partial_t\left(\theta(t_n)-\theta_n^h\right), v\right)+\left(Q\nabla(\bar\theta_n-\bar\theta_n^h),\nabla v\right)=-\kappa\left(\bar\theta_t(t_n)-\partial_t\theta(t_n), v\right), \quad \forall v\in\mathcal{V}^h. \tag{5.1.13}$$

The term $\eta(t_n)$ is the error in an elliptic problem which depends only on the exact solution and may be handled as such, whereas the term ζ_n will be the main object of the analysis. Using definitions (5.1.10), (5.1.13) now takes the following form,

$$\kappa\left(\partial_t\zeta_n, v\right) + \left(Q\nabla\bar{\zeta}_n, \nabla v\right) = -\kappa\left(\partial_t\theta(t_n) - \bar{\theta}_t(t_n), v\right) \\ + \kappa\left(\partial_t\eta(t_n), v\right) + \left(Q\nabla\bar{\eta}(t_n), \nabla v\right), \quad \forall v \in \mathcal{V}^h, \quad (5.1.14)$$

where we have moved $\eta(t_n)$ to the right as a "known" term. Also note that the last term above is zero, by definition.

Next, choose $v = 2k\bar{\zeta}_n \in \mathcal{V}^h$ in (5.1.14) to get,

$$\kappa\|\zeta_n\|^2_{L_2(\Omega)} - \kappa\|\zeta_{n-1}\|^2_{L_2(\Omega)} + 2k\|Q\nabla\bar{\zeta}_n\|^2_{L_2(\Omega)} \\ = 2k\kappa\left(\partial_t\theta(t_n) - \bar{\theta}_t(t_n), \bar{\zeta}_n\right) + 2k\kappa\left(\partial_t\eta(t_n), \bar{\zeta}_n\right). \quad (5.1.15)$$

Summing the above over $n = 1, \ldots, m \leqslant N$, yields,

$$\kappa\|\zeta_m\|^2_{L_2(\Omega)} + 2k\sum_{n=1}^{m}\|Q\nabla\bar{\zeta}_n\|^2_{L_2(\Omega)} \\ = \kappa\|\zeta_0\|^2_{L_2(\Omega)} + 2k\sum_{n=1}^{m}\kappa\left[\left(\partial_t\theta(t_n) - \bar{\theta}_t(t_n), \bar{\zeta}_n\right) + \left(\partial_t\eta(t_n), \bar{\zeta}_n\right)\right] \\ \leqslant \kappa\|\zeta_0\|^2_{L_2(\Omega)} + 2k\kappa\sum_{n=1}^{m}\|\partial_t\theta(t_n) - \bar{\theta}_t(t_n)\|_{L_2(\Omega)}\|\bar{\zeta}_n\|_{L_2(\Omega)} \\ + 2k\kappa\sum_{n=1}^{m}\|\partial_t\eta(t_n)\|_{L_2(\Omega)}\|\bar{\zeta}_n\|_{L_2(\Omega)}, \quad (5.1.16)$$

where we have used Cauchy-Schwartz. Next, using Theorem (1.3.1) (Friedrich's inequality) followed by Inequality (1.3.1) with $\epsilon = 2$, we can write (5.1.16) as,

$$\begin{aligned}
&\kappa\|\zeta_m\|^2_{L_2(\Omega)} + 2k\sum_{n=1}^{m}\|Q\nabla\bar{\zeta}_n\|^2_{L_2(\Omega)} \\
&\leqslant \kappa\|\zeta_0\|^2_{L_2(\Omega)} + 2C_F^2\kappa^2Q^{-1}k\sum_{n=1}^{m}\|\partial_t\theta(t_n) - \bar{\theta}_t(t_n)\|^2_{L_2(\Omega)} + \frac{k}{2}\sum_{n=1}^{m}\|\nabla Q\bar{\zeta}_n\|^2_{L_2(\Omega)} \\
&+ 2C_F^2\kappa^2Q^{-1}k\sum_{n=1}^{m}\|\partial_t\eta(t_n)\|^2_{L_2(\Omega)} + \frac{k}{2}\sum_{n=1}^{m}\|Q\nabla\bar{\zeta}_n\|^2_{L_2(\Omega)}. \qquad (5.1.17)
\end{aligned}$$

Rearranging this, yields,

$$\begin{aligned}
&\kappa\|\zeta_m\|^2_{L_2(\Omega)} + k\sum_{n=1}^{m}\|Q\nabla\bar{\zeta}_n\|^2_{L_2(\Omega)} \\
&\leqslant \kappa\|\zeta_0\|^2_{L_2(\Omega)} + Ck\sum_{n=1}^{m}\left(\|\partial_t\eta(t_n)\|^2_{L_2(\Omega)} + \|\partial_t\theta(t_n) - \bar{\theta}_t(t_n)\|^2_{L_2(\Omega)}\right). \qquad (5.1.18)
\end{aligned}$$

Next we deal with term $\|\partial_t\eta(t_n)\|^2_{L_2(\Omega)}$ above. We aim to bound this term by the exact solution θ and/or its derivatives. Again using Friedrich's inequality and the estimate (5.1.6), gives,

$$\begin{aligned}
\|\partial_t\eta(t_n)\|^2_{L_2(\Omega)} &\leqslant \|\partial_t\eta(t_n)\|^2_{H^1(\Omega)} \\
&\leqslant (C_F + 1)\|\nabla\partial_t\eta(t_n)\|^2_{L_2(\Omega)} \\
&\leqslant Ch^2\|\partial_t\theta(t_n)\|^2_{H^2(\Omega)}. \qquad (5.1.19)
\end{aligned}$$

But,

$$\begin{aligned}
\|\partial_t\theta(t_n)\|^2_{H^2(\Omega)} &= (\partial_t\theta(t_n), \partial_t\theta(t_n))_{H^2(\Omega)} \\
&= \frac{1}{k^2}\left(\int_{t_{n-1}}^{t_n} \theta_t(t)dt, \int_{t_{n-1}}^{t_n} \theta_s(s)ds\right)_{H^2(\Omega)} \\
&= \frac{1}{k^2}\int_{t_{n-1}}^{t_n}\int_{t_{n-1}}^{t_n} (\theta_t(t), \theta_s(s))_{H^2(\Omega)}\, dtds \\
&\leqslant \frac{1}{k^2}\int_{t_{n-1}}^{t_n}\int_{t_{n-1}}^{t_n} \|\theta_t(t)\|_{H^2(\Omega)}\|\theta_s(s)\|_{H^2(\Omega)}dtds, \quad \text{(Cauchy-Schwartz)} \\
&= \Big(\frac{1}{k}\int_{t_{n-1}}^{t_n} 1\|\theta_t(t)\|_{H^2(\Omega)}dt\Big)^2 \\
&\leqslant \frac{1}{k^2}\int_{t_{n-1}}^{t_n} 1^2dt\int_{t_{n-1}}^{t_n} \|\theta_t(t)\|^2_{H^2(\Omega)}dt = \frac{1}{k}\int_{t_{n-1}}^{t_n} \|\theta_t(t)\|^2_{H^2(\Omega)}dt
\end{aligned} \tag{5.1.20}$$

Hence, from (5.1.19) and (5.1.20), we have the following estimate,

$$\|\partial_t\eta(t_n)\|^2_{L_2(\Omega)} \leqslant \frac{Ch^2}{k}\int_{t_{n-1}}^{t_n} \|\theta_t(t)\|^2_{H^2(\Omega)}dt. \tag{5.1.21}$$

For the term $\|\partial_t\theta(t_n) - \bar{\theta}_t(t_n)\|^2_{L_2(\Omega)}$ in (5.1.18), using Lemma (5.1.1) with $\omega = \theta_t$, we can derive the following estimate,

$$\begin{aligned}
\|\partial_t\theta(t_n) - \bar{\theta}_t(t_n)\|^2_{L_2(\Omega)} &= \frac{1}{k^2}\Big\| \int_{t_{n-1}}^{t_n} \theta_t(t)dt - \frac{k}{2}\left(\theta_t(t_n) + \theta_t(t_{n-1})\right)\Big\|^2_{L_2(\Omega)} \\
&= \frac{1}{k^2}\int_\Omega \Big|\frac{k}{2}\left(\theta_t(t_n) + \theta_t(t_{n-1})\right) - \int_{t_{n-1}}^{t_n} \theta_t(t)dt\Big|^2 d\Omega \\
&\leqslant \frac{1}{k^2}\int_\Omega C^2k^4\left(\int_{t_{n-1}}^{t_n} 1|\theta_{ttt}|dt\right)^2 d\Omega \\
&\leqslant Ck^2\int_{t_{n-1}}^{t_n} 1^2dt\int_{t_{n-1}}^{t_n} \|\theta_{ttt}\|^2_{L_2(\Omega)}dt \\
&= Ck^3\int_{t_{n-1}}^{t_n} \|\theta_{ttt}\|^2_{L_2(\Omega)}dt.
\end{aligned} \tag{5.1.22}$$

Next, substituting (5.1.21) and (5.1.22) in (5.1.18), gives,

$$\begin{aligned}\kappa\|\zeta_m\|^2_{L_2(\Omega)} + k\sum_{n=1}^{m}\|Q\nabla\bar{\zeta}_n\|^2_{L_2(\Omega)} &\leqslant \kappa\|\zeta_0\|^2_{L_2(\Omega)} + Ch^2\sum_{n=1}^{m}\int_{t_{n-1}}^{t_n}\|\theta_t\|^2_{H^2(\Omega)}dt \\ &+ Ck^3\sum_{n=1}^{m}\int_{t_{n-1}}^{t_n}\|\theta_{ttt}\|^2_{L_2(\Omega)}dt \\ &\leqslant \kappa\|\zeta_0\|^2_{L_2(\Omega)} + Ch^2\|\theta_t\|^2_{L^2(0,T;H^2(\Omega))} + Ck^4\|\theta_{ttt}\|^2_{L_2(0,T;L_2(\Omega))}. \quad (5.1.23)\end{aligned}$$

To derive an estimate for $\|\zeta_0\|^2_{L_2(\Omega)}$, we use the fact that,

$$\left(\theta_0^h, v\right) = (\theta(0), v) \quad \forall v \in \mathcal{V}^h, \quad (5.1.24)$$

which is given in (3.3.6). Thus, we have,

$$\begin{aligned}\|\zeta_0\|^2_{L_2(\Omega)} &= \left(\theta_0^h - R\theta(0), \theta_0^h - R\theta(0)\right) = \left(\theta_0^h, \theta_0^h - R\theta(0)\right) - \left(R\theta(0), \theta_0^h - R\theta(0)\right) \\ &= \left(\theta(0) - R\theta(0), \theta_0^h - R\theta(0)\right) = \left(\eta(0), \theta_0^h - R\theta(0)\right) \\ &\leqslant \|\eta(0)\|_{L_2(\Omega)}\|\theta_0^h - R\theta(0)\|_{L_2(\Omega)} \\ &\Longrightarrow \|\zeta_0\|_{L_2(\Omega)} \leqslant \|\eta(0)\|_{L_2(\Omega)}. \quad (5.1.25)\end{aligned}$$

Then, using Friedrich's inequality and the estimate (5.1.6), for the term $\|\zeta(t_0)\|^2_{L_2(\Omega)}$ we can write,

$$\|\zeta(t_0)\|^2_{L_2(\Omega)} \leqslant \|\eta(0)\|^2_{L_2(\Omega)} \leqslant Ch^2\|\theta(0)\|^2_{H^2(\Omega)}. \quad (5.1.26)$$

From (5.1.11), using the triangle inequality, we have,

$$\begin{aligned}\|\theta(t_m) - \theta_m^h\|^2_{L_2(\Omega)} &= \|\zeta(t_m) - \eta_m\|^2_{L_2(\Omega)} \\ &\leqslant \left(\|\zeta(t_m)\|_{L_2(\Omega)} + \|\eta_m\|_{L_2(\Omega)}\right)^2 \\ &\leqslant 2\|\zeta(t_m)\|^2_{L_2(\Omega)} + 2\|\eta_m\|^2_{L_2(\Omega)}. \quad (5.1.27)\end{aligned}$$

Similarly,

$$k\sum_{n=1}^{m}\|Q\nabla\left(\bar{\theta}(t_n)-\bar{\theta}_n^h\right)\|_{L_2(\Omega)}^2 \leqslant 2k\sum_{n=1}^{m}\|Q\nabla\bar{\zeta}_n\|_{L_2(\Omega)}^2 + 2k\sum_{n=1}^{m}\|Q\nabla\bar{\eta}(t_n)\|_{L_2(\Omega)}^2. \tag{5.1.28}$$

Adding (5.1.27) and (5.1.28), gives

$$\begin{aligned}\|\theta(t_m)-\theta_m^h\|_{L_2(\Omega)}^2 &+ k\sum_{n=1}^{m}\|Q\nabla\left(\bar{\theta}(t_n)-\bar{\theta}_n^h\right)\|_{L_2(\Omega)}^2\\ &\leqslant 2\|\eta(t_m)\|_{L_2(\Omega)}^2 + 2k\sum_{n=1}^{m}\|Q\nabla\bar{\eta}(t_n)\|_{L_2(\Omega)}^2\\ &+ Ch^2\|\theta(0)\|_{H^2(\Omega)}^2 + Ch^2\|\theta_t\|_{L^2(0,T;H^2(\Omega))}^2 + Ck^4\|\theta_{ttt}\|_{L_2(0,T;L_2(\Omega))}^2.\end{aligned} \tag{5.1.29}$$

For the term $2\|\eta(t_m)\|_{L_2(\Omega)}^2$, we have,

$$2\|\eta(t_m)\|_{L_2(\Omega)}^2 \leqslant Ch^2\|\theta(t_m)\|_{H^2(\Omega)}^2. \tag{5.1.30}$$

Similarly,

$$2k\sum_{n=1}^{m}\|Q\nabla\bar{\eta}(t_n)\|_{L_2(\Omega)}^2 \leqslant Ckh^2\sum_{n=1}^{m}\|\bar{\theta}(t_n)\|_{H^2(\Omega)}^2 \leqslant CTh^2\|\theta\|_{L_\infty(0,T;H^2(\Omega))}^2. \tag{5.1.31}$$

Finally, substituting (5.1.30) and (5.1.31) in (5.1.29), yields the required estimate,

$$\begin{aligned}\kappa\|\theta(t_m)-\theta_m^h\|_{L_2(\Omega)}^2 &+ k\sum_{n=1}^{m}\|Q\nabla\left(\bar{\theta}(t_n)-\bar{\theta}_n^h\right)\|_{L_2(\Omega)}^2\\ &\leqslant Ch^2\|\theta(t_m)\|_{H^2(\Omega)}^2 + CTh^2\|\theta\|_{L_\infty(0,T;H^2(\Omega))}^2\\ &+ Ch^2\|\theta(0)\|_{H^2(\Omega)}^2 + Ch^2\|\theta_t\|_{L^2(0,T;H^2(\Omega))}^2 + Ck^4\|\theta_{ttt}\|_{L_2(0,T;L_2(\Omega))}^2\\ &\leqslant Ch^2\|\theta(t_m)\|_{H^2(\Omega)}^2 + Ch^2\|\theta(0)\|_{H^2(\Omega)}^2\\ &+ Ch^2\|\theta_t\|_{L^2(0,T;H^2(\Omega))}^2 + Ck^4\|\theta_{ttt}\|_{L_2(0,T;L_2(\Omega))}^2,\end{aligned} \tag{5.1.32}$$

□

and this proves the theorem.

5.2 A priori error analysis for the linear problem

Having derived the error estimate for the heat problem, we now have to hand an important result towards the main aim of this chapter: to derive an a *priori* error estimate for the linear problem. We proceed in a similar fashion as we did with the heat problem in the previous section. We recall that the weak formulation for the linear problem is given by (2.4.21), whereas the fully discrete formulation is given by (3.4.1). We now present the following theorem.

Theorem 5.2.1. *Let Assumptions 2.4.1 hold. Let $\boldsymbol{u}$ and $\boldsymbol{u}_i^h$ be the solutions of (2.4.21) and (3.4.1), respectively. For k a positive constant, small enough, the following estimate holds:*

$$\|\boldsymbol{u}(t_i) - \boldsymbol{u}_i^h\|_E \leqslant C(h + k^2)$$

where the positive constant C depends on exact solutions, derivatives of exact solutions and other constants.

Proof. We define the Ritz projection, $R\boldsymbol{u}(t_i)$ as:

$$a\left((\boldsymbol{u} - R\boldsymbol{u})(t_i), v\right) = 0 \quad \forall \boldsymbol{v} \in V^h,\ \ t_i \in I^k,$$

where $i \in \{0, \ldots, N\}$, and set, for $t_i \in I^k$,

$$\eta(t_i) := \boldsymbol{u}(t_i) - R\boldsymbol{u}(t_i) \quad \text{and} \quad \zeta_i := \boldsymbol{u}_i^h - R\boldsymbol{u}(t_i),$$

which then gives,

$$\boldsymbol{u}_i^h - \boldsymbol{u}(t_i) = \zeta_i - \eta(t_i) \tag{5.2.1}$$

Note that η and ζ here are analogous to the those used in the previous section, however they have different meanings. We subtract the weak formulation (2.4.21) with $t = t_i$ from the fully discrete scheme (3.4.1). In the result that follows, we have added and subtracted the following terms,

$$\begin{aligned}
&\frac{k}{2}\sum_{j=1}^{i}\Big(\varphi_s(t_i - t_j)a(\boldsymbol{u}(t_j), \boldsymbol{v}) + \varphi_s(t_i - t_{j-1})a(\boldsymbol{u}(t_{j-1}), \boldsymbol{v})\Big) \quad \text{and} \\
&\frac{k}{2}\sum_{j=1}^{i}\Big[\Big(\alpha\boldsymbol{D}\varphi_s(t_i - t_j)(\theta(t_j) - \theta_r)\boldsymbol{I_0}, \boldsymbol{\varepsilon}(\boldsymbol{v})\Big) \\
&\qquad\qquad + \Big(\alpha\boldsymbol{D}\varphi_s(t_i - t_{j-1})(\theta(t_{j-1}) - \theta_r)\boldsymbol{I_0}, \boldsymbol{\varepsilon}(\boldsymbol{v})\Big)\Big].
\end{aligned} \tag{5.2.2}$$

These terms give us the error terms $\boldsymbol{u}_j^h - \boldsymbol{u}(t_j)$ and $\theta_j^h - \theta(t_j)$, respectively. In addition, we are also able to use the trapezoidal rule for approximation. Thus we have,

$$
\begin{aligned}
a(\boldsymbol{u}_i^h - \boldsymbol{u}(t_i), \boldsymbol{v}) = \frac{k}{2}\sum_{j=1}^{i} \Big[&\varphi_s(t_i - t_j) a(\boldsymbol{u}_j^h - \boldsymbol{u}(t_j), \boldsymbol{v}) \\
&+ \varphi_s(t_i - t_{j-1}) a(\boldsymbol{u}_{j-1}^h - \boldsymbol{u}(t_{j-1}), \boldsymbol{v})\Big] + \big(\alpha \boldsymbol{D}(\theta_i^h - \theta(t_i))\boldsymbol{I_0}, \boldsymbol{\varepsilon}(\boldsymbol{v})\big)_\Omega \\
- \frac{k}{2}\sum_{j=1}^{i} \Big[&\Big(\alpha \boldsymbol{D}\varphi_s(t_i - t_j)(\theta_j^h - \theta(t_j))\boldsymbol{I_0}, \boldsymbol{\varepsilon}(\boldsymbol{v})\Big) \\
&+ \Big(\alpha \boldsymbol{D}\varphi_s(t_i - t_{j-1})(\theta_{j-1}^h - \theta(t_{j-1}))\boldsymbol{I_0}, \boldsymbol{\varepsilon}(\boldsymbol{v})\Big)\Big] \\
- \Big[\int_0^{t_i} &\varphi_s(t_i - s) a(\boldsymbol{u}(s), \boldsymbol{v}) ds \\
&- \frac{k}{2}\sum_{j=1}^{i}\Big(\varphi_s(t_i - t_j) a(\boldsymbol{u}(t_j), \boldsymbol{v}) + \varphi_s(t_i - t_{j-1}) a(\boldsymbol{u}(t_{j-1}), \boldsymbol{v})\Big)\Big] \\
+ \int_0^{t_i} &\Big(\alpha \boldsymbol{D}\varphi_s(t_i - s)(\theta(s) - \theta_r)\boldsymbol{I_0}, \boldsymbol{\varepsilon}(\boldsymbol{v})\Big) ds \\
- \frac{k}{2}\sum_{j=1}^{i} \Big[&\Big(\alpha \boldsymbol{D}\varphi_s(t_i - t_j)(\theta(t_j) - \theta_r)\boldsymbol{I_0}, \boldsymbol{\varepsilon}(\boldsymbol{v})\Big) \\
&+ \Big(\alpha \boldsymbol{D}\varphi_s(t_i - t_{j-1})(\theta(t_{j-1}) - \theta_r)\boldsymbol{I_0}, \boldsymbol{\varepsilon}(\boldsymbol{v})\Big)\Big]. \qquad (5.2.3)
\end{aligned}
$$

Using (5.2.1), this can be re-written as,

$$
\begin{aligned}
a(\zeta_i,\boldsymbol{v}) &= a(\eta(t_i),\boldsymbol{v}) + \frac{k}{2}\sum_{j=1}^{i}\left[\varphi_s(t_i-t_j)a(\zeta_j,\boldsymbol{v}) + \varphi_s(t_i-t_{j-1})a(\zeta_{j-1},\boldsymbol{v})\right] \\
&- \frac{k}{2}\sum_{j=1}^{i}\left[\varphi_s(t_i-t_j)a(\eta(t_j),\boldsymbol{v}) + \varphi_s(t_i-t_{j-1})a(\eta(t_{j-1}),\boldsymbol{v})\right] + \big(\alpha\boldsymbol{D}(\theta_i^h-\theta(t_i))\boldsymbol{I_0},\boldsymbol{\varepsilon}(\boldsymbol{v})\big)_\Omega \\
&- \frac{k}{2}\sum_{j=1}^{i}\Big[\big(\alpha\boldsymbol{D}\varphi_s(t_i-t_j)(\theta_j^h-\theta(t_j))\boldsymbol{I_0},\boldsymbol{\varepsilon}(\boldsymbol{v})\big) \\
&\qquad + \big(\alpha\boldsymbol{D}\varphi_s(t_i-t_{j-1})(\theta_{j-1}^h-\theta(t_{j-1}))\boldsymbol{I_0},\boldsymbol{\varepsilon}(\boldsymbol{v})\big)\Big] \\
&- \Big[\int_0^{t_i}\varphi_s(t_i-s)a(\boldsymbol{u}(s),\boldsymbol{v})ds \\
&\qquad - \frac{k}{2}\sum_{j=1}^{i}\big[\varphi_s(t_i-t_j)a(\boldsymbol{u}(t_j),\boldsymbol{v}) + \varphi_s(t_i-t_{j-1})a(\boldsymbol{u}(t_{j-1}),\boldsymbol{v})\big]\Big] \\
&+ \int_0^{t_i}\left(\alpha\boldsymbol{D}\varphi_s(t_i-s)(\theta(s)-\theta_r)\boldsymbol{I_0},\boldsymbol{\varepsilon}(\boldsymbol{v})\right)ds \\
&\qquad - \frac{k}{2}\sum_{j=1}^{i}\Big[\big(\alpha\boldsymbol{D}\varphi_s(t_i-t_j)(\theta(t_j)-\theta_r)\boldsymbol{I_0},\boldsymbol{\varepsilon}(\boldsymbol{v})\big) \\
&\qquad + \big(\alpha\boldsymbol{D}\varphi_s(t_i-t_{j-1})(\theta(t_{j-1})-\theta_r)\boldsymbol{I_0},\boldsymbol{\varepsilon}(\boldsymbol{v})\big)\Big]. \qquad (5.2.4)
\end{aligned}
$$

Next, put $\boldsymbol{v} = \zeta_i \in V^h$ above, to get

$$
\begin{aligned}
a(\zeta_i, \zeta_i) &= a(\eta(t_i), \zeta_i) + \frac{k}{2}\sum_{j=1}^{i}\Big[\varphi_s(t_i - t_j)a(\zeta_j, \zeta_i) + \varphi_s(t_i - t_{j-1})a(\zeta_{j-1}, \zeta_i)\Big] \\
&- \frac{k}{2}\sum_{j=1}^{i}\Big[\varphi_s(t_i - t_j)a(\eta(t_j), \zeta_i) + \varphi_s(t_i - t_{j-1})a(\eta(t_{j-1}), \zeta_i)\Big] \\
&\qquad + \big(\alpha \boldsymbol{D}(\theta_i^h - \theta(t_i))\boldsymbol{I_0}, \boldsymbol{\varepsilon}(\zeta_i)\big)_\Omega \\
&- \frac{k}{2}\sum_{j=1}^{i}\Big[\Big(\alpha \boldsymbol{D}\varphi_s(t_i - t_j)(\theta_j^h - \theta(t_j))\boldsymbol{I_0}, \boldsymbol{\varepsilon}(\zeta_i)\Big) \\
&\qquad + \Big(\alpha \boldsymbol{D}\varphi_s(t_i - t_{j-1})(\theta_{j-1}^h - \theta(t_{j-1}))\boldsymbol{I_0}, \boldsymbol{\varepsilon}(\zeta_i)\Big)\Big] \\
&- \Big[\int_0^{t_i}\varphi_s(t_i - s)a(\boldsymbol{u}(s), \zeta_i)ds \\
&\qquad - \frac{k}{2}\sum_{j=1}^{i}\Big(\varphi_s(t_i - t_j)a(\boldsymbol{u}(t_j), \zeta_i) + \varphi_s(t_i - t_{j-1})a(\boldsymbol{u}(t_{j-1}), \zeta_i)\Big)\Big] \\
&+ \int_0^{t_i}\Big(\alpha \boldsymbol{D}\varphi_s(t_i - s)(\theta(s) - \theta_r)\boldsymbol{I_0}, \boldsymbol{\varepsilon}(\zeta_i)\Big)ds \\
&\qquad - \frac{k}{2}\sum_{j=1}^{i}\Big[\Big(\alpha \boldsymbol{D}\varphi_s(t_i - t_j)(\theta(t_j) - \theta_r)\boldsymbol{I_0}, \boldsymbol{\varepsilon}(\zeta_i)\Big) \\
&\qquad + \Big(\alpha \boldsymbol{D}\varphi_s(t_i - t_{j-1})(\theta(t_{j-1}) - \theta_r)\boldsymbol{I_0}, \boldsymbol{\varepsilon}(\zeta_i)\Big)\Big].
\end{aligned}
\tag{5.2.5}
$$

The first two sums above give,

$$
\begin{aligned}
&\frac{k}{2}\sum_{j=1}^{i}[\varphi_s(t_i - t_j)a(\zeta_j, \zeta_i) + \varphi_s(t_i - t_{j-1})a(\zeta_{j-1}, \zeta_i)] \\
&- \frac{k}{2}\sum_{j=1}^{i}[\varphi_s(t_i - t_j)a(\eta(t_j), \zeta_i) + \varphi_s(t_i - t_{j-1})a(\eta(t_{j-1}), \zeta_i)] \\
&= k\sum_{j=0}^{i}\varphi_s(t_i - t_j)a(\zeta_j, \zeta_i) - k\sum_{j=0}^{i}\varphi_s(t_i - t_j)a(\eta(t_j), \zeta_i) + \frac{k}{2}\varphi_s(t_i)a(\eta(t_0), \zeta_i) \\
&- \frac{k}{2}\varphi_s(t_i)a(\zeta_0, \zeta_i) - \frac{k}{2}\varphi_s(0)a(\zeta_i, \zeta_i) + \frac{k}{2}\varphi_s(0)a(\eta(t_i), \zeta_i).
\end{aligned}
\tag{5.2.6}
$$

Substituting this in (5.2.5) and using the definition of the energy norm, that is $\|\cdot\|_E^2 = a(\cdot,\cdot)$, yields,

$$\begin{aligned}
&\|\zeta_i\|_E^2 \leqslant \|\eta(t_i)\|_E\|\zeta_i\|_E + C_1 k\sum_{j=0}^{i}\|\zeta_j\|_E\|\zeta_i\|_E + C_1 k\sum_{j=0}^{i}\|\eta(t_j)\|_E\|\zeta_i\|_E \\
&+ \frac{k}{2}\varphi_s(t_i)\|\zeta_0\|_E\|\zeta_i\|_E + \frac{k}{2}\varphi_s(t_i)\|\eta(t_0)\|_E\|\zeta_i\|_E + \frac{k}{2}\varphi_s(0)\|\zeta_i\|_E^2 + \frac{k}{2}\varphi_s(0)\|\eta(t_i)\|_E\|\zeta_i\|_E \\
&+ C(\alpha,\boldsymbol{D})\|\theta_i^h - \theta(t_i)\|_{L_2(\Omega)}\|\zeta_i\|_E + C(\alpha,\boldsymbol{D})C_1 k\sum_{j=1}^{i}\|\theta_j^h - \theta(t_j)\|_{L_2(\Omega)}\|\zeta_i\|_E \\
&+ C(\alpha,\boldsymbol{D})C_2 k\sum_{j=1}^{i}\|\theta_{j-1}^h - \theta(t_{j-1})\|_{L_2(\Omega)}\|\zeta_i\|_E \\
&+ \sum_{j=1}^{i}\left[Ck^2\int_{t_{j-1}}^{t_j}|\,(\varphi_s(t_i-s)a(\boldsymbol{u}(s),\zeta_i))''\,|ds\right] \\
&+ \sum_{j=1}^{i}\left[Ck^2\int_{t_{j-1}}^{t_j}|\,((\alpha\boldsymbol{D}\varphi_s(t_i-s)(\theta(s)-\theta_r)\boldsymbol{I_0},\boldsymbol{\varepsilon}(\zeta_i)))''\,|ds\right]. \qquad (5.2.7)
\end{aligned}$$

Here $C_1 = C_2 = \max\limits_{0\leqslant j\leqslant i}\varphi_s(t_i - t_j)$. The last two terms above have been obtained by applying the trapezoidal rule (Lemma 5.1.1) to the appropriate terms in (5.2.5). Thus, we have

$$\begin{aligned}
&\int_0^{t_i}\varphi_s(t_i-s)a(\boldsymbol{u}(s),\boldsymbol{v})ds \\
&\qquad - \frac{k}{2}\sum_{j=1}^{i}\left[\varphi_s(t_i-t_j)a(\boldsymbol{u}(t_j),\boldsymbol{v}) + \varphi_s(t_i-t_{j-1})a(\boldsymbol{u}(t_{j-1}),\boldsymbol{v})\right] \\
&\qquad \leqslant \sum_{j=1}^{i}\left[Ck^2\int_{t_{j-1}}^{t_j}|\,(\varphi_s(t_i-s)a(\boldsymbol{u}(s),\zeta_i))''\,|ds\right], \qquad (5.2.8)
\end{aligned}$$

and,

$$\begin{aligned}
&\int_0^{t_i} \Big(\alpha \boldsymbol{D}\varphi_s(t_i - s)(\theta(s) - \theta_r)\boldsymbol{I_0}, \boldsymbol{\varepsilon}(\zeta_i)\Big) ds \\
&\qquad - \frac{k}{2}\sum_{j=1}^{i} \Big[\Big(\alpha \boldsymbol{D}\varphi_s(t_i - t_j)(\theta(t_j) - \theta_r)\boldsymbol{I_0}, \boldsymbol{\varepsilon}(\zeta_i)\Big) \\
&\qquad + \Big(\alpha \boldsymbol{D}\varphi_s(t_i - t_{j-1})(\theta(t_{j-1}) - \theta_r)\boldsymbol{I_0}, \boldsymbol{\varepsilon}(\zeta_i)\Big)\Big] \\
&\qquad \leqslant \sum_{j=1}^{i} \left[Ck^2 \int_{t_{j-1}}^{t_j} |\left((\alpha \boldsymbol{D}\varphi_s(t_i - s)(\theta(s) - \theta_r)\boldsymbol{I_0}, \boldsymbol{\varepsilon}(\zeta_i)\right))'' | ds\right]. \qquad (5.2.9)
\end{aligned}$$

Labelling the terms on the right-hand side of (5.2.7) in order as $I, II, \ldots, XII$, using the Inequality 1.3.1 we can derive the following estimates by considering these terms individually:

Term I:

$$\begin{aligned}
\|\eta(t_i)\|_E \|\zeta_i\|_E &\leqslant \frac{1}{2\epsilon_1 2}\|\eta(t_i)\|_E^2 + \frac{2\epsilon_1}{2}\|\zeta_i\|_E^2 \\
&= \frac{1}{4\epsilon_1}\|\eta(t_i)\|_E^2 + \epsilon_1\|\zeta_i\|_E^2. \qquad (5.2.10)
\end{aligned}$$

Term II:

$$\begin{aligned}
C_1 k \sum_{j=0}^{i} \|\zeta_j\|_E \|\zeta_i\|_E &\leqslant C_1 k \left[\sum_{j=0}^{i} \left(\frac{C_1 T}{2\epsilon_2}\frac{1}{2}\|\zeta_j\|_E^2 + \frac{2\epsilon_2}{C_1 T}\frac{1}{2}\|\zeta_i\|_E^2\right)\right] \\
&= C_1 k \frac{C_1 T}{4\epsilon_2}\sum_{j=0}^{i}\|\zeta_j\|_E^2 + C_1 k \frac{2\epsilon_2}{C_1 T}\frac{1}{2}\sum_{j=0}^{i}\|\zeta_i\|_E^2 \\
&\leqslant \frac{CkT}{4\epsilon_2}\sum_{j=0}^{i-1}\|\zeta_j\|_E^2 + \frac{CkT}{4\epsilon_2}\|\zeta_i\|_E^2 + \epsilon_2\|\zeta_i\|_E^2. \qquad (5.2.11)
\end{aligned}$$

Term III:

$$
\begin{aligned}
C_1k\sum_{j=0}^{i}\|\eta(t_j)\|_E\|\zeta_i\|_E &\leqslant C_1k\left[\sum_{j=0}^{i}\left(\frac{C_1T}{2\epsilon_3}\frac{1}{2}\|\eta(t_j)\|_E^2+\frac{2\epsilon_3}{C_1T}\frac{1}{2}\|\zeta_i\|_E^2\right)\right]\\
&= C_1k\frac{C_1T}{2\epsilon_3}\frac{1}{2}\sum_{j=0}^{i}\|\eta(t_j)\|_E^2+C_1k\frac{2\epsilon_3}{C_1T}\frac{1}{2}\sum_{j=0}^{i}\|\zeta_i\|_E^2\\
&\leqslant \frac{CTk}{4\epsilon_3}\sum_{j=0}^{i}\|\eta(t_j)\|_E^2+\epsilon_3\|\zeta_i\|_E^2. \qquad (5.2.12)
\end{aligned}
$$

Term IV:

$$
\begin{aligned}
\frac{k}{2}\varphi_s(t_i)\|\zeta_0\|_E\|\zeta_i\|_E &\leqslant \tilde{C}_\varphi k\left(\frac{\tilde{C}_\varphi k}{2\epsilon_4}\frac{1}{2}\|\zeta_0\|_E^2+\frac{2\epsilon_4}{\tilde{C}_\varphi k}\frac{1}{2}\|\zeta_i\|_E^2\right)\\
&= \frac{Ck^2}{4\epsilon_4}\|\zeta_0\|_E^2+\epsilon_4\|\zeta_i\|_E^2, \qquad (5.2.13)
\end{aligned}
$$

where $\frac{1}{2}\varphi_s(t_i)\leqslant\frac{1}{2}|\varphi'(0)|=\tilde{C}_\varphi$. Here we first need to deal with the error term $\|\zeta_0\|_E$. From (2.4.21) with $t=0$ and (3.4.1) with $i=0$, and $v=\zeta_0\in V^h$, we get

$$
a\big(\boldsymbol{u}_0^h-R\boldsymbol{u}(0),\zeta_0\big)=a\big(\boldsymbol{u}(0)-R\boldsymbol{u}(0),\zeta_0\big)+\big(\alpha\boldsymbol{D}(\theta_0^h-\theta(0))\boldsymbol{I_0},\boldsymbol{\varepsilon}(\zeta_0)\big). \qquad (5.2.14)
$$

This then gives,

$$
\begin{aligned}
\|\zeta_0\|_E^2 &\leqslant \|\eta(0)\|_E\|\zeta_0\|_E+C(\alpha,\boldsymbol{D})\|\theta_0^h-\theta(0)\|_{L_2(\Omega)}\\
&= \frac{\epsilon}{2}\|\eta(0)\|_E^2+\frac{1}{2\epsilon}\|\zeta_0\|_E^2+\frac{1}{2\epsilon}\|\zeta_0\|_E^2+\frac{\epsilon}{2}Ch^2\|\theta(0)\|_{H^2(\Omega)}^2, \qquad (5.2.15)
\end{aligned}
$$

which, with $\epsilon=2$, becomes

$$
\|\zeta_0\|_E^2\leqslant 2\|\eta(0)\|_E^2+Ch^2\|\theta(0)\|_{H^2(\Omega)}^2\leqslant Ch^2\|\theta(0)\|_{H^2(\Omega)}^2. \qquad (5.2.16)
$$

Term V:

$$\frac{k}{2}\varphi_s(t_i)\|\eta(t_0)\|_E\|\zeta_i\|_E \leqslant \tilde{C}_\varphi k\left(\frac{\tilde{C}_\varphi k}{2\epsilon_5}\frac{1}{2}\|\eta(t_0)\|_E^2 + \frac{2\epsilon_5}{\tilde{C}_\varphi k}\frac{1}{2}\|\zeta_i\|_E^2\right)$$
$$= \frac{Ck^2}{4\epsilon_5}\|\eta(t_0)\|_E^2 + \epsilon_5\|\zeta_i\|_E^2, \tag{5.2.17}$$

Term VI:

$$\frac{k}{2}\varphi_s(0)\|\zeta_i\|_E^2 \leqslant Ck\|\zeta_i\|_E^2$$

Term VII:

$$\frac{k}{2}\varphi_s(0)\|\eta(t_i)\|_E\|\zeta_i\|_E \leqslant Ck\left(\frac{Ck}{2\epsilon_6}\frac{1}{2}\|\eta(t_i)\|_E^2 + \frac{2\epsilon_6}{Ck}\frac{1}{2}\|\zeta_i\|_E^2\right)$$
$$= \frac{Ck^2}{2\epsilon_6}\|\eta(t_i)\|_E^2 + \epsilon_6\|\zeta_i\|_E^2. \tag{5.2.18}$$

Term VIII:

$$C\|\theta_i^h - \theta(t_i)\|_{L_2(\Omega)}\|\zeta_i\|_E \leqslant C\left(\frac{C}{2\epsilon_7}\frac{1}{2}\|\theta_i^h - \theta(t_i)\|_{L_2(\Omega)}^2 + \frac{2\epsilon_7}{C}\frac{1}{2}\|\zeta_i\|_E^2\right)$$
$$= \frac{C}{4\epsilon_7}\|\theta_i^h - \theta(t_i)\|_{L_2(\Omega)}^2 + \epsilon_7\|\zeta_i\|_E^2. \tag{5.2.19}$$

Term IX:

$$Ck\sum_{j=1}^{i}\|\theta_j^h - \theta(t_j)\|_{L_2(\Omega)}\|\zeta_i\|_E \leqslant Ck\sum_{j=1}^{i}\left(\frac{CT}{2\epsilon_8}\frac{1}{2}\|\theta_j^h - \theta(\theta_j)\|_{L_2(\Omega)}^2 + \frac{2\epsilon_8}{CT}\frac{1}{2}\|\zeta_i\|_E^2\right)$$
$$\leqslant \frac{CkT}{4\epsilon_8}\sum_{j=1}^{i}\|\theta_j^h - \theta(t_j)\|_{L_2(\Omega)}^2 + \epsilon_8\|\zeta_i\|_E^2. \tag{5.2.20}$$

Term X:

$$Ck\sum_{j=i}^{i}\|\theta_{j-1}^h-\theta(t_{j-1})\|_{L_2(\Omega)}\|\zeta_i\|_E \leqslant Ck\sum_{j=0}^{i-1}\left(\frac{CT}{2\epsilon_9}\frac{1}{2}\|\theta_j^h-\theta(\theta_j)\|^2_{L_2(\Omega)}+\frac{2\epsilon_9}{CT}\frac{1}{2}\|\zeta_i\|_E^2\right)$$
$$\leqslant \frac{CkT}{4\epsilon_9}\sum_{j=0}^{i-1}\|\theta_j^h-\theta(t_j)\|^2_{L_2(\Omega)}+\epsilon_9\|\zeta_i\|^2_E. \quad (5.2.21)$$

Term XI:

$$\int_{t_{j-1}}^{t_j}|\big(\varphi_s(t_i-s)a(\boldsymbol{u}(s),\boldsymbol{\zeta}_i)\big)''|ds \leqslant C_\varphi''' \int_{t_{j-1}}^{t_j}\Big(\|\boldsymbol{u}(s)\|_E+\|\boldsymbol{u}'(s)\|_E+\|\boldsymbol{u}''(s)\|_E\Big)\|\boldsymbol{\zeta}_i\|_E ds$$
$$\leqslant \sqrt{3}C_\varphi'''\int_{t_{j-1}}^{t_j}\Big(\|\boldsymbol{u}(s)\|^2_E+\|\boldsymbol{u}'(s)\|^2_E+\|\boldsymbol{u}''(s)\|^2_E\Big)^{\frac{1}{2}}ds\|\boldsymbol{\zeta}_i\|_E$$
$$\leqslant \frac{CTk}{2\epsilon_{10}}\frac{1}{2}\left(\int_{t_{j-1}}^{t_j}\Big(\|\boldsymbol{u}(s)\|^2_E+\|\boldsymbol{u}'(s)\|^2_E+\|\boldsymbol{u}''(s)\|^2_E\Big)^{\frac{1}{2}}ds\right)^2+\frac{2\epsilon_{10}}{CTk}\frac{1}{2}\|\boldsymbol{\zeta}_i\|^2_E$$
$$\leqslant \frac{CTk}{4\epsilon_{10}}\left(\int_{t_{j-1}}^{t_j}1^2ds\right)\int_{t_{j-1}}^{t_j}\Big(\|\boldsymbol{u}(s)\|^2_E+\|\boldsymbol{u}'(s)\|^2_E+\|\boldsymbol{u}''(s)\|^2_E\Big)ds+\frac{\epsilon_{10}}{CTk}\|\boldsymbol{\zeta}_i\|^2_E$$
$$=\frac{CTk^2}{4\epsilon_{10}}\int_{t_{j-1}}^{t_j}\Big(\|\boldsymbol{u}(s)\|^2_E+\|\boldsymbol{u}'(s)\|^2_E+\|\boldsymbol{u}''(s)\|^2_E\Big)ds+\frac{\epsilon_{10}}{CTk}\|\boldsymbol{\zeta}_i\|^2_E. \quad (5.2.22)$$

The notations: " $'$ ", " $''$ " and " $'''$ ", denote the first, second and third order derivatives, respectively. Hence,

$$\sum_{j=1}^{i}Ck^2\int_{t_{j-1}}^{t_j}|\big(\varphi_s(t_i-s)a(\boldsymbol{u}(s),\boldsymbol{\zeta}_i)\big)''|ds \leqslant \frac{CTk^4}{4\epsilon_9}\|\boldsymbol{u}\|_{H^2(0,T;E)}+\frac{k\epsilon_{10}}{T}\sum_{j=1}^{i}\|\boldsymbol{\zeta}_i\|^2_E$$
$$\leqslant \frac{CTk^4}{4\epsilon_{10}}\|\boldsymbol{u}\|^2_{H^2(0,T;E)}+\epsilon_{10}\|\boldsymbol{\zeta}_i\|^2_E. \quad (5.2.23)$$

Term XII:

$$\begin{aligned}
&\int_{t_{j-1}}^{t_j} |\big(\alpha \boldsymbol{D}\varphi_s(t_i-s)(\theta(s)-\theta_r)\boldsymbol{I_0}, \boldsymbol{\varepsilon}(\boldsymbol{\zeta}_i)\big)''|ds \\
&\leqslant C(\alpha,\boldsymbol{D})C_\varphi''' \int_{t_{j-1}}^{t_j} \Big(\|\theta(s)-\theta_r\|_{L_2(\Omega)} + \|(\theta(s)-\theta_r)'\|_{L_2(\Omega)} \\
&\qquad\qquad + \|(\theta(s)-\theta_r)''\|_{L_2(\Omega)}\Big)\|\boldsymbol{\zeta}_i\|_E ds \\
&\leqslant \sqrt{3}C(\alpha,\boldsymbol{D})C_\varphi''' \int_{t_{j-1}}^{t_j} \Big(\|\theta(s)-\theta_r\|^2_{L_2(\Omega)} + \|(\theta(s)-\theta_r)'\|^2_{L_2(\Omega)} \\
&\qquad\qquad + \|(\theta(s)-\theta_r)''\|^2_{L_2(\Omega)}\Big)^{\frac{1}{2}} ds \|\boldsymbol{\zeta}_i\|_E \\
&\leqslant \frac{CTk}{2\epsilon_{11}}\frac{1}{2}\Big(\int_{t_{j-1}}^{t_j} \big(\|\theta(s)-\theta_r\|^2_{L_2(\Omega)} + \|(\theta(s)-\theta_r)'\|^2_{L_2(\Omega)} + \|(\theta(s)-\theta_r)''\|^2_{L_2(\Omega)}\big)^{\frac{1}{2}} ds\Big)^2 \\
&\qquad\qquad + \frac{\epsilon_{11}}{CTk}\|\boldsymbol{\zeta}_i\|^2_E \\
&\leqslant \frac{CTk^2}{4\epsilon_{11}} \int_{t_{j-1}}^{t_j} \big(\|\theta(s)-\theta_r\|^2_{L_2(\Omega)} + \|(\theta(s)-\theta_r)'\|^2_{L_2(\Omega)} + \|(\theta(s)-\theta_r)''\|^2_{L_2(\Omega)}\big) ds \\
&\qquad\qquad + \frac{\epsilon_{11}}{CTk}\|\boldsymbol{\zeta}_i\|^2_E. \qquad (5.2.24)
\end{aligned}$$

Hence,

$$\begin{aligned}
&\sum_{j=1}^{i} Ck^2 \int_{t_{j-1}}^{t_j} |\big(\alpha \boldsymbol{D}\varphi_s(t_i-s)(\theta(s)-\theta_r)\boldsymbol{I_0}, \boldsymbol{\varepsilon}(\boldsymbol{\zeta}_i)\big)''|ds \\
&\qquad \leqslant \frac{CTk^4}{4\epsilon_{11}}\|\theta-\theta_r\|^2_{H^2(0,T;L_2(\Omega))} + \frac{k\epsilon_{11}}{T}\sum_{j=1}^{i}\|\boldsymbol{\zeta}_i\|^2_E \\
&\qquad \leqslant \frac{CTk^4}{4\epsilon_{11}}\|\theta-\theta_r\|^2_{H^2(0,T;L_2(\Omega))} + \epsilon_{11}\|\boldsymbol{\zeta}_i\|^2_E. \qquad (5.2.25)
\end{aligned}$$

Substitute these estimates back in (5.2.7), by choosing $\epsilon_1 = \epsilon_2 = \ldots = \epsilon_{11} = \dfrac{1}{12}$. We also make use of the estimate $\|\eta(t)\| \leqslant C_R h|\boldsymbol{u}(t)|_{H^2(\Omega)}$, see Shaw et al. (1997). Then, taking $\|\boldsymbol{\zeta}_i\|_E^2$ to the left as a common factor, we can write (5.2.7) as,

$$\begin{aligned}
&\left(\frac{1}{12} - k\big(\frac{3CT}{11} + C\big)\right)\|\boldsymbol{\zeta}_i\|_E^2 \\
&\leqslant Ch^2|\boldsymbol{u}(t_i)|^2_{H^2(\Omega)} + CT^2h^2|\boldsymbol{u}|^2_{L_\infty(0,T;H^2(\Omega))} + Ch^2k^2|\boldsymbol{u}(t_0)|^2_{H^2(\Omega)} + Ch^2k^2\|\theta(0)\|^2_{H^2(\Omega)} \\
&+ Ch^2k^2|\boldsymbol{u}(t_i)|_{H^2(\Omega)} + C\|\theta_i^h - \theta(t_i)\|^2_{L_2(\Omega)} + CTk\sum_{j=1}^{i}\|\theta_j^h - \theta(t_j)\|^2_{L_2(\Omega)} \\
&+ CTk\sum_{j=0}^{i-1}\|\theta_j^h - \theta(t_j)\|^2_{L_2(\Omega)} + CTk^4\|\boldsymbol{u}\|^2_{H^2(0,T;E)} + CTk^4\|\theta - \theta_r\|^2_{H^2(0,T;L_2(\Omega))} \\
&+ CTk\sum_{j=0}^{i-1}\|\boldsymbol{\zeta}_j\|_E^2. \qquad (5.2.26)
\end{aligned}$$

Let $\epsilon_0 := \dfrac{1}{12} - k\big(\dfrac{3CT}{11} + C\big)$. We require that $\epsilon_0 > 0$, which implies that $k < \dfrac{1}{12C}$. Dividing (5.2.26) through by ϵ_0, and recalling that T is also a constant, yields

$$\begin{aligned}
\|\zeta_i\|_E^2 &\leqslant Ch^2|\boldsymbol{u}(t_i)|^2_{H^2(\Omega)} + Ch^2|\boldsymbol{u}|^2_{L_\infty(0,T;H^2(\Omega))} + Ch^2k^2|\boldsymbol{u}(t_0)|^2_{H^2(\Omega)} + Ch^2k^2\|\theta(0)\|^2_{H^2(\Omega)} \\
&+ Ch^2k^2|\boldsymbol{u}(t_i)|^2_{H^2(\Omega)} + C\|\theta_i^h - \theta(t_i)\|^2_{L_2(\Omega)} + Ck\sum_{j=1}^{i}\|\theta_j^h - \theta(t_j)\|^2_{L_2(\Omega)} \\
&+ Ck\sum_{j=0}^{i-1}\|\theta_j^h - \theta(t_j)\|^2_{L_2(\Omega)} + Ck^4\|\boldsymbol{u}\|^2_{H^2(0,T;E)} + Ck^4\|\theta - \theta_r\|^2_{H^2(0,T;L_2(\Omega))} \\
&+ Ck\sum_{j=0}^{i-1}\|\boldsymbol{\zeta}_j\|_E^2. \qquad (5.2.27)
\end{aligned}$$

Substituting the result for the heat error estimate from (5.1.32) gives,

$$\begin{aligned}
\|\zeta_i\|_E^2 \leqslant{}& Ch^2|\boldsymbol{u}(t_i)|^2_{H^2(\Omega)} + Ch^2|\boldsymbol{u}|^2_{L_\infty(0,T;H^2(\Omega))} + Ch^2k^2|\boldsymbol{u}(t_0)|^2_{H^2(\Omega)} + Ch^2k^2\|\theta(0)\|^2_{H^2(\Omega)} \\
&+ Ch^2k^2|\boldsymbol{u}(t_i)|^2_{H^2(\Omega)} + Ch^2\|\theta\|^2_{L_\infty(0,T;H^2(\Omega))} + Ch^2\|\theta(0)\|^2_{H^2(\Omega)} \\
&+ Ch^2\|\theta_t\|^2_{L^2(0,T;H^2(\Omega))} + Ck^4\|\theta_{ttt}\|^2_{L_2(0,T;L_2(\Omega))} + Ck^4\|\boldsymbol{u}\|^2_{H^2(0,T;E)} \\
&+ Ck^4\|\theta - \theta_r\|^2_{H^2(0,T;L_2(\Omega))} + Ck\sum_{j=0}^{i-1}\|\zeta_j\|_E^2 \\
\leqslant{}& C(h^2 + k^4) + Ck\sum_{j=0}^{i-1}\|\zeta_j\|_E^2. \qquad (5.2.28)
\end{aligned}$$

And using the Gronwall inequality (Lemma (1.4.2)), yields

$$\|\zeta_i\|_E^2 \leqslant Ce^{c_1 T}(h^2 + k^4). \qquad (5.2.29)$$

Using the triangle inequality, we can write

$$\begin{aligned}
\|\boldsymbol{u}(t_i) - \boldsymbol{u}_i^h\|_E^2 &\leqslant 2\|\eta(t_i)\|_E^2 + 2\|\zeta_i\|_E^2 \\
&\leqslant Ch^2|\boldsymbol{u}|^2_{H^2(\Omega)} + Ce^{c_1 T}(h^2 + k^4). \qquad (5.2.30)
\end{aligned}$$

Finally, taking square roots, we are arrive at,

$$\|\boldsymbol{u}(t_i) - \boldsymbol{u}_i^h\|_E \leqslant C(h + k^2). \qquad (5.2.31)$$

This completes the proof. □

5.3 Numerical results

In this section we derive an algorithm which computes the fully approximate solution $\boldsymbol{u}_i^h$ for the discrete linear problem (3.4.1). The first summation on the right-hand side of (3.4.1), including the factor $\frac{k}{2}$, can be written as

$$\frac{k}{2}\alpha\varphi_s(0)\hat{\boldsymbol{F}}_i + k\alpha\sum_{j=1}^{i-1}\varphi_s(t_i - t_j)\hat{\boldsymbol{F}}_j + \frac{k}{2}\alpha\varphi_s(t_i)\hat{\boldsymbol{F}}_0, \tag{5.3.1}$$

where

$$\hat{\boldsymbol{F}}_i = \Big(\boldsymbol{D}(\theta_i^h - \theta_r)\boldsymbol{I_0}, \boldsymbol{\varepsilon}(\boldsymbol{v})\Big)_\Omega. \tag{5.3.2}$$

Similarly, for $\hat{\boldsymbol{F}}_j$ and $\hat{\boldsymbol{F}}_0$, with t_i replaced with t_j and $t_0 = 0$, respectively. The sum of the last two terms in (5.3.1) gives,

$$\begin{aligned}
& k\alpha\sum_{j=1}^{i-1}\varphi_s(t_i - t_j)\hat{\boldsymbol{F}}_j + \frac{k}{2}\alpha\varphi_s(t_i)\hat{\boldsymbol{F}}_0 \\
&= \sum_{q=1}^{N_\varphi}\left[\frac{k}{2}\alpha\alpha_q\varphi_q e^{-\alpha_q t_i}\hat{\boldsymbol{F}}_0 + \sum_{j=1}^{i-1}k\alpha\alpha_q\varphi_q e^{-\alpha_q(t_i - t_j)}\hat{\boldsymbol{F}}_j\right] \\
&= \sum_{q=1}^{N_\varphi}\hat{\boldsymbol{H}}_{iq}.
\end{aligned} \tag{5.3.3}$$

Using the identity (3.2.10), we can write

$$\hat{\boldsymbol{H}}_{iq} = e^{-\alpha_q k}\hat{\boldsymbol{H}}_{(i-1)q} + k\alpha\alpha_q\varphi_q e^{-\alpha_q(t_i - t_{i-1})}\hat{\boldsymbol{F}}_{i-1}, \tag{5.3.4}$$

because

$$\hat{\boldsymbol{H}}_{(i-1)q} = \frac{k}{2}\alpha\alpha_q\varphi_q e^{-\alpha_q t_{i-1}}\hat{\boldsymbol{F}}_0 + \sum_{j=1}^{i-2}k\alpha\alpha_q\varphi_q e^{-\alpha_q(t_{i-1} - t_j)}\hat{\boldsymbol{F}}_j. \tag{5.3.5}$$

The last recursive relation is derived mainly to save computer memory thus increasing the efficiency of the computer code. We are now able to write an algorithm for solving the linear coupled problem.

`Algorithm 2:  Linear problem (no reduced time)`

---

1. Given $\theta(0)$, i.e temperature at t=0
2. Find $\hat{F}_0$
3. Solve $AU_0 = L_0 + \alpha\hat{F}_0$, i.e find displacement at t=0
4. Initialize $H_q = \frac{k}{2}\alpha_q\varphi_q e^{-\alpha_q t_1}U_0, \qquad q = 1,\ldots,N_q$
5. Initialize $\hat{H}_q = \frac{k}{2}\alpha\alpha_q\varphi_q e^{-\alpha_q t_1}\hat{F}_0, \qquad q = 1,\ldots,N_q$
6. for i=1,...,N
7. Solve $A(1 - \frac{k}{2}\varphi_s(0))U_i = L_i + A\sum_{q=1}^{N_q} H_q - \sum_{q=1}^{N_q}\hat{H}_q + \alpha(1 - \frac{k}{2}\varphi_s(0))\hat{F}_i$
8. update H_q
9. $H_q \leftarrow e^{-\alpha_q k}H_q + k\alpha_q\varphi_q e^{-\alpha_q k}U_i$
10. update $\hat{H}_q$
11. $\hat{H}_q \leftarrow e^{-\alpha_q k}\hat{H}_q + k\alpha\alpha_q\varphi_q e^{-\alpha_q k}\hat{F}_i$
12. next i

As the above algorithm shows, we first give the initial condition for temperature: this is just the exact solution for temperature θ computed at $t = 0$. With this to hand, we can proceed to compute the displacement at $t = 0$, U_0, as shown in line 3 of the algorithm, by feeding $\theta(0)$ in the thermal load vector given by (5.3.2). L_i is the load vector. Using the recursive relations 5.3.4 and 3.2.11 we make two initialisations as shown in lines 4 and 5. Then, inside the time loop, for each discrete time, we solve the matrix equation shown in line 7 of algorithm, which corresponds to (3.4.1). We also update H_q and $\hat{H}_q$. In order to see that the algorithm convergences, we consider the following example of exact solution:

$$\boldsymbol{u}(\boldsymbol{x},t) = (5t(x+3y), 2t(4x-5y)) \text{ for displacement, and}$$

$$\theta(\boldsymbol{x},t) = (1+3t)(4x-2y) \text{ for heat.}$$

Table 5.1 shows the max error. As we can see, there is second order convergence vertically, that is, as the number of time steps is doubled the max error is reduced by a factor of four in each column. This is because of the trapezoidal rule for approximation and also due to the exponentials in the algorithm. Also recall that the heat conduction problem is discretized using the Crank-Nicolson method which gives a second order convergence for the error when computing the finite element approximate value for temperature. There are no spatial errors present since the exact solution is linear in spatial variables. For computational purposes, throughout this thesis, the value of the thermal expansion coefficient is taken to be $\alpha = 0.001$ and the reference temperature is taken to be θ_r=20. We can see that the error has some dependency on the parameter h. The error changes slightly as the mesh size is changed. This is probably due to the fact that the integrals involved are not computed exactly. Only one quadrature point is used to compute the integrals (center of gravity). This is evident in all three tables.

Table 5.1: Max displacement errors $\times\ 10^{-3}$, linear problem

time steps	mesh size 2	4	8	16	32	64
2	0.150173	0.160440	0.165797	0.168077	0.168663	0.168879
4	0.037541	0.040108	0.041447	0.042017	0.042163	0.042217
8	0.009385	0.010026	0.010361	0.010504	0.010540	0.010554
16	0.002346	0.002506	0.002590	0.002626	0.002635	0.002638
32	0.000586	0.000626	0.000647	0.000656	0.000658	0.000659
64	0.000146	0.000156	0.000161	0.000164	0.000164	0.000164

Table 5.3 shows the error in the L_2 norm. We see that, along the diagonal as the mesh and time steps are doubled, the error is reduced by a factor of four. The error in the L_2 norm is bounded by $C(h^2 + k^2)$, this is due to the fact that as one moves

from L_2 to H^1, a power of h is lost, due to gradients. The error estimate that we derived earlier in the energy norm, which is equivalent to the H^1 norm, was $C(h+k^2)$. The errors in the L_2 and H^1 norm are computed using their corresponding norm definitions which were introduced in Chapter 1. Thus, for the L_2 error we have,

$$\max_{1\leqslant i\leqslant N} \|\boldsymbol{u}(t_i) - \boldsymbol{u}_i^h\|_{L_2(\Omega)} = \max_{1\leqslant i\leqslant N} \left(\int_\Omega |\boldsymbol{u}(t_i) - \boldsymbol{u}_i^h|^2 d\Omega \right)^{1/2}. \tag{5.3.6}$$

This means that for each discrete time we compute the L_2 error by adding the contributions from all elements of the mesh, in the form $\int_e |\boldsymbol{u}(t_i) - \boldsymbol{u}_i^h|^2 de$, and then finally taking the maximum value over all times.

Table 5.2 shows the error in the H^1 norm. As the mesh size and time steps are

Table 5.2: Displacement errors in the H^1 norm, $\times 10^{-3}$: linear problem

time steps	mesh size 2	4	8	16	32	64
2	0.339976	0.382661	0.402686	0.414343	0.420468	0.423402
4	0.084989	0.095660	0.100666	0.103580	0.105111	0.105845
8	0.021247	0.023914	0.025166	0.025894	0.026277	0.026460
16	0.005311	0.005978	0.006291	0.006473	0.006569	0.006615
32	0.001327	0.001494	0.001572	0.001618	0.001642	0.001653
64	0.000331	0.000373	0.000393	0.000404	0.000410	0.000413

Table 5.3: Displacement errors in the L_2 norm, $\times 10^{-3}$: linear problem

time steps	mesh size 2	4	8	16	32	64
2	0.059182	0.071358	0.076145	0.078202	0.079002	0.079290
4	0.014794	0.017838	0.019035	0.019549	0.019749	0.019821
8	0.003698	0.004459	0.004758	0.004887	0.004937	0.004955
16	0.000924	0.001114	0.001189	0.001221	0.001234	0.001238
32	0.000231	0.000278	0.000297	0.000305	0.000308	0.000309
64	0.000057	0.000069	0.000074	0.000076	0.000077	0.000077

doubled, we see that the error is reduced by a factor of four. This is probably due to the fact that the exact solution is linear in space. For a solution which is not linear in space one would expect the error along the diagonal to reduce by a factor of two, consistent with the error estimate $C(h+k^2)$; we explain why. Taking h as a measure, then we are interested to know what is the value of k, such that we can get a solution without loosing any significant accuracy in a reasonable amount of time. If we take $h = k$, we obtain an accuracy $h + k^2 \sim h$, but then we need $1/k^2 = 1/h^2$ time steps, which are many. On the other hand, if we take $h = k^2$, then we obtain an accuracy $h + k^2 = 2h$, in which case one needs $1/k^2 = 1/h$ time steps which are by far less than before. In both cases we get an estimate $C(h)$, with the second choice being much more efficient. Now halving h, would half the previous value of error. For the H^1 error we have,

$$\max_{1 \leqslant i \leqslant N} \|\boldsymbol{u}(t_i) - \boldsymbol{u}_i^h\|_{H^1(\Omega)} = \max_{1 \leqslant i \leqslant N} \left(\int_\Omega \left(|\boldsymbol{u}(t_i) - \boldsymbol{u}_i^h|^2 + |\nabla(\boldsymbol{u}(t_i) - \boldsymbol{u}_i^h)|^2 \right) d\Omega \right)^{1/2}. \tag{5.3.7}$$

The procedure for computing this is similar to that for computing (5.3.6), with the only difference being the presence of gradients.

We shall use (5.3.6) and (5.3.7) to compute the L_2 and H^1 errors throughout this thesis.

5.4 Summary

Error estimates for the heat conduction and the linear coupled problem were derived. Some numerical results were shown as well, indicating that the algorithm works correctly: the results are as expected.

Chapter 6

Stability Analysis for the Nonlinear Problem

6.1 The continuous formulation

The aim here is to derive a stability estimate for the continuous formulation for the nonlinear coupled problem 2.4.22, which involves the *reduced time*. We derive a stability bound in the energy norm for the exact solution $\boldsymbol{u}$. We now present a theorem giving a stability estimate for this problem.

Theorem 6.1.1. *Let Assumptions 2.4.1 and Corollary 2.2.1 hold and let* $\alpha > 0$*. Also assume that* $\theta > \theta_g - 51.6$*, in which case the shift factor* $\dfrac{1}{\psi(\theta)}$ *has an upper bound, that is,* $\|\dfrac{1}{\psi(\theta)}\|_{L_\infty([0,T]\times\Omega)} \leqslant C_\rho$*. Then for* $\boldsymbol{u}$*, the exact solution of (2.4.22), we have the following bound in energy norm:*

$$\|\boldsymbol{u}(t)\|_E \leqslant C_1 e^{C_2 T}, \tag{6.1.1}$$

where C_1 and C_2 are non-negative constants. C_1 depends on initial conditions, data and other constants.

Proof. Choose $\boldsymbol{v} = \boldsymbol{u}(t)$ in (2.4.22) and use the definition of the energy norm, $\| \cdot \|_E^2 = a(\cdot, \cdot)$, to get,

$$\begin{aligned}\|\boldsymbol{u}(t)\|_E^2 = L(t; \boldsymbol{u}(t)) + \int_0^t \Big(\boldsymbol{D}\varphi_s(\rho(t) - \rho(s))\boldsymbol{\varepsilon}(\boldsymbol{u}(s)), \boldsymbol{\varepsilon}(\boldsymbol{u}(t))\Big)_\Omega ds \\ + \Big(\alpha \boldsymbol{D}(\theta(t) - \theta_r)\boldsymbol{I_0}, \boldsymbol{\varepsilon}(\boldsymbol{u}(t))\Big)_\Omega \\ - \int_0^t \Big(\alpha \boldsymbol{D}\varphi_s(\rho(t) - \rho(s))(\theta(s) - \theta_r)\boldsymbol{I_0}, \boldsymbol{\varepsilon}(\boldsymbol{u}(t))\Big)_\Omega ds. \qquad (6.1.2)\end{aligned}$$

Next step is to bound the terms on the right. Thus, labelling them in order as I, II, III and IV, we can now derive the following estimates:

Term I: Using the definition of the dual norm we can write,

$$|\langle L, \boldsymbol{u}\rangle| \leqslant \|L\|_{E'}\|\boldsymbol{u}(t)\|_E. \qquad (6.1.3)$$

Term II: First, note that we have $\varphi_s(\rho(t) - \rho(s)) = \sum_{q=1}^{N_\varphi} \alpha_q \varphi_q e^{-\alpha_q(\rho(t) - \rho(s))}\rho'(s)$. Using the upper bound of $\rho'(s) = 1/\psi(\theta)$ denoted by C_ρ we have,

$$\|\varphi_s(\rho(t) - \rho(s))\|_{L_\infty([0,T]\times\Omega)} \leqslant \Big(\sum_{q=1}^{N_\varphi} \alpha_q \varphi_q\Big) C_\rho =: C'_\varphi C_\rho. \qquad (6.1.4)$$

Then,

$$\begin{aligned}\int_0^t \Big(\boldsymbol{D}\varphi_s(\rho(t) - \rho(s))\boldsymbol{\varepsilon}(\boldsymbol{u}(s)), \boldsymbol{\varepsilon}(\boldsymbol{u}(t))\Big)_\Omega ds \\ \leqslant \big\|\varphi_s(\rho(t) - \rho(s))\big\|_{L_\infty(0,T;L_\infty(\Omega))} \int_0^t \big|a((\boldsymbol{u}(s), \boldsymbol{u}(t))\big| ds \\ \leqslant C'_\varphi C_\rho \|\boldsymbol{u}(t)\|_E \int_0^t \|\boldsymbol{u}(s)\|_E ds. \qquad (6.1.5)\end{aligned}$$

Term III: Similarly to the linear problem, since $\alpha > 0$, using Cauchy-Schwartz we have,

$$\begin{aligned}\Big(\alpha \boldsymbol{D}(\theta(t)-\theta_r)\boldsymbol{I_0},\boldsymbol{\varepsilon}(\boldsymbol{u}(t))\Big)_\Omega &= \int_\Omega \alpha \boldsymbol{D}^{1/2}\boldsymbol{I_0} : \boldsymbol{D}^{1/2}\boldsymbol{\varepsilon}(\boldsymbol{u}(t))(\theta(t)-\theta_r)d\Omega \\ &\leqslant \alpha\|\boldsymbol{D}^{1/2}\boldsymbol{I_0}\|_{L_\infty(\Omega)}\|\boldsymbol{D}^{1/2}\boldsymbol{\varepsilon}(\boldsymbol{u}(t))\|_{L_2(\Omega)}\|\theta(t)-\theta_r\|_{L_2(\Omega)} \\ &\leqslant C(\alpha,\boldsymbol{D})\|\boldsymbol{u}(t)\|_E\|\theta(t)-\theta_r\|_{L_2(\Omega)}, \end{aligned} \tag{6.1.6}$$

where $\alpha\|\boldsymbol{D}^{1/2}\boldsymbol{I_0}\|_{L_\infty(\Omega)} \leqslant C(\alpha,\boldsymbol{D})$, a positive constant.

Term IV:

$$\begin{aligned}&-\int_0^t \Big(\alpha \boldsymbol{D}\varphi_s(\rho(t)-\rho(s))(\theta(s)-\theta_r)\boldsymbol{I_0},\boldsymbol{\varepsilon}(\boldsymbol{u}(t))\Big)_\Omega ds \\ &\qquad\leqslant TC(\alpha,\boldsymbol{D})\big\|\varphi_s(\rho(t)-\rho(s))\big\|_{L_\infty(0,T;L_\infty(\Omega))}\|\theta-\theta_r\|_{L_\infty(0,T;L_2(\Omega))}\|\boldsymbol{u}(t)\|_E \\ &\qquad\leqslant TC(\alpha,\boldsymbol{D})C'_\varphi C_\rho\|\theta-\theta_r\|_{L_\infty(0,T;L_2(\Omega))}\|\boldsymbol{u}(t)\|_E. \end{aligned} \tag{6.1.7}$$

With these estimates, (6.1.2) now becomes,

$$\begin{aligned}\|\boldsymbol{u}(t)\|_E &\leqslant \|L\|_{E'} + C'_\varphi C_\rho\int_0^t \|u(s)\|_E ds + C(\alpha,\boldsymbol{D})\|\theta(t)-\theta_r\|_{L_2(\Omega)} \\ &\quad + TC(\alpha,\boldsymbol{D})C'_\varphi C_\rho\|\theta-\theta_r\|_{L_\infty(0,T;L_2(\Omega))} \\ &\leqslant \|L\|_{E'} + C\|\theta(t)-\theta_r\|_{L_2(\Omega)} + C\|\theta-\theta_r\|_{L_\infty(0,T;L_2(\Omega))} + C\int_0^t \|u(s)\|_E ds. \end{aligned} \tag{6.1.8}$$

Next, using the triangle inequality and the bound on temperature given by (4.1.13), we can write,

$$\begin{aligned}\|\theta(t)-\theta_r\|^2_{L_2(\Omega)} &\leqslant 2\|\theta(t)\|^2_{L_2(\Omega)} + 2\|\theta_r\|^2_{L_2(\Omega)} \\ &\leqslant 2\|\theta(0)\|^2_{L_2(\Omega)} + 2\|G(s)\|^2_{L_2(0,t;\mathcal{A}')} + |\theta_r|^2\mathrm{Vol}(\Omega), \end{aligned} \tag{6.1.9}$$

and, taking the *supremum* over all times of this, gives,

$$\|\theta - \theta_r\|^2_{L_\infty(0,T;L_2(\Omega))} \leqslant 2\|\theta(0)\|^2_{L_\infty(0,T;L_2(\Omega))} + 2T\|G\|^2_{L_2(0,T;\mathcal{A}')} + |\theta_r|^2\mathrm{Vol}(\Omega). \tag{6.1.10}$$

Substituting (6.1.9) and (6.1.10) (after taking square roots) in (6.1.8), and using the Gronwall's lemma (1.4.1), gives,

$$\|\boldsymbol{u}(t)\|_E \leqslant \tilde{C}e^{CT}, \tag{6.1.11}$$

where $\tilde{C} \geqslant 0$ represents everything on the right-hand side of (6.1.8), excluding the last (integral) term. This proves the theorem. □

6.2 The fully-discrete formulation

In this section we derive a stability estimate for the fully-discrete formulation given by (3.4.2). This can be re-written in a more explicit form as,

find, for each t_i, $i = 1, \ldots, N$, a $\boldsymbol{u}_i^h \in V^h$ such that,

$$\begin{aligned}
&a(\boldsymbol{u}_i^h, \boldsymbol{v}) = L(t_i; \boldsymbol{v}) \\
&+ \frac{k}{2}\sum_{j=1}^{i}\Big(\big(\boldsymbol{D}\varphi_s(\rho_i^h - \rho_j^h)\boldsymbol{\varepsilon}(\boldsymbol{u}_j^h), \boldsymbol{\varepsilon}(\boldsymbol{v})\big)_\Omega\Big) \\
&+ \frac{k}{2}\sum_{j=1}^{i}\Big(\big(\boldsymbol{D}\varphi_s(\rho_i^h - \rho_{j-1}^h)\boldsymbol{\varepsilon}(\boldsymbol{u}_{j-1}^h), \boldsymbol{\varepsilon}(\boldsymbol{v})\big)_\Omega\Big) \\
&+ \Big(\alpha\boldsymbol{D}(\theta_i^h - \theta_r)\boldsymbol{I_0}, \boldsymbol{\varepsilon}(\boldsymbol{v})\Big)_\Omega - \frac{k}{2}\sum_{j=1}^{i}\Big(\big(\alpha\boldsymbol{D}\varphi_s(\rho_i^h - \rho_j^h)(\theta_j^h - \theta_r)\boldsymbol{I_0}, \boldsymbol{\varepsilon}(\boldsymbol{v})\big)\Big) \\
&- \frac{k}{2}\sum_{j=1}^{i}\Big(\big(\alpha\boldsymbol{D}\varphi_s(\rho_i^h - \rho_{j-1}^h)(\theta_{j-1}^h - \theta_r)\boldsymbol{I_0}, \boldsymbol{\varepsilon}(\boldsymbol{v})\big)\Big) \qquad \forall \boldsymbol{v} \in V^h.
\end{aligned} \tag{6.2.1}$$

This may be re-arranged further as,

$$
\begin{aligned}
a(\boldsymbol{u}_i^h, \boldsymbol{v}) = L(t; \boldsymbol{v}) &+ \frac{k}{2}\big(\boldsymbol{D}\varphi_s(0)\boldsymbol{\varepsilon}(\boldsymbol{u}_i^h), \boldsymbol{\varepsilon}(\boldsymbol{v})\big)_\Omega - \frac{k}{2}\big(\boldsymbol{D}\varphi_s(\rho_i^h - \rho_0^h)\boldsymbol{\varepsilon}(\boldsymbol{u}_0^h), \boldsymbol{\varepsilon}(\boldsymbol{v})\big)_\Omega \\
&+ k\sum_{j=0}^{i-1}\big(\boldsymbol{D}\varphi_s(\rho_i^h - \rho_j^h)\boldsymbol{\varepsilon}(\boldsymbol{u}_j^h), \boldsymbol{\varepsilon}(\boldsymbol{v})\big)_\Omega + \big(\alpha\boldsymbol{D}(\theta_i^h - \theta_r)\boldsymbol{I_0}, \boldsymbol{\varepsilon}(\boldsymbol{v})\big)_\Omega \\
&- \frac{k}{2}\sum_{j=1}^{i}\big(\alpha\boldsymbol{D}\varphi_s(\rho_i^h - \rho_j^h)(\theta_j^h - \theta_r)\boldsymbol{I_0}, \boldsymbol{\varepsilon}(\boldsymbol{v})\big)_\Omega \\
&- \frac{k}{2}\sum_{j=0}^{i-1}\big(\alpha\boldsymbol{D}\varphi_s(\rho_i^h - \rho_j^h)(\theta_j^h - \theta_r)\boldsymbol{I_0}, \boldsymbol{\varepsilon}(\boldsymbol{v})\big)_\Omega. \qquad (6.2.2)
\end{aligned}
$$

We are now able to introduce the following theorem.

Theorem 6.2.1. *Let Assumptions 2.4.1 and Corollary 2.2.1 hold and let $\alpha > 0$. Also assume that $\theta > \theta_g - 51.6$, in which case the shift factor $\dfrac{1}{\psi(\theta_i^h)}$ has an upper bound, that is, $\big\|\dfrac{1}{\psi(\theta_i^h)}\big\|_{L_\infty([0,T]\times\Omega)} \leqslant C_\rho$. Then for $\boldsymbol{u}_i^h$, the approximate solution of (6.2.2), for k small enough, we have the following bound in energy norm:*

$$
\|\boldsymbol{u}_i^h\|_E \leqslant \tilde{C}_1 e^{CT}, \qquad (6.2.3)
$$

where $\tilde{C}_1$ and C are non-negative constants. $\tilde{C}_1$ depends on data, initial conditions and other constants.

Proof. First, choose $\boldsymbol{v} = \boldsymbol{u}_i^h$ above. Then, labelling the terms on the right in order as I,II,III,IV,V,VI and VII, the following bounds can be derived for each of the terms.

Term I: Using the definition of the dual norm we have,

$$
|L(t_i; \boldsymbol{u}_i^h)| \leqslant \|L\|_{E'}\|\boldsymbol{u}_i^h\|_E. \qquad (6.2.4)
$$

Term II:

$$\begin{aligned}\frac{k}{2}\big(\boldsymbol{D}\varphi_s(0)\boldsymbol{\varepsilon}(\boldsymbol{u}_i^h),\boldsymbol{\varepsilon}(\boldsymbol{u}_i^h)\big)_\Omega &\leqslant \frac{k}{2}\|\varphi_s(0)\|_{L_\infty(0,T;L_\infty(\Omega))}\big(\boldsymbol{D}\boldsymbol{\varepsilon}(\boldsymbol{u}_i^h),\boldsymbol{\varepsilon}(\boldsymbol{u}_i^h)\big)_\Omega\\ &\leqslant \frac{k}{2}C'_\varphi C_\rho\|\boldsymbol{u}_i^h\|_E^2,\end{aligned}\tag{6.2.5}$$

where C_ρ is an upper bound for $\dfrac{1}{\psi(\theta_j^h)}$.

Term III:

$$\begin{aligned}-\frac{k}{2}\big(\boldsymbol{D}\varphi_s(\rho_i^h-\rho_0^h)\boldsymbol{\varepsilon}(\boldsymbol{u}_0^h),\boldsymbol{\varepsilon}(\boldsymbol{v})\big)_\Omega &\leqslant \frac{k}{2}\|\varphi_s(\rho_i^h-\rho_0^h)\|_{L_\infty(0,T;L_\infty(\Omega))}\|\boldsymbol{u}_0^h\|_E\|\boldsymbol{u}_i^h\|_E\\ &\leqslant \frac{k}{2}C'_\varphi C_\rho\|\boldsymbol{u}_0^h\|_E\|\boldsymbol{u}_i^h\|_E.\end{aligned}\tag{6.2.6}$$

Term IV:

$$\begin{aligned}k\sum_{j=0}^{i-1}\big(\boldsymbol{D}\varphi_s(\rho_i^h-\rho_j^h)\boldsymbol{\varepsilon}(\boldsymbol{u}_j^h),\boldsymbol{\varepsilon}(\boldsymbol{v})\big)_\Omega &\leqslant kC'_\varphi C_\rho\sum_{j=0}^{i-1}\big(\boldsymbol{D}\boldsymbol{\varepsilon}(\boldsymbol{u}_j^h),\boldsymbol{\varepsilon}(\boldsymbol{u}_i^h)\big)_\Omega\\ &\leqslant kC'_\varphi C_\rho\sum_{j=0}^{i-1}\|\boldsymbol{u}_j^h\|_E\|\boldsymbol{u}_i^h\|_E.\end{aligned}\tag{6.2.7}$$

Term V:

$$\big(\alpha\boldsymbol{D}(\theta_i^h-\theta_r)\boldsymbol{I_0},\boldsymbol{\varepsilon}(\boldsymbol{v})\big)_\Omega \leqslant C(\alpha,\boldsymbol{D})\|\theta_i^h-\theta_r\|_{L_2(\Omega)}\|\boldsymbol{u}_i^h\|_E.\tag{6.2.8}$$

Term VI:

$$-\frac{k}{2}\sum_{j=1}^{i}\big(\alpha\boldsymbol{D}\varphi_s(\rho_i^h-\rho_j^h)(\theta_j^h-\theta_r)\boldsymbol{I_0},\boldsymbol{\varepsilon}(\boldsymbol{v})\big)_\Omega \leqslant \frac{k}{2}C'_\varphi C_\rho\sum_{j=1}^{i}\|\theta_j^h-\theta_r\|_{L_2(\Omega)}\|\boldsymbol{u}_i^h\|_E.\tag{6.2.9}$$

The same estimate can be derived for term VII as for the term VI. Putting all of these estimates together, using (6.2.2), gives

$$\begin{aligned}\big(1 - Ck\big)\|\boldsymbol{u}_i^h\|_E \leqslant \|L\|_{E'} + CT\|\boldsymbol{u}_0^h\|_E + C\|\theta_i^h - \theta_r\|_{L_2(\Omega)} + CT \max_{1\leqslant j\leqslant i} \|\theta_j^h - \theta_r\|_{L_2(\Omega)} \\ + CT \max_{0\leqslant j\leqslant i-1} \|\theta_j^h - \theta_r\|_{L_2(\Omega)} + Ck\sum_{j=0}^{i-1} \|\boldsymbol{u}_j^h\|_E. \qquad (6.2.10)\end{aligned}$$

We require that $1 - Ck > 0$, which implies that $k < \dfrac{1}{C}$. Dividing (6.2.10) through by $1 - Ck$, and using the bound on temperature given by (4.2.9), we can write,

$$\|\boldsymbol{u}_i^h\|_E \leqslant \tilde{C}_1 + Ck\sum_{j=0}^{i-1} \|\boldsymbol{u}_j^h\|_E. \qquad (6.2.11)$$

Finally, using the discrete version of Gronwall inequality, yields,

$$\|\boldsymbol{u}_i^h\|_E \leqslant \tilde{C}_1 e^{CT}. \qquad (6.2.12)$$

This completes the proof of the theorem. □

6.3 Summary

Stability estimates were derived for the nonlinear problem for the continuous and the fully-discrete formulations.

Chapter 7

A Priori Error Analysis for the Nonlinear Problem

7.1 Motivation

In this chapter we aim to derive an error estimate in the energy norm for the nonlinear coupled problem. For this purpose, we refer to the weak formulation for this problem given by (2.4.22) and correspondingly to the fully-discrete approximation given by (3.4.2).

7.2 Error estimate

We begin by introducing the following theorem.

Theorem 7.2.1. *Let $\boldsymbol{u}$ and $\boldsymbol{u}_i^h$ be the solutions of (2.4.22) and (3.4.2), respectively. Provided that Assumptions 2.4.1 hold and that k is small enough, then the following* *estimate holds:*

$$\|\boldsymbol{u}(t_i) - \boldsymbol{u}_i^h\|_E \leqslant C(h + k^2), \tag{7.2.1}$$

where the positive constant C depends on data, exact solutions and derivatives of exact solutions.

Proof. Subtract (2.4.22) from (3.4.2), with (2.4.22) at $t = t_i$, to get,

$$
\begin{aligned}
a(\boldsymbol{u}_i^h - \boldsymbol{u}(t_i), \boldsymbol{v}) = \frac{k}{2}\sum_{j=1}^{i} \Big[& \big(\boldsymbol{D}\varphi_s(\rho_i^h - \rho_j^h)\boldsymbol{\varepsilon}(\boldsymbol{u}_j^h), \boldsymbol{\varepsilon}(\boldsymbol{v})\big)_\Omega \\
& + \big(\boldsymbol{D}\varphi_s(\rho_i^h - \rho_{j-1}^h)\boldsymbol{\varepsilon}(\boldsymbol{u}_{j-1}^h), \boldsymbol{\varepsilon}(\boldsymbol{v})\big)_\Omega\Big] \\
- \frac{k}{2}\sum_{j=1}^{i} \Big[& \big(\boldsymbol{D}\varphi_s(\rho(t_i) - \rho(t_j))\boldsymbol{\varepsilon}(\boldsymbol{u}(t_j)), \boldsymbol{\varepsilon}(\boldsymbol{v})\big)_\Omega \\
& + \big(\boldsymbol{D}\varphi_s(\rho(t_i) - \rho(t_{j-1}))\boldsymbol{\varepsilon}(\boldsymbol{u}(t_{j-1})), \boldsymbol{\varepsilon}(\boldsymbol{v})\big)_\Omega\Big] \\
- \int_0^{t_i} & \Big(\boldsymbol{D}\varphi_s(\rho(t_i) - \rho(s))\boldsymbol{\varepsilon}(\boldsymbol{u}(s)), \boldsymbol{\varepsilon}(\boldsymbol{v})\Big)_\Omega ds \\
& + \frac{k}{2}\sum_{j=1}^{i} \Big[\big(\boldsymbol{D}\varphi_s(\rho(t_i) - \rho(t_j))\boldsymbol{\varepsilon}(\boldsymbol{u}(t_j)), \boldsymbol{\varepsilon}(\boldsymbol{v})\big)_\Omega \\
& + \big(\boldsymbol{D}\varphi_s(\rho(t_i) - \rho(t_{j-1}))\boldsymbol{\varepsilon}(\boldsymbol{u}(t_{j-1})), \boldsymbol{\varepsilon}(\boldsymbol{v})\big)_\Omega\Big] \\
+ \big(\alpha\boldsymbol{D}(\theta_i^h - \theta_r)\boldsymbol{I_0}, & \boldsymbol{\varepsilon}(\boldsymbol{v})\big)_\Omega - \big(\alpha\boldsymbol{D}(\theta(t_i) - \theta_r)\boldsymbol{I_0}, \boldsymbol{\varepsilon}(\boldsymbol{v})\big)_\Omega \\
- \frac{k}{2}\sum_{j=1}^{i} \Big[& \big(\alpha\boldsymbol{D}\varphi_s(\rho_i^h - \rho_j^h)(\theta_j^h - \theta_r)\boldsymbol{I_0}, \boldsymbol{\varepsilon}(\boldsymbol{v})\big)_\Omega \\
& + \big(\alpha\boldsymbol{D}\varphi_s(\rho_i^h - \rho_{j-1}^h)(\theta_{j-1}^h - \theta_r)\boldsymbol{I_0}, \boldsymbol{\varepsilon}(\boldsymbol{v})\big)_\Omega\Big] \\
+ \int_0^{t_i} & \Big(\alpha\boldsymbol{D}\varphi_s(\rho(t_i) - \rho(s))(\theta(s) - \theta_r)\boldsymbol{I_0}, \boldsymbol{\varepsilon}(\boldsymbol{v})\Big)_\Omega ds \\
& - \frac{k}{2}\sum_{j=1}^{i} \Big[\Big(\alpha\boldsymbol{D}\varphi_s(\rho(t_i) - \rho(t_j))(\theta(t_j) - \theta_r)\boldsymbol{I_0}, \boldsymbol{\varepsilon}(\boldsymbol{v})\Big)_\Omega \\
& + \Big(\alpha\boldsymbol{D}\varphi_s(\rho(t_i) - \rho(t_{j-1}))(\theta(t_{j-1}) - \theta_r)\boldsymbol{I_0}, \boldsymbol{\varepsilon}(\boldsymbol{v})\Big)_\Omega\Big] \\
+ \frac{k}{2}\Big[& \Big(\alpha\boldsymbol{D}\varphi_s(\rho(t_i) - \rho(t_j))(\theta(t_j) - \theta_r)\boldsymbol{I_0}, \boldsymbol{\varepsilon}(\boldsymbol{v})\Big)_\Omega \\
& + \Big(\alpha\boldsymbol{D}\varphi_s(\rho(t_i) - \rho(t_{j-1}))(\theta(t_{j-1}) - \theta_r)\boldsymbol{I_0}, \boldsymbol{\varepsilon}(\boldsymbol{v})\Big)_\Omega\Big].
\end{aligned} \tag{7.2.2}
$$

It is important to note that in (7.2.2) we have added and subtracted terms for our convenience. This will be made clearer as we progress in our analysis. As in the linear case, we make use of relations: $\eta(t_i) := \boldsymbol{u}(t_i) - R\boldsymbol{u}(t_i)$ and

$\zeta_i := \boldsymbol{u}_i^h - R\boldsymbol{u}(t_i)$, implying that $\boldsymbol{u}_i^h - \boldsymbol{u}(t_i) = \zeta_i - \eta(t_i)$. Thus we can write,

$$\begin{aligned}
&\frac{k}{2}\sum_{j=1}^{i}\Big[\big(\boldsymbol{D}\varphi_s(\rho_i^h - \rho_j^h)\boldsymbol{\varepsilon}(\boldsymbol{u}_j^h), \boldsymbol{\varepsilon}(\boldsymbol{v})\big)_\Omega - \big(\boldsymbol{D}\varphi_s(\rho(t_i) - \rho(t_j))\boldsymbol{\varepsilon}(\boldsymbol{u}(t_j)), \boldsymbol{\varepsilon}(\boldsymbol{v})\big)_\Omega\Big] \\
&= \frac{k}{2}\sum_{j=1}^{i}\Big[\big(\boldsymbol{D}\varphi_s(\rho_i^h - \rho_j^h)\boldsymbol{\varepsilon}(\boldsymbol{u}_j^h - \boldsymbol{u}(t_j)), \boldsymbol{\varepsilon}(\boldsymbol{v})\big)_\Omega + \big(\boldsymbol{D}\varphi_s(\rho_i^h - \rho_j^h)\boldsymbol{\varepsilon}(\boldsymbol{u}(t_j)), \boldsymbol{\varepsilon}(\boldsymbol{v})\big)_\Omega \\
&\qquad\qquad - \big(\boldsymbol{D}\varphi_s(\rho(t_i) - \rho(t_j))\boldsymbol{\varepsilon}(\boldsymbol{u}(t_j)), \boldsymbol{\varepsilon}(\boldsymbol{v})\big)_\Omega\Big] \\
&= \frac{k}{2}\sum_{j=1}^{i}\Big[\big(\boldsymbol{D}\varphi_s(\rho_i^h - \rho_j^h)\boldsymbol{\varepsilon}(\zeta_j - \eta(t_j)), \boldsymbol{\varepsilon}(\boldsymbol{v})\big)_\Omega \\
&\qquad\qquad + \big(\boldsymbol{D}\big[\varphi_s(\rho_i^h - \rho_j^h) - \varphi_s(\rho(t_i) - \rho(t_j))\big]\boldsymbol{\varepsilon}(\boldsymbol{u}(t_j)), \boldsymbol{\varepsilon}(\boldsymbol{v})\big)_\Omega\Big].
\end{aligned} \tag{7.2.3}$$

Using Assumption 2.4.1 (iv), we proceed by choosing $\boldsymbol{v} = \zeta_i$. Thus for the first term in the last line of (7.2.3), we have the following:

$$\begin{aligned}
\big|\big(\boldsymbol{D}\varphi_s(\rho_i^h - \rho_j^h)\boldsymbol{\varepsilon}(\zeta_j - \eta(t_j)), \boldsymbol{\varepsilon}(\boldsymbol{v})\big)_\Omega\big| &\leqslant C'_\varphi C_\rho \big|a(\zeta_j, \zeta_i)\big| + C'_\varphi C_\rho \big|a(\eta(t_j), \zeta_i)\big| \\
&\leqslant C'_\varphi C_\rho \Big(\|\zeta_j\|_E + \|\eta(t_j)\|_E\Big)\|\zeta_i\|_E.
\end{aligned} \tag{7.2.4}$$

With respect to the second term in the last line of (7.2.3), we first deal with the difference involving the stress relaxation function φ_s. In order to make the analysis easier, we introduce the following lemma,

Lemma 7.2.1. *Let Assumptions 2.4.1 (iv) hold. Then,*

$$\begin{aligned}
&\|\varphi_s(\rho_i^h - \rho_j^j) - \varphi_s(\rho(t_i) - \rho(t_j))\|_{L_2(\Omega)} \\
&\qquad \leqslant Ck^2 + Ck\sum_{m=0}^{i}\|\theta_m^h - \theta(t_m)\|_{L_2(\Omega)} + C\|\theta_j^h - \theta(t_j)\|_{L_2(\Omega)}.
\end{aligned} \tag{7.2.5}$$

Proof. We have,

$$\varphi_s(\rho_i^h - \rho_j^h) - \varphi_s(\rho(t_i) - \rho(t_j)) = \varphi'(\rho(t_i) - \rho(t_j))\frac{1}{\psi(\theta(t_j))} - \varphi'(\rho_i^h - \rho_j^h)\frac{1}{\psi(\theta_j^h)}$$
$$= \frac{\Big[\varphi'(\rho(t_i) - \rho(t_j)) - \varphi'(\rho_i^h - \rho_j^h)\Big]\psi(\theta_j^h) + \Big[\psi(\theta_j^h) - \psi(\theta(t_j))\Big]\varphi'(\rho_i^h - \rho_j^h)}{\psi(\theta(t_j))\psi(\theta_j^h)}. \tag{7.2.6}$$

But,

$$\begin{aligned}\varphi'(\rho(t_i) - \rho(t_j)) - \varphi'(\rho_i^h - \rho_j^h) &= \int_{\rho_i^h - \rho_j^h}^{\rho(t_i) - \rho(t_j)} \varphi''(\xi)d\xi \\ &\leqslant \|\varphi''\|_{L_\infty([0,T]\times\Omega)}\big[\big(\rho(t_i) - \rho(t_j)\big) - \big(\rho_i^h - \rho_j^h\big)\big] \\ &\leqslant \|\varphi''\|_{L_\infty([0,T]\times\Omega)}\big(|\rho(t_i) - \rho_i^h| + |\rho(t_j) - \rho_j^h|\big).\end{aligned} \tag{7.2.7}$$

For the error $\rho(t_j) - \rho_j^h$ we can write,

$$\begin{aligned}\rho(t_j) - \rho_j^h &= \int_0^{t_j} \frac{d\xi}{\psi(\theta(\xi))} - \frac{k}{2}\sum_{m=1}^{j}\Big(\frac{1}{\psi(\theta_m^h)} + \frac{1}{\psi(\theta_{m-1}^h)}\Big) \\ &= \int_0^{t_j} \frac{d\xi}{\psi(\theta(\xi))} - \frac{k}{2}\sum_{m=1}^{j}\Big(\frac{1}{\psi(\theta(t_m))} + \frac{1}{\psi(\theta(t_{m-1}))}\Big) + \frac{k}{2}\sum_{m=1}^{j}\Big(\frac{1}{\psi(\theta(t_m))} - \frac{1}{\psi(\theta_m^h)}\Big) \\ &\leqslant Ck^2\sum_{m=1}^{j}\Big|\Big(\frac{1}{\psi(\theta(\xi))}\Big)''\Big|d\xi + \frac{k}{2}C_\rho^2\|\psi\|_{L_\infty([0,T]\times\Omega)}\sum_{m=1}^{j}|\theta_m^h - \theta(t_m)| \\ &+ \frac{k}{2}C_\rho^2\|\psi\|_{L_\infty([0,T]\times\Omega)}\sum_{m=1}^{j}|\theta_{m-1}^h - \theta(t_{m-1})| \\ &\leqslant Ck^2\sum_{m=1}^{j}\Big|\Big(\frac{1}{\psi(\theta(\xi))}\Big)''\Big|d\xi + kC_\rho^2\|\psi\|_{L_\infty([0,T]\times\Omega)}\sum_{m=0}^{j}|\theta_m^h - \theta(t_m)|.\end{aligned} \tag{7.2.8}$$

Hence,

$$|\rho(t_j)-\rho_j^h|\leqslant Ck^2\sum_{m=1}^{j}\Big|\Big(\frac{1}{\psi(\theta(\xi))}\Big)''\Big|d\xi+kC_\rho^2\|\psi\|_{L_\infty([0,T]\times\Omega)}\sum_{m=0}^{j}|\theta_m^h-\theta(t_m)|, \tag{7.2.9}$$

where we have used the fact that,

$$\begin{aligned}\frac{1}{\psi(\theta_m^h)}-\frac{1}{\psi(\theta(t_m))}&=\frac{\psi(\theta(t_m))-\psi(\theta_m^h)}{\psi(\theta_m^h)\psi(\theta(t_m))}\\&=\frac{\int_{\theta_m^h}^{\theta(t_m)}\psi'(\xi)d\xi}{\psi(\theta_m^h)\psi(\theta(t_m))}\leqslant C_\rho^2\|\psi'\|_{L_\infty([0,T]\times\Omega)}|\theta_m^h-\theta(t_m)|.\end{aligned} \tag{7.2.10}$$

In an analogous way, for the error $\rho(t_j)-\rho_j^h$, we get,

$$|\rho(t_i)-\rho_i^h|\leqslant Ck^2\sum_{m=1}^{i}\Big|\Big(\frac{1}{\psi(\theta(\xi))}\Big)''\Big|d\xi+kC_\rho^2\|\psi\|_{L_\infty([0,T]\times\Omega)}\sum_{m=0}^{i}|\theta_m^h-\theta(t_m)|. \tag{7.2.11}$$

We also have that,

$$\psi(\theta_j^h)-\psi(\theta(t_j))=\int_{\theta(t_j)}^{\theta_j^h}\psi'(\xi)d\xi\leqslant\|\psi'\|_{L_\infty([0,T]\times\Omega)}|\theta_j^h-\theta(t_j)|. \tag{7.2.12}$$

Returning now to (7.2.6), we can write,

$$\begin{aligned}&\varphi_s(\rho_i^h-\rho_j^h)-\varphi_s(\rho(t_i)-\rho(t_j))\\&\leqslant C_\rho\|\varphi''\|_{L_\infty([0,T]\times\Omega)}\big(|\rho(t_i)-\rho_i^h|+|\rho(t_j)-\rho_j^h|\big)+C_\rho C_\varphi\|\psi'\|_{L_\infty([0,T]\times\Omega)}|\theta_j^h-\theta(t_j)|\\&\leqslant Ck^2+C|\theta_j^h-\theta(t_j)|+Ck\sum_{m=0}^{j}|\theta_m^h-\theta(t_m)|+Ck\sum_{m=0}^{i}|\theta_m^h-\theta(t_m)|\\&\leqslant Ck^2+C|\theta_j^h-\theta(t_j)|+Ck\sum_{m=0}^{i}|\theta_m^h-\theta(t_m)|,\quad\text{since}\quad j\leqslant i.\end{aligned} \tag{7.2.13}$$

Finally,

$$\|\varphi_s(\rho_i^h - \rho_j^h) - \varphi_s(\rho(t_i) - \rho(t_j))\|_{L_2(\Omega)}$$
$$\leqslant Ck^2 + Ck\sum_{m=0}^{i}\|\theta_m^h - \theta(t_m)\|_{L_2(\Omega)} + C\|\theta_j^h - \theta(t_j)\|_{L_2(\Omega)}, \quad (7.2.14)$$

which proves our lemma. □

Returning to the second term in the last line of (7.2.3), using Lemma (7.2.1) and Inequality 1.3.2, we can now write,

$$\Big(\boldsymbol{D}\big[\varphi_s(\rho_i^h - \rho_j^h) - \varphi_s(\rho(t_i) - \rho(t_j))\big]\boldsymbol{\varepsilon}(\boldsymbol{u}(t_j)), \boldsymbol{\varepsilon}(\boldsymbol{v})\Big)_\Omega$$
$$\leqslant \|\varphi_s(\rho_i^h - \rho_j^h) - \varphi_s(\rho(t_i) - \rho(t_j))\|_{L_2(\Omega)}\|\boldsymbol{u}\|_{L_\infty([0,T]\times\Omega)}\|\zeta\|_E$$
$$\leqslant Ck^2\|\zeta_i\|_E + Ck\sum_{m=0}^{i}\|\theta_m^h - \theta(t_m)\|_{L_2(\Omega)}\|\zeta_i\|_E + C\|\theta_j^h - \theta(t_j)\|_{L_2(\Omega)}\|\zeta_i\|_E. \quad (7.2.15)$$

Similarly, for the terms containing thermal expansion, we can write,

$$\sum_{j=1}^{i}\Big[\Big(\alpha\boldsymbol{D}\varphi_s(\rho_i^h - \rho_j^h)(\theta_j^h - \theta_r)\boldsymbol{I_0}, \boldsymbol{\varepsilon}(\boldsymbol{v})\Big)_\Omega$$
$$- \Big(\alpha\boldsymbol{D}\varphi_s(\rho(t_i) - \rho(t_j))(\theta(t_j) - \theta_t)\boldsymbol{I_0}, \boldsymbol{\varepsilon}(\boldsymbol{v})\Big)_\Omega\Big]$$
$$= \sum_{j=1}^{i}\Big[\Big(\alpha\boldsymbol{D}\varphi_s(\rho_i^h - \rho_j^h)(\theta_j^h - \theta(t_j))\boldsymbol{I_0}, \boldsymbol{\varepsilon}(\boldsymbol{v})\Big)_\Omega\Big]$$
$$+ \Big(\alpha\boldsymbol{D}\big[\varphi_s(\rho_i^h - \rho_j^h) - \varphi_s(\rho(t_i) - \rho(t_j))\big](\theta(t_j) - \theta_r)\boldsymbol{I_0}, \boldsymbol{\varepsilon}(\boldsymbol{v})\Big)_\Omega\Big]. \quad (7.2.16)$$

For the first term of (7.2.16), by choosing $\boldsymbol{v} = \zeta_i \in V^h$, we can write,

$$\left|\Big(\alpha \boldsymbol{D}\varphi_s(\rho_i^h - \rho_j^h)(\theta_j^h - \theta(t_j))\boldsymbol{I_0}, \boldsymbol{\varepsilon}(\zeta_i)\Big)_\Omega\right| \leqslant C'_\varphi C_\rho \cdot C(\alpha, \boldsymbol{D})\|\theta_j^h - \theta(t_j)\|_{L_2(\Omega)}\|\zeta_i\|_E$$
$$\leqslant C\|\theta_j^h - \theta(t_j)\|_{L_2(\Omega)}\|\zeta_i\|_E. \qquad (7.2.17)$$

Using Lemma (7.2.1) again, the second term of (7.2.16) gives,

$$\begin{aligned}
&\Big(\alpha \boldsymbol{D}\big[\varphi_s(\rho_i^h - \rho_j^h) - \varphi_s(\rho(t_i) - \rho(t_j))\big](\theta(t_j) - \theta_r)\boldsymbol{I_0}, \boldsymbol{\varepsilon}(\zeta_i)\Big)_\Omega \\
&\leqslant C(\alpha, \boldsymbol{D})\|\varphi_s(\rho_i^h - \rho_j^h) - \varphi_s(\rho(t_i) - \rho(t_j))\|_{L_2(\Omega)}\|\theta(t_j) - \theta_r\|_{L_\infty(\Omega)}\|\zeta_i\|_E \\
&\leqslant Ck^2\|\zeta_i\|_E + Ck\sum_{m=0}^{i}\|\theta_m^h - \theta(t_m)\|_{L_2(\Omega)}\|\zeta_i\|_E + C\|\theta_j^h - \theta(t_j)\|_{L_2(\Omega)}\|\zeta_i\|_E. \qquad (7.2.18)
\end{aligned}$$

Using the trapezoidal rule, for the terms in lines 5, 6 and 7 of (7.2.2), choosing $\boldsymbol{v} = \zeta_i$, gives

$$\begin{aligned}
&\int_0^{t_i}\Big(\boldsymbol{D}\varphi_s(\rho(t_i) - \rho(s))\boldsymbol{\varepsilon}(\boldsymbol{u}(s)), \boldsymbol{\varepsilon}(\zeta_i)\Big)_\Omega ds \\
&\qquad - \frac{k}{2}\sum_{j=1}^{i}\Big[\big(\boldsymbol{D}\varphi_s(\rho(t_i) - \rho(t_j))\boldsymbol{\varepsilon}(\boldsymbol{u}(t_j)), \boldsymbol{\varepsilon}(\zeta_i)\big)_\Omega \\
&\qquad + \big(\boldsymbol{D}\varphi_s(\rho(t_i) - \rho(t_{j-1}))\boldsymbol{\varepsilon}(\boldsymbol{u}(t_{j-1})), \boldsymbol{\varepsilon}(\zeta_i)\big)_\Omega\Big] \\
&\qquad \leqslant \sum_{j=1}^{i}\Big[Ck^2\int_{t_{j-1}}^{t_j}\left|\Big(\boldsymbol{D}\varphi_s(\rho(t_i) - \rho(s))\boldsymbol{\varepsilon}(\boldsymbol{u}(s)), \boldsymbol{\varepsilon}(\zeta_i)\Big)''_\Omega\right| ds\Big] \\
&\qquad \leqslant Ck^2C'''_\rho\sqrt{3}\int_0^{t_i}\Big(\|\boldsymbol{u}(s)\|_E^2 + \|\boldsymbol{u}'(s)\|_E^2 + \|\boldsymbol{u}''(s)\|_E^2\Big)^{\frac{1}{2}} ds\|\boldsymbol{\zeta}_i\|_E \\
&\qquad \leqslant Ck^2\|\zeta_i\|_E. \qquad (7.2.19)
\end{aligned}$$

Similarly, for the terms with thermal expansion,

$$\begin{aligned}
&\int_0^{t_i}\Big(\alpha\boldsymbol{D}\varphi_s(\rho(t_i)-\rho(s))(\theta(s)-\theta_r)\boldsymbol{I_0},\boldsymbol{\varepsilon}(\zeta_i)\Big)_\Omega ds\\
&\quad-\frac{k}{2}\sum_{j=1}^{i}\Big[\Big(\alpha\boldsymbol{D}\varphi_s(\rho(t_i)-\rho(t_j))(\theta(t_j)-\theta_r)\boldsymbol{I_0},\boldsymbol{\varepsilon}(\zeta_i)\Big)_\Omega\\
&\quad+\Big(\alpha\boldsymbol{D}\varphi_s(\rho(t_i)-\rho(t_{j-1}))(\theta(t_{j-1})-\theta_r)\boldsymbol{I_0},\boldsymbol{\varepsilon}(\zeta_i)\Big)_\Omega\Big]\\
&\quad\leqslant\sum_{j=1}^{i}\Big[Ck^2\int_{t_{j-1}}^{t_j}\Big|\Big(\alpha\boldsymbol{D}\varphi_s(\rho(t_i)-\rho(s))(\theta(s)-\theta_r)\boldsymbol{I_0},\boldsymbol{\varepsilon}(\zeta_i)\Big)''_\Omega\Big|ds\Big]\\
&\quad\leqslant\sqrt{3}Ck^2C(\alpha,\boldsymbol{D})C'''_\rho\int_{t_{j-1}}^{t_j}\Big(\|\theta(s)-\theta_r\|^2_{L_2(\Omega)}+\|(\theta(s)-\theta_r)'\|^2_{L_2(\Omega)}\\
&\qquad\qquad+\|(\theta(s)-\theta_r)''\|^2_{L_2(\Omega)}\Big)^{\frac{1}{2}}ds\|\boldsymbol{\zeta}_i\|_E\\
&\quad\leqslant Ck^2\|\zeta_i\|_E. \qquad (7.2.20)
\end{aligned}$$

Putting all these ingredients together in (7.2.2), yields

$$\begin{aligned}
\|\zeta_i\|_E^2 &\leqslant \|\eta(t_i)\|_E\|\zeta_i\|_E + C\frac{k}{2}\sum_{j=1}^{i}\Big(\|\zeta_j\|_E+\|\eta(t_j)\|_E\Big)\|\zeta_i\|_E\\
&+C\frac{k}{2}\sum_{j=0}^{i-1}\Big(\|\zeta_j\|_E+\|\eta(t_j)\|_E\Big)\|\zeta_i\|_E+C\|\theta_i^h-\theta(t_i)\|_{L_2(\Omega)}\|\zeta_i\|_E\\
&+C\frac{k}{2}\sum_{j=1}^{i}\Big(k^2\|\zeta_i\|_E+k\sum_{m=0}^{i}\|\theta_m^h-\theta(t_m)\|_{L_2(\Omega)}\|\zeta_i\|_E+\|\theta_j^h-\theta(t_j)\|_{L_2(\Omega)}\|\zeta_i\|_E\Big)\\
&+C\frac{k}{2}\sum_{j=0}^{i-1}\Big(k^2\|\zeta_i\|_E+k\sum_{m=0}^{i}\|\theta_m^h-\theta(t_m)\|_{L_2(\Omega)}\|\zeta_i\|_E+\|\theta_j^h-\theta(t_j)\|_{L_2(\Omega)}\|\zeta_i\|_E\Big)\\
&+C\frac{k}{2}\sum_{j=1}^{i}\|\theta_j^h-\theta(t_j)\|_{L_2(\Omega)}\|\zeta_i\|_E+C\frac{k}{2}\sum_{j=0}^{i-1}\|\theta_j^h-\theta(t_j)\|_{L_2(\Omega)}\|\zeta_i\|_E\\
&+Ck^2\|\zeta_i\|_E+Ck^2\|\zeta_i\|_E. \qquad (7.2.21)
\end{aligned}$$

Simplifying this further and dividing through by $\|\zeta_i\|_E$, we get

$$\begin{aligned}\big(1 - Ck\big)\|\zeta_i\|_E \leqslant \|\eta(t_i)\|_E + Ck\sum_{j=0}^{i-1}\|\zeta_j\|_E + Ck\sum_{j=0}^{i}\|\eta(t_j)\|_E \\ + Ck\sum_{j=0}^{i}\Big[k^2 + T\max_{0\leqslant m\leqslant N}\|\theta_m^h - \theta(t_m)\|_{L_2(\Omega)} + \|\theta_j^h - \theta(t_j)\|_{L_2(\Omega)}\Big] \\ + Ck\sum_{j=0}^{i}\|\theta_j^h - \theta(t_j)\|_{L_2(\Omega)} + C\|\theta_i^h - \theta(t_i)\|_{L_2(\Omega)}, \\ + Ck^2 + Ck^2 \end{aligned} \tag{7.2.22}$$

where we require that $1 - Ck > 0$. Using the estimate $\|\eta(t)\| \leqslant Ch|u(t)|_{H^2(\Omega)}$ (as we did for the linear case) and the bound on error for the heat problem given by (5.1.32), after dividing by $1 - Ck$ yields

$$\|\zeta_i\|_E \leqslant C(h + k^2) + Ck\sum_{j=0}^{i-1}\|\zeta_j\|_E. \tag{7.2.23}$$

Using the discrete version of Gronwall inequality, one gets

$$\|\zeta_i\|_E \leqslant C(h + k^2)e^{c_2T}. \tag{7.2.24}$$

Using the triangle inequality, we have

$$\begin{aligned}\|\boldsymbol{u}_i^h - \boldsymbol{u}(t_i)\|_E &\leqslant \|\eta(t_i)\|_E + \|\zeta_i\|_E \\ &\leqslant Ch|\boldsymbol{u}|_{H^2(\Omega)} + Ce^{c_2T}(h + k^2) \\ &\leqslant C(h + k^2). \end{aligned} \tag{7.2.25}$$

□

We have thus proved the theorem.

7.3 Numerical results

After deriving an error estimate in the previous section, we now show some numerical results. In this section we show computational results in terms of convergence rates for a number of exact solutions for the nonlinear problem. First we introduce a shorthand notation. Let

$$\begin{aligned} b(t_i, t_j; \boldsymbol{u}_j^h, \boldsymbol{v}) :&= \int_\Omega \boldsymbol{\varepsilon}(\boldsymbol{v}) \cdot \boldsymbol{D}\boldsymbol{\varepsilon}(\boldsymbol{u}_j^h)\varphi_s(\rho_i^h - \rho_j^h) d\Omega \\ &= \Big(\boldsymbol{\varepsilon}(\boldsymbol{v}), \boldsymbol{D}\boldsymbol{\varepsilon}(\boldsymbol{u}_j^h)\varphi_s(\rho_i^h - \rho_j^h)\Big)_\Omega. \end{aligned} \tag{7.3.1}$$

Note that $\boldsymbol{\varepsilon}(\boldsymbol{v})$ as argument of the bilinear form appears on the left side now, compared with the previous notation. Next, let

$$\begin{aligned} d(t_i, t_j; \theta_j^h, \boldsymbol{v}) :&= \int_\Omega \boldsymbol{\varepsilon}(\boldsymbol{v}) \cdot \alpha \boldsymbol{D}\varphi_s(\rho_i^h - \rho_j^h)(\theta_j^h - \theta_r)\boldsymbol{I_0} d\Omega \\ &= \Big(\boldsymbol{\varepsilon}(\boldsymbol{v}), \alpha \boldsymbol{D}\varphi_s(\rho_i^h - \rho_j^h)(\theta_j^h - \theta_r)\boldsymbol{I_0}\Big)_\Omega. \end{aligned} \tag{7.3.2}$$

Next, we establish two relations. We will make use of the fact that,

$$\varphi_s(\rho_i^h - \rho_j^h) = \sum_{q=1}^{N_\varphi} \alpha_q \varphi_q e^{-\alpha_q(\rho_i^h - \rho_j^h)} (\rho_j^h)'. \tag{7.3.3}$$

This will enable us to rewrite parts of (3.4.2) in terms of (7.3.3). Thus, we can write,

$$
\begin{aligned}
&\frac{k}{2}b(t_i,t_0;\boldsymbol{u}_0^h,\boldsymbol{v}) + k\sum_{j=1}^{i-1} b(t_i,t_j;\boldsymbol{u}_j^h,\boldsymbol{v}) \\
&\quad = k\int_\Omega \sum_{q=1}^{N_\varphi}\left[\frac{1}{2}\boldsymbol{\varepsilon}(\boldsymbol{v})\cdot\boldsymbol{D}\boldsymbol{\varepsilon}(\boldsymbol{u}_0^h)\alpha_q\varphi_q e^{-\alpha_q(\rho_i^h-\rho_0^h)}(\rho_0^h)'\right] d\Omega \\
&\quad + k\int_\Omega \sum_{q=1}^{N_\varphi}\left[\sum_{j=1}^{i-1}\boldsymbol{\varepsilon}(\boldsymbol{v})\cdot\boldsymbol{D}\boldsymbol{\varepsilon}(\boldsymbol{u}_j^h)\alpha_q\varphi_q e^{-\alpha_q(\rho_i^h-\rho_j^h)}(\rho_j^h)'\right] d\Omega \\
&\quad = k\int_\Omega \sum_{q=1}^{N_\varphi}\boldsymbol{K}_{iq}, \qquad (7.3.4)
\end{aligned}
$$

where,

$$
\begin{aligned}
\boldsymbol{K}_{iq} &= \frac{1}{2}\boldsymbol{\varepsilon}(\boldsymbol{v})\cdot\boldsymbol{D}\boldsymbol{\varepsilon}(\boldsymbol{u}_0^h)\alpha_q\varphi_q e^{-\alpha_q(\rho_i^h-\rho_0^h)}(\rho_0^h)' \\
&\quad + \sum_{j=1}^{i-1}\boldsymbol{\varepsilon}(\boldsymbol{v})\cdot\boldsymbol{D}\boldsymbol{\varepsilon}(\boldsymbol{u}_j^h)\alpha_q\varphi_q e^{-\alpha_q(\rho_i^h-\rho_j^h)}(\rho_j^h)'. \qquad (7.3.5)
\end{aligned}
$$

Next, we can again rewrite parts of (3.4.2) in terms of (7.3.3). Thus we can write,

$$
\begin{aligned}
&-\frac{k}{2}d(t_i,t_0;\theta_0^h,\boldsymbol{v}) - k\sum_{j=1}^{i-1} d(t_i,t_j;\theta_j^h,\boldsymbol{v}) \\
&\quad = -k\int_\Omega \sum_{q=1}^{N_\varphi}\left[\frac{1}{2}\boldsymbol{\varepsilon}(\boldsymbol{v})\cdot\alpha\boldsymbol{D}\alpha_q\varphi_q e^{-\alpha_q(\rho_i^h-\rho_0^h)}(\rho_0^h)'(\theta_0^h-\theta_r)\boldsymbol{I_0}\right] d\Omega \\
&\quad - k\int_\Omega \sum_{q=1}^{N_\varphi}\left[\sum_{j=1}^{i-1}\boldsymbol{\varepsilon}(\boldsymbol{v})\cdot\alpha\boldsymbol{D}\alpha_q\varphi_q e^{-\alpha_q(\rho_i^h-\rho_j^h)}(\rho_j^h)'(\theta_j^h-\theta_r)\boldsymbol{I_0}\right] d\Omega \\
&\quad = -k\int_\Omega \sum_{q=1}^{N_\varphi}\boldsymbol{P}_{iq}, \qquad (7.3.6)
\end{aligned}
$$

where,

$$\begin{aligned} \boldsymbol{P}_{iq} &= \frac{1}{2}\boldsymbol{\varepsilon}(\boldsymbol{v}) \cdot \alpha \boldsymbol{D} \alpha_q \varphi_q e^{-\alpha_q(\rho_i^h - \rho_0^h)} (\rho_0^h)'(\theta_0^h - \theta_r)\boldsymbol{I_0} \\ &+ \sum_{j=1}^{i-1} \boldsymbol{\varepsilon}(\boldsymbol{v}) \cdot \alpha \boldsymbol{D} \alpha_q \varphi_q e^{-\alpha_q(\rho_i^h - \rho_j^h)} (\rho_j^h)'(\theta_j^h - \theta_r)\boldsymbol{I_0}. \end{aligned} \tag{7.3.7}$$

We are now able to give an algorithm for solving the thermoviscoelasticity problem with the nonlinearity. For this, we will make use of equations (7.3.4) and (7.3.6).

`Algorithm 3:  Nonlinear problem (with reduced time)`

---

1. `Given` $\theta(0),$ `i.e temperature at t=0`
2. `Find` $\hat{\mathtt{F}}_0$
3. `Solve` $\mathtt{AU}_0 = \mathtt{L}_0 + \alpha \hat{\mathtt{F}}_0,$ `i.e find displacement at t=0`
4. `Find` $\rho(t=0),$ `reduced time at t=0`
5. `for i=1,...,N`
6.   `Compute` $\theta_{\mathtt{i}}$, `i.e solve the heat conduction problem for each time i`
7.   `Compute` $\rho_{\mathtt{i}} = \frac{\mathtt{k}}{2}\left[\frac{1}{\psi(\theta_{\mathtt{i}})} + \frac{1}{\psi(\theta_{\mathtt{i-1}})}\right] + \rho_{\mathtt{i-1}}$
8.   `Solve` $\mathtt{A}(1 - \frac{\mathtt{k}}{2}\varphi_{\mathtt{s}}(0))\mathtt{U}_{\mathtt{i}} = \mathtt{L}_i + \sum_{\mathtt{q}=1}^{\mathtt{N_q}} \mathtt{K}_{\mathtt{q}} - \sum_{\mathtt{q}=1}^{\mathtt{N_q}} \mathtt{P}_{\mathtt{q}} + \alpha(1 - \frac{\mathtt{k}}{2}\varphi_{\mathtt{s}}(0))\hat{\mathtt{F}}_{\mathtt{i}}$
9. `next i`

It is probably impossible to find an exact solution in a closed form using WLF formula for the *reduced time* given by (2.3.7), from which

$$\frac{1}{\psi[\theta(\zeta)]} = 10^{\frac{k_2 + \theta - \theta_g}{k_1(\theta - \theta_g)}} \tag{7.3.8}$$

One always obtains an integral which cannot be evaluated in closed form when trying to compute the stress using the stress-strain law given by (2.4.7). We investigate two different forms of the shift factor ψ.

CASE 1. We propose a simpler form for the shift factor: $\frac{1}{\psi[\theta(\zeta)]} = 10^{\theta(\zeta)}$, where we take the temperature $\theta(\zeta) = \beta$, β constant, and displacement $u(\boldsymbol{x}, t) = (3x - 2y, 4x + y)t$. Tabulation of displacement errors when $\beta = 2$, is shown in Table 7.1. These are the same type of errors that were computed for the viscoelasticity and the linear problems, that is, the maximum errors over *all* discrete times and over all nodes. We can see that the error due to time steps is decreasing by a factor of 4, except in the first row, where the time steps are doubled from 2 to 4. This is probably because of the large value of the shift factor when $\beta = 2$. In other words, at least 4 time steps are needed before the error starts to reduce by a factor of 4. So each column indicates $O(k^2)$ convergence, k being the size of time step. As expected, there are no spatial errors and this is because the exact solution for the displacement is linear in spatial coordinates. In Tables (7.2) and (7.3) we show the errors in the L_2 and H^1 norms, respectively. Both tables show a convergence rate by a factor of 4 as the number of time steps is doubled. There are no errors as the number of elements in the mesh is increased. We see in all three tables that there is some dependency on h parameter, similarly to the viscoelasticity problem in Section 3.2.2. This is is due to quadrature error in computing the integrals. This is evident in all three tables showing the different types of error.

CASE 2. Taking $1/\psi$ to be $\frac{1}{\psi(\theta(\zeta))} = \theta(\zeta, \boldsymbol{x})$, one can evaluate the stress in closed form, by taking the temperature to be $\theta(\zeta, \boldsymbol{x}) = \mathcal{M}(x, y)e^t$ and displacement $\boldsymbol{u}(\boldsymbol{x}, t) = (u_1(x, y), u_2(x, y))e^t$. We give four different numerical examples where convergence rates are shown in the L_2 and H^1 norms, as well as in the max norm.

Table 7.1: *Max* errors for displacement: nonlinearity, Case 1

time steps	mesh size 2	4	8	16	32
2	18.612156	19.906652	20.583299	20.870252	20.941361
4	0.543710	0.581136	0.600668	0.608964	0.611018
8	0.105918	0.113208	0.117012	0.118628	0.119028
16	0.025116	0.026844	0.027747	0.028130	0.028225
32	0.006199	0.006626	0.006849	0.006943	0.006967
64	0.001545	0.001651	0.001706	0.001730	0.001736

Table 7.2: L^2 errors for displacement: nonlinearity, Case 1

time steps	mesh size 2	4	8	16	32
2	7.320330	8.835289	9.434735	9.692902	9.793268
4	0.214164	0.258332	0.275741	0.283231	0.286143
8	0.041721	0.050325	0.053716	0.055175	0.055742
16	0.009893	0.011933	0.012737	0.013083	0.013218
32	0.002442	0.002945	0.003144	0.003229	0.003262
64	0.000608	0.000734	0.000783	0.000804	0.000813
128	0.000152	0.000183	0.000195	0.000201	0.000203

Numerical Example 1: $\theta(\zeta, \boldsymbol{x}) = e^t$

$$\boldsymbol{u}(\boldsymbol{x}, t) = (3x - 2y, 4x + y)e^t$$

Tables 7.4 and 7.5 show the L_2 and H^1 norms, respectively. We see that in both cases, the errors are decreasing only as time steps are doubled. This is due to the presence of exponential in the exact solution and the trapezoidal rule approximation. Both tables show that the error is decreasing by a factor of four along the diagonal. This is consistent with the error estimate derived in this Chapter. Taking $h = k^2$ gives an estimate $C(h)$. This is much more efficient than taking $h = k$, which would require many more time steps. With regards to the H^1 norm the decrease by a factor of four is because the exact solution is linear in space. Otherwise, this we would see a decrease by a factor of two, if the solution was not linear in space. Later

Table 7.3: H^1 errors for displacement: nonlinearity, Case 1

time steps	mesh size 2	4	8	16	32
2	42.052094	47.339318	49.826943	51.279971	52.045258
4	1.230281	1.384831	1.457418	1.499733	1.521988
8	0.239671	0.269778	0.283919	0.292161	0.296497
16	0.056833	0.063972	0.067325	0.069280	0.070308
32	0.014028	0.015790	0.016618	0.017101	0.017354
64	0.003496	0.003935	0.004141	0.004261	0.004325
128	0.000873	0.000983	0.001034	0.001064	0.001080

Table 7.4: Displacement errors in the L_2 norm: nonlinearity, Case 2, Example 1

time steps	mesh size 2	4	8	16	32	64	128
2	0.005180	0.006267	0.006694	0.006877	0.006948	0.006974	0.006983
4	0.001306	0.001580	0.001688	0.001734	0.001752	0.001758	0.001760
8	0.000327	0.000395	0.000422	0.000434	0.000438	0.000440	0.000441
16	0.000081	0.000099	0.000105	0.000108	0.000109	0.000110	0.000110
32	0.000020	0.000024	0.000026	0.000027	0.000027	0.000027	0.000027
64	0.000005	0.000006	0.000006	0.000006	0.000006	0.000006	0.000006
128	0.000001	0.000001	0.000001	0.000001	0.000001	0.000001	0.000001

examples will show just that. We also see some dependency on the h parameter for all three types of error in this example. This may be due to quadrature error for not computing the integrals exactly.

Table 7.5: Displacement errors in the H^1 norm: nonlinearity, Case 2, Example 1

time steps	mesh size 2	4	8	16	32	64	128
2	0.029758	0.033588	0.035373	0.036407	0.036948	0.037206	0.037321
4	0.007506	0.008470	0.008919	0.009180	0.009316	0.009381	0.009410
8	0.001880	0.002122	0.002234	0.002300	0.002334	0.002350	0.002357
16	0.000470	0.000530	0.000559	0.000575	0.000583	0.000587	0.000589
32	0.000117	0.000132	0.000139	0.000143	0.000145	0.000147	0.000147
64	0.000029	0.000033	0.000034	0.000035	0.000035	0.000035	0.000035
128	0.000007	0.000008	0.000008	0.000009	0.000009	0.000009	0.000009

Table 7.6: *Max* errors for displacement: nonlinearity, Case 2, Example 1

time steps	mesh size 2	4	8	16	32	64	128
2	0.013165	0.014116	0.014599	0.014803	0.014854	0.014871	0.014874
4	0.003320	0.003558	0.003680	0.003731	0.003744	0.003748	0.003749
8	0.000832	0.000891	0.000922	0.000934	0.000938	0.000939	0.000939
16	0.000208	0.000223	0.000230	0.000233	0.000234	0.000234	0.000234
32	0.000052	0.000055	0.000057	0.000058	0.000058	0.000058	0.000058
64	0.000013	0.000014	0.000014	0.000014	0.000014	0.000014	0.000014
128	0.000003	0.000003	0.000003	0.000003	0.000003	0.000003	0.000003

Numerical Example 2:

$$\theta(\zeta, \boldsymbol{x}) = (2 + \sin(2x + 3y))e^t$$

$$\boldsymbol{u}(\boldsymbol{x}, t) = (3x - 2y, 4x + y)e^t$$

In Example 2, again we see the same behaviour as in Example 1. See Tables 7.7, 7.8 and 7.9. The only difference seems to be that the corresponding errors for the same norm differ by a factor of four. The only reason for this may be the fact that in Example 2, the temperature depends on spatial coordinates and is not linear. This is true for all the norms. Again we see the the errors have some dependency on h, the reason being that given in Example 1. Also, the consistency between theoretical estimate and numerical results shown can be justified in the same way

Table 7.7: Displacement errors in the L_2 norm: nonlinearity, Case 2, Example 2

time steps	mesh size 2	4	8	16	32	64	128
2	0.019563	0.018390	0.021251	0.022401	0.022764	0.022873	0.022906
4	0.015843	0.005595	0.004971	0.005498	0.005685	0.005738	0.005753
8	0.016121	0.005044	0.001473	0.001279	0.001390	0.001427	0.001437
16	0.016271	0.005335	0.001366	0.000377	0.000323	0.000348	0.000357
32	0.016314	0.005431	0.001458	0.000351	0.000095	0.000081	0.000087
64	0.016325	0.005457	0.001487	0.000375	0.000088	0.000023	0.000020

as for Example 1.

Table 7.8: Displacement errors in the H^1 norm: nonlinearity, Case 2, Example 2

time steps	mesh size 2	4	8	16	32	64	128
2	0.096756	0.099016	0.109223	0.113956	0.115887	0.116677	0.116999
4	0.062343	0.028337	0.026391	0.028218	0.028991	0.029270	0.029371
8	0.062072	0.021485	0.007658	0.006796	0.007156	0.007299	0.007344
16	0.062687	0.022293	0.006035	0.001980	0.001722	0.001800	0.001829
32	0.062883	0.022658	0.006283	0.001569	0.000502	0.000433	0.000451
64	0.062934	0.022759	0.006385	0.001633	0.000397	0.000126	0.000108

Table 7.9: *Max* errors for displacement: nonlinearity, Case 2, Example 2

time steps	mesh size 2	4	8	16	32	64	128
2	0.051171	0.044912	0.046054	0.046719	0.046978	0.047038	0.047059
4	0.027033	0.012642	0.011799	0.011754	0.011767	0.011770	0.011773
8	0.027926	0.007418	0.003233	0.003008	0.002958	0.002947	0.002944
16	0.028150	0.007820	0.001903	0.000822	0.000756	0.000740	0.000737
32	0.028206	0.008121	0.002115	0.000481	0.000207	0.000189	0.000185

Numerical Example 3: $\theta(\zeta, \boldsymbol{x}) = e^t$

$$\boldsymbol{u}(\boldsymbol{x}, t) = (\sin(x/2 + 2y/3), \sin(x/3 - 3y/4))\, e^t$$

Referring to Example 3, Table 7.10 tabulates the errors in the L_2 norm. We see that, along the diagonal as the mesh size and time steps are doubled, the error decreases by a factor of four. This is consistent with the estimate $C(h^2 + k^2)$. This is because if h and k are halved, then a factor of $1/4$ comes in front of error error estimate, due to the squares in h^2 and k^2. On the other hand, the error in the H^1 norm decreases by a factor of two along the diagonal, as shown in Table 7.11. This is consistent with the error estimate, which we derived in this chapter, $C(h+k^2)$. Taking $h = k^2$, gives an estimate $C(h)$, and then halving h, the error is halved as a result. Table 7.12 shows the max errors. We would expect the error here to decrease as $C(h^2+k^2)$ which is consistent with what the table shows: along the diagonal the error reduces by a factor of four.

Table 7.10: Displacement errors in the L_2 norm: nonlinearity, Case 2, Example 3

time steps	mesh size 2	4	8	16	32	64	128
2	0.040147	0.010162	0.002508	0.001591	0.001739	0.001802	0.001821
4	0.040326	0.010490	0.002572	0.000632	0.000408	0.000441	0.000455
8	0.040373	0.010588	0.002682	0.000646	0.000158	0.000103	0.000110
16	0.040384	0.010613	0.002714	0.000676	0.000161	0.000039	0.000025
32	0.040387	0.010620	0.002723	0.000685	0.000169	0.000040	0.000009
64	0.040388	0.010621	0.002725	0.000687	0.000171	0.000042	0.000010

Table 7.11: Displacement errors in the H^1 norm: nonlinearity, Case 2, Example 3

time steps	mesh size 2	4	8	16	32	64	128
2	0.248989	0.124410	0.062504	0.032317	0.018292	0.012584	0.010708
4	0.249148	0.124537	0.062192	0.031136	0.015712	0.008152	0.004624
8	0.249198	0.124609	0.062226	0.031092	0.015551	0.007794	0.003935
16	0.249212	0.124629	0.062242	0.031097	0.015545	0.007773	0.003888
32	0.249215	0.124635	0.062246	0.031099	0.015546	0.007772	0.003886
64	0.249216	0.124636	0.062247	0.031100	0.015546	0.007772	0.003886

Table 7.12: *Max* errors for displacement: nonlinearity, Case 2, Example 3

time steps	mesh size 2	4	8	16	32	64	128
2	0.015856	0.005200	0.002943	0.003567	0.003741	0.003784	0.003795
4	0.016156	0.006381	0.001538	0.000762	0.000907	0.000944	0.000954
8	0.016232	0.006680	0.001967	0.000403	0.000192	0.000227	0.000236
16	0.016251	0.006755	0.002075	0.000521	0.000102	0.000048	0.000057
32	0.016256	0.006773	0.002102	0.000551	0.000132	0.000025	0.000012

Numerical Example 4: $\theta(\zeta, \boldsymbol{x}) = (2 + \sin(2x + 3y))e^t$

$$\boldsymbol{u}(\boldsymbol{x}, t) = (\sin(x/2 + 2y/3), \sin(x/3 - 3y/4))\, e^t$$

Example 4 is probably the most interesting, since neither $\boldsymbol{u}$ nor θ are linear in space and time. Table 7.13 shows how the error in L_2 norm behaves. As the mesh size and time steps are doubled (i.e. along the diagonal of the table), the error reduces by a factor of four. This is again consistent with the theoretical estimate $C(h^2 + k^2)$.

Table 7.13: Displacement errors in the L_2 norm: nonlinearity, Case 2, Example 4

time steps	mesh size 2	4	8	16	32	64	128
2	0.040181	0.010024	0.004806	0.005462	0.005825	0.005935	0.005967
4	0.040577	0.010432	0.002517	0.001288	0.001410	0.001475	0.001494
8	0.040691	0.010687	0.002661	0.000631	0.000330	0.000356	0.000370
16	0.040721	0.010760	0.002752	0.000670	0.000158	0.000083	0.000089
32	0.040729	0.010778	0.002778	0.000696	0.000168	0.000039	0.000020
64	0.040731	0.010783	0.002785	0.000703	0.000174	0.000042	0.000009

The behaviour of error in the H^1 norm is shown in Table 7.14. As the table shows, the error reduces by a factor of two along the diagonal as the mesh size and time steps are doubled. The theoretical estimate $C(h + k^2)$ which we derived confirms just that, since as explained the earlier Example 3, $h = k^2$ gives an estimate $C(h)$. Then halving h, this halves the previous value of error. The max error also behaves confirm the theoretical estimate, which we would expect to be exactly the same as for the L_2 norm. The max error behaviour is shown in Table 7.15.

The estimate $C(h + k^2)$ tells us that the contribution from h and k are not the same with respect to convergence of the error. For example, Table 7.14 shows that the error does not start to decrease simultaneously for the same values of mesh size and time steps. Looking at the columns of the table, we see that only in the

Table 7.14: Displacement errors in the H^1 norm: nonlinearity, Case 2, Example 4

time steps	mesh size 2	4	8	16	32	64	128
2	0.249108	0.125230	0.066962	0.043047	0.035169	0.033073	0.032586
4	0.249306	0.124491	0.062322	0.031831	0.017369	0.011172	0.008993
8	0.249428	0.124655	0.062210	0.031110	0.015645	0.008017	0.004379
16	0.249464	0.124718	0.062251	0.031094	0.015547	0.007785	0.003917
32	0.249473	0.124735	0.062266	0.031101	0.015545	0.007772	0.003887
64	0.249475	0.124740	0.062270	0.031103	0.015546	0.007772	0.003886

Table 7.15: *Max* errors for displacement: nonlinearity, Case 2, Example 4

time steps	mesh size 2	4	8	16	32	64	128
2	0.014004	0.008655	0.012630	0.014158	0.014653	0.014774	0.014806
4	0.014915	0.005792	0.002415	0.003343	0.003620	0.003690	0.003708
8	0.015141	0.006839	0.001781	0.000631	0.000852	0.000909	0.000924
16	0.015198	0.007100	0.002183	0.000472	0.000160	0.000214	0.000227
32	0.015212	0.007166	0.002284	0.000586	0.000119	0.000040	0.000053

forth column the error starts to reduce as the times steps are doubled (i.e. going downwards). Therefore there is a need to investigate how the error behaves if we make " $h = k^2$ ". In this case, we have: error $= \|\boldsymbol{u}(t_i) - \boldsymbol{u}_i^h\|_E \leqslant Ch = \dfrac{C}{m}$, where m is the mesh size. In terms of log, this takes the form: $\log \text{error} = \log C - \log m$. Thus plotting the error vs m in the loglog scale, we would expect a graph of slope approximately equal to -1, see Fig. 7.1. Choosing two points on the graph, we can compute the slope.

$$\text{slope} = \frac{\log(0.015895) - \log(0.031831)}{\log(64) - \log(32)} = \frac{-0.6944}{0.6931} = -1.009 \tag{7.3.9}$$

The slope of approximately -1, confirms that the codes are working correctly and

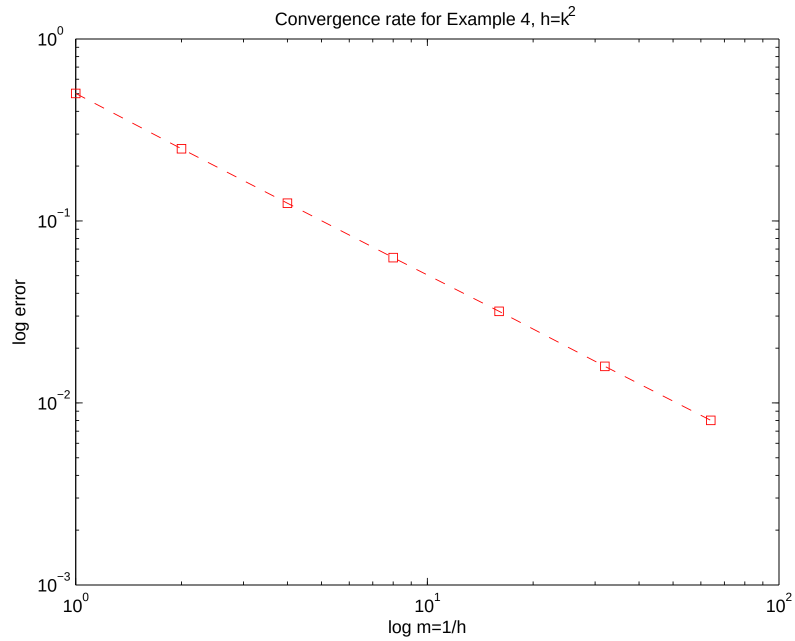

Figure 7.1: Loglog plot of error vs mesh size

that the convergence rates are correct. We show this only for Example 4, as all other examples use the same code.

Numerical results for the heat problem

Since we are dealing with a coupled problem, and temperature is embedded in this coupling, it is worthwhile to show that the part of the coupling code which which solves the heat problem also works correctly in terms of the convergence.

Example 1. $\theta(\zeta, \boldsymbol{x}) = e^t$

Table 7.16: Heat errors in the L_2 norm: $\times 10^3$, $T = 10$, Example 1

time steps	mesh size 2	4	8	16	32	64	128
2	0.931609	1.111466	1.155729	1.166751	1.169504	1.170192	1.170364
4	0.483505	0.574926	0.597263	0.602814	0.604200	0.604546	0.604633
8	0.166726	0.197784	0.205333	0.207207	0.207674	0.207791	0.207820
16	0.046081	0.054616	0.056686	0.057200	0.057328	0.057360	0.057368
32	0.011833	0.014021	0.014551	0.014683	0.014716	0.014724	0.014726
64	0.002978	0.003529	0.003662	0.003695	0.003703	0.003705	0.003706
128	0.000745	0.000883	0.000917	0.000925	0.000927	0.000928	0.000928

Table 7.17: Heat errors in the H^1 norm: $\times 10^3$, $T = 10$, Example 1

time steps	mesh size 2	4	8	16	32	64	128
2	3.358964	3.759067	3.852780	3.875864	3.881614	3.883050	3.883409
4	1.743302	1.944676	1.991577	2.003115	2.005988	2.006705	2.006885
8	0.601139	0.669059	0.684818	0.688691	0.689656	0.689896	0.689957
16	0.166148	0.184761	0.189074	0.190133	0.190397	0.190463	0.190479
32	0.042665	0.047432	0.048537	0.048808	0.048876	0.048893	0.048897
64	0.010739	0.011938	0.012216	0.012284	0.012301	0.012305	0.012306
128	0.002689	0.002989	0.003059	0.003076	0.003080	0.003081	0.003081

Table 7.17 shows the error in the L_2 norm. The error reduces by a factor of four along the diagonal. This is consistent with the estimate for the heat problem given by 5.1.1. Looking on the left side of this estimate, the second term is dominant.

Thus, the error in the L_2 norm behaves as $C(h^2 + k^2)$. The H^1 error reduces by a factor of four as well (rather than a factor of two), but this is due to the fact that the exact solution does not depend on spatial coordinates.

Example 2. $\theta(\zeta, \boldsymbol{x}) = (2 + \sin(2x + 3y))e^t$

Table 7.18: Heat errors in the L_2 norm: $\times 10^3$, $T = 10$, Example 2

time steps	mesh size 2	4	8	16	32	64	128
2	6.601375	2.914935	2.651746	2.737765	2.770018	2.778750	2.780975
4	6.604605	2.188074	1.381707	1.401830	1.427141	1.434713	1.436683
8	6.702427	2.022107	0.637621	0.475438	0.485571	0.491734	0.493493
16	6.759839	2.058266	0.537015	0.168596	0.131529	0.134318	0.135829
32	6.778099	2.078375	0.547806	0.136444	0.042817	0.033786	0.034497
64	6.782960	2.084254	0.553501	0.139288	0.034253	0.010747	0.008504
128	6.784194	2.085779	0.555117	0.140763	0.034974	0.008572	0.002689

Table 7.19: Heat errors in the H^1 norm: $\times 10^3$, $T = 10$, Example 2

time steps	mesh size 2	4	8	16	32	64	128
2	41.59911	23.61615	14.44124	10.82397	9.69744	9.39381	9.31629
4	40.95527	22.30510	12.09001	7.35795	5.55464	5.00149	4.85325
8	40.69755	21.84448	11.21976	5.81534	3.24339	2.16263	1.79309
16	40.64333	21.77662	11.10267	5.59252	2.82742	1.46825	0.83365
32	40.63238	21.76830	11.09222	5.57431	2.79246	1.40034	0.70752
64	40.62986	21.76693	11.09117	5.57293	2.79005	1.39569	0.69836
128	40.62925	21.76664	11.09101	5.57280	2.78987	1.39538	0.69777

In Example 2, the exact solution is not linear either in space or in time. The L_2 error is behaving as is supposed to behave. This time the H^1 error is also behaving consistent with the theoretical estimate $C(h + k^2)$. The explanation is similar to that given in the examples for displacement. In both examples we take $T = 10$ as for smaller values of T it is hard to see how the error behaves; this is probably due to the presence of the factor e^t in the exact solutions.

7.4 Summary

An error estimate in the energy norm was derived for the nonlinear problem. Numerical results were shown for a number of exact solution to demonstrate that the error converges in consistency with the theoretical estimates, both for displacement and temperature.

Chapter 8

Conclusions and Future Work

Conclusions. In this thesis the model problem introduced in Section 2.4 has been considered. The study has been conducted in two aspects: theoretical and computational.

In view of the theoretical results, the focus has been on deriving stability and a *priori* error estimates in the defined energy norm.

In the case of the linear problem, stability bounds have been derived for continuous and discrete formulations. Stability bounds which have been derived for the discrete case contain exponentials; this is due to Gronwall's lemma. Such results containing exponentials are common in literature. The bounds show that the solution, in both cases, depends continuously on data, as well as initial conditions and constants. The existence has have been assumed *a priori* for the linear problem, whereas the uniqueness has been proved. Hence we can conclude that both formulations are well-posed. In the case of nonlinear problem, the challenge has been on dealing with the presence of the reduced time. The only possibility to overcome this was by assuming the temperature to be in some allowed range, as assumed in Assumptions 2.4.1 (iv). With this to hand, we then have been able to show that, for the nonlinear problem too, the bound for both formulations, continuous and discrete, contains only data, initial conditions and constants, again using Gronwall. Thus, for the reasons mentioned above, both formulations are well-posed.

A *priori* error estimates have been derived for the linear and nonlinear problems. Again, the challenge has been in dealing with the nonlinearity due to the reduced time. In both cases, it has been shown, using the Gronwall's lemma, that the error in the energy norm is bounded by $C(h + k^2)$.

In view of computational results, convergence rates have been shown for a number of exact solutions, in the L_2 and H^1 norms as well as in the "max norms". All computational results show the expected convergence rates. For the nonlinear problem we have been unable to use the WLF formula for the shift factor in the reduced time formula. This is due to the fact that it has not been possible to solve the integrals in a closed form in the stress-strain law in order to compute the stresses. One case $\dfrac{1}{\psi} = 10^{\beta}$ (for β constant) has been the closest to WLF formula (2.3.7), however this case corresponds to a constant temperature.

Future work. One can consider the possibility of extending the work presented in this thesis. Some of the ideas are as follows:

- Use the viscoelastic energy dissipation, due to particle frictions, to create a source term in the temperature equation (2.4.4). Then, implement a discrete approximation and obtain numerical results. This would include dealing with the non-trivial nonlinear coupling that would result by linearising with extrapolation of temperature from previous time steps. This is a novel idea.

- Include the inertia term $\ddot{\boldsymbol{u}}$ in the equilibrium equations (2.4.1) and consider a viscodynamic rather then a quasistatic problem. Then perform stability and error analysis for this problem. This also constitutes a novel idea. Even without the thermal effects, such a problem would be considered for the first time, as so far we have not come across a study, textbook or paper, which deals with the numerical analysis of this model.

- Consider large deformations instead. This would imply moving to the non-linear theory of deformation which is by far more complicated then the linear theory. For our coupled problem, this would be the first time to study such a model.

- Include hereditary effects in the temperature equation and also explore the possibility of deriving well-posedness results for the continuous problem. So far, we are not aware that this problem has been dealt with.

Bibliography

J. Alberty, C. Carstensen and S. Funken, *Remarks around 50 lines of Matlab: short finite element implementation*. Numerical Algorithms 20, 117-137, (1999)

J. Alberty, C. Carstensen, S. Funken and R. Klose *Matlab implementation of the finite element method in elasticity*. Computing 69, 239-263, (2002)

K. Atkinson and W. Han, *Theoretical Numerical Analysis: a functional analysis framework*(Springer-Verlag, New York, 2010)

S.C.Brenner and L.R. Scott, *The Mathematical Theory of Finite Element Methods* (Springer, New York, 2002)

G.R. Buchanan, *Finite Element Analysis* (McGraw-Hill, USA, 1995)

R. Courant, *Variational methods for the solution of problems of equilibrium and vibrations*. Bull. Amer. Math. Soc., 49, pp.1-23 (1943)

M.J Fagan, *Finite Element Analysis* (Longman, Scientific and Technical, 1992)

W.N. Findley, J.S. Lai, K. Onaran, *Creep and Relaxation of Nonlinear Viscoelastic Materials - with introduction to linear viscoelasticity* (Dover Publications, New York, 1989)

J.M. Hill and J.N. Dewynne, *Heat Conduction* (Black Scientific Publications, 1987, USA)

J.M. Golden and G.A.C. Graham, *Boundary value problems in linear viscoelasticity* (Springer-Verlag, Berlin, 1988)

C. Johnson, *Numerical Solution of Partial Differential Equations by the Finite Element Method* (Dover, 2009, New York)

J. Kiusalaas, *Numerical methods in engineering with MATLAB* (Cambridge University Press, New York, 2005)

H. Kopka and P.W. Daly, *Guide to LaTeX. Tools and techniques for computer typesetting* (Addison-Wesley, Massachusetts, 2009)

R.S. Lakes, *Viscoelastic solids* (CRC Press, Florida, 1998)

S. Larsson and V. Thomée, *Partial differential equations with numerical methods* (Springer, Berlin, 2005)

M. Lees, *A priori estimates for the solution of difference approximations to parabolic partial differential equations*. Duke Math 27, 297-311, (1960)

P. Linz, *Analytical and numerical methods for Volterra equations* (SIAM, Philadelphia, 1985)

G.E. Masse, *Continuum mechanics* (McGraw-Hill, USA, 1970)

L.W. Morland and E.H. Lee, *Stress Analysis for Linear Viscoelastic Materials with Temperature Variation*. Transactions of the society of rheology IV, 233-263, (1960)

J.T. Oden and J.N. Reddy, *An introduction to the mathematical theory of finite elements* (Wiley Interscience Publication, John Wiley and Sons, 1976)

M.N. Ozisik, *Boundary Value Problems of Heat Conduction* (International Textbook Company, Pennsylvania, 1968)

A.C. Pipkin, *A course on integral equations* (Springer-Verlag, New York, 1976)

Y. Qin and Z. Ma, *Energy Decay and Global Attractors for Thermoviscoelastic Systems*. Acta Appl Math(2012), 117:195-214

B.D. Reddy, *Introductory Functional Analysis with Applications to Boundary Value Problems and Finite Elements* (Springer, New York, 1998)

F. Schwarzl and A.J. Staverman, *Time-Temperature Dependence of Linear Viscoelastic Behavior*. Journal of Applied Physics, Volume 23, Number 8, (1952)

L.R. Scott, *Numerical Analysis* (Princeton University Press, New Jersey, 2011)

L.R. Scott and S. Zhang, *Finite element interpolation of nonsmooth functions satisfying boundary conditions*. Mathematics of Computation Volume 54, Number 190, 483-493, (1990)

S. Shaw, *Finite element and discrete time methods for continuous problems with memory and applications to viscoelasticity* (PhD thesis, Brunel University, 1993)

S. Shaw, M.K. Warby, J.R. Whiteman, C. Dawson, M.F. Wheeler, *Numerical techniques for the treatment of quasistatic viscoelastic stress problems in linear isotropic solids*. Computer methods in applied mechanics and engineering 118, 211-237, (1994)

S. Shaw, M.K. Warby, J.R. Whiteman, *Discrete schemes for treating hereditary problems of viscoelasticity and applications*. Journal of Computational and Applied Mathematics 74, 313-329, (1996)

S. Shaw, M.K. Warby, J.R. Whiteman, *Error estimates with sharp constants for a fading memory volterra problem in linear solid viscoelasticity*. SIAM J. NUMER. ANAL. Vol. 34, No. 3, pp.1237-1254, (1997)

S. Shaw and J.R. Whiteman, *Optimal long-time* $L_p(0,T)$ *stability and semidiscrete error estimates for the Volterra formulation of the linear quasistatic viscoelasticity problem*. Numer.Math.(2001)88:743-770

S. Shaw, M.K. Warby, J.R. Whiteman, *An Introduction to the Theory and Numerical Analysis of Viscoelasticity Problems - Notes*. BICOM, Brunel University,(2009)

V. Thomée, *Galerkin finite element methods for parabolic problems* (Springer, Second edition, New York, 2006)

P. Tong and J.N. Rossettos, *Finite element method - basic technique and implementation* (Dover Publications, New York, 2008)

F. Trèves , *Topological Vector Spaces, Distributions and Kernels* (Academic Press, New York, 2006)

B. Venkatraman and S.A. Patel, *Structural mechanics with introductions to elasticity and plasticity* (McGraw-Hill Inc., 1970)

M.L. Williams, R.F. Landel, J.D. Ferry, *The Temperature Dependence of Relaxation Mechanisms in Amorphous Polymers and Other Glass-forming Liquids*. Temperature Dependence of Relaxation Mechanisms 3701, (1955)

A. Wineman and R. Kolberg, *Response of Beams of Non-Linear Viscoelastic Materials Exhibiting Strain-Dependent Stress Relaxation*. Int. J. Non-Linear Mechanics Vol. 32, No. 5, 863-883, (1997)

M. Zlámal, *On the finite element method*. Numerische Mathematik, 12, pp. 394-402, (1968)

O.C. Zienkiewicz, *The birth of the finite element method and of computational mechanics*. Int. J. Numer. Meth. Engng, 60:3-10, (2004)